UNIVERSITA' DI PISA

Facoltà di Scienze Matematiche Fisiche e Naturali

Tesi di

Dottorato in Scienze Chimiche (PhD Thesis)

(XXIV Ciclo)

CHIM 04

"Rheological, mechanical, thermal and flame retardant properties of EVA composites highly filled with natural inorganic fillers"

SUPERVISOR: Prof. Giacomo Ruggeri

CANDIDATE: Angela Cardelli

President of the Doctorate School in Chemistry:

Prof. Benedetta Mennucci

A Bruno

Summary

In this PhD thesis the properties of highly filled composites, consisting of poly(ethylene-co-vinyl acetate) as matrix with different natural fillers, have been studied in order to understand how the presence of fillers can modify composites behaviour depending on their specific properties. The physicochemical properties of the chosen natural fillers have been analysed in comparison with two synthetic fillers in order to point out the main differences.

Rheological properties of the highly filled EVA composites have been studied, taking into account the effects of shear rate, temperature and in particular filler properties and concentration. A theoretical approach has been applied on the rheological results in order to rationalize and find indications about filler dispersion and its main effects on composite properties. Processing phenomena of composites, such as swelling and surface roughness of the extrudates, have been analysed in order to evaluate how the differences among filler properties can affect the melt elasticity behaviour. Filler properties influence has been evaluated also on mechanical behaviour of the composites to point out the reinforcing and elongation behaviour of the materials.

Thermal degradation behaviour of pristine EVA in comparison with the composites has been studied in order to understand how the introduction of the natural fillers affect the degradation mechanism of polymer; particular attention has been given to the behaviour of composites filled with natural carbonates.

Flame retardant properties of EVA composite filled with natural magnesium hydroxide have been investigated alone and in combination with other flame retardant additives, in order to find positive effects on performance reducing the total amount of filler. In this regard a screening study with a parameterization method of flame retardant behaviour has been developed and applied to a set of additives in order to evaluate their performance in combination with the natural magnesium hydroxide.

A specific combination of EVA composite filled with magnesium hydroxide, including a silicon and a boron containing additives, has been investigated by applying chemometric approach in order to rationalize the flame retardant behaviour of the system and to tailor formulations with the desired properties.

Index

1. Introduction

1.1. Fillers for polymeric composites

Originally fillers were introduced into polymeric materials in order to reduce the total cost of the compounds. Nowadays, it is ascertained that fillers enhance also specific properties of the materials and for this reason the term *functional filler* has been introduced: there are a lot of fillers used for different applications due to their functionalities. One of the most important factors, still influent on the industrial use of filler for polymer application, is their cost, different for each filler type and affected by raw material, production, transports and their specific properties[1]. A wide variety of fillers can be found, which are different for their properties and origin. Their behaviour in the polymeric composite is deeply influenced by many factors, such as morphology, colour, refractive index, presence of impurities, density, hardness, moisture content, thermal stability, modulus, surface chemistry and toxicity.

The morphology of fillers can be considered the key for understanding their performance in polymers and it includes particle size, shape, surface area and particle packing capacity. All these properties are related to the primary particles composing the filler, but it must be taken into account that fillers can easily form assemblies defined as aggregates, with very strong interaction among the particles, and agglomerates, characterized by weaker interactions. The tendency of the filler to assembly influences strongly the dispersion in the compound, even if it can be possible to break down aggregates and agglomerates by increasing the processing conditions severity and so dispersion energy[2] (Figure 1.1.1).

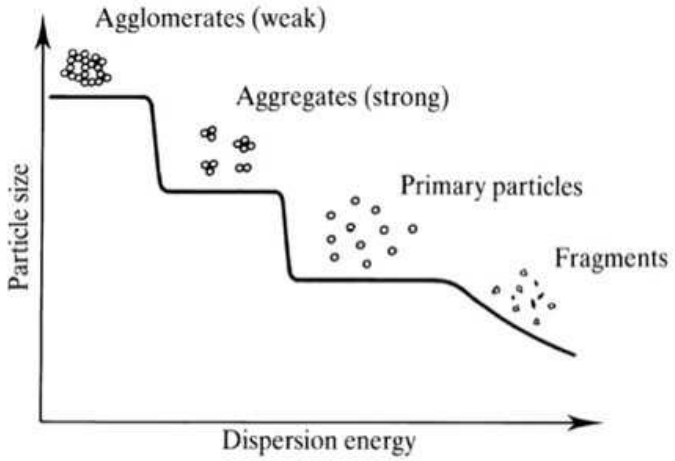

Figure 1.1.1: Different particle forms of dispersion of filler in compounds, depending on the applied dispersion energy.

The size, the specific surface area and the shape of the particles are strictly correlated each other. The most used parameter is the particle size and the distribution, but often the irregularity of the shapes makes its determination quite difficult and not so meaningful. The concept of equivalent spherical diameter (*eds*) is diffused for size identification and it corresponds to the diameter of a sphere having the same volume of the particle; the main defect of its use as indicative parameter is that fillers with different particle characteristics (porosity, surface roughness, shape, etc) can have the same esd. In technical datasheets, for practicalness, the particle size and distribution (PSD) are usually given by the average diameter values of particles at different percentage (indicated as D_{10}, D_{50}, D_{90}).

The main parameter introduced for the determination of particle shape is the aspect ratio, which is really useful for distinguishing anisotropic and isotropic particles. It represents the ratio of the length to the diameter of a rod, or of the thickness to the diameter of plates and its value is 1 for a sphere; for filler characterized by irregular shape it is not easy to obtain an average significant value. Both particle size and shape play an essential role in determining how the particles can pack together[3].

Specific surface area (SSA) describes the area of particles surface for weight unit of filler and its determination gives an idea of the surface available for polymer in composite: higher specific surface area commonly corresponds to more possibility of interaction

points between filler and matrix. It is deeply related to the particle size of the filler and usually higher is the size and smaller is the surface area.

It is important to underline that all these factors could be changed by processing of filler in the compounds: especially in case of "soft" fillers, particles breakdown can occur generating different shape, size and additional specific surface area.

One of the main aspects influencing filler properties, is their origin: the use of natural or synthetic fillers can involve different production devices and final product properties due to their different characteristics[1, 4, 5].

Table 1.1.1: Key properties of some common fillers.

Filler	Chemical formula	Shape	Colour	Density	Mohs hardness
Carbon black	C (83-99%)	spherical	black	1.7-1.9	1
Precipitated silica	SiO_2	spherical	white	2.0	7
Aluminium hydroxide	$Al(OH)_3$	spherical/ platy	white	2.3-2.4	-
Magnesium hydroxide	$Mg(OH)_2$	platy (hexagonal)	white	2.3	-
Calcium carbonate	$CaCO_3$	spherical	white	2.7	3
Magnesium carbonate	$MgCO_3$	irregular	white/ brown	2.9	4
Huntite/ hydromagnesite	$Mg_3Ca(CO_3)_4$ / $MgCO_3.Mg(OH)_2.4H_2O$	irregular	white/ brown	-	-
Talc	$Mg_3(Si_4O_{10})(OH)_2$	platy	grey/ white	2.7	1
Mica	$KM(AlSi_3O_{10})(OH)_2$	platy	white/ brown	2.8-2.9	2-2.5
Kaolin	$Al_2O_3.2SiO_2.2H_2O$	platy	white/ brown	2.6	2.5-3

Synthetic fillers

Synthetic fillers are commonly produced by precipitation and usually synthetic routes are chosen when the desired natural mineral is not available and/or high purity, particular shapes and sizes are required than that obtainable for natural fillers; obviously the cost of the final product is higher due to the necessary raw materials, production routes and final properties.

Among the synthetic fillers carbon black is the most widely used especially for elastomer applications due to its electrical properties and surface capacity of interacting strongly

with elastomer molecules without the use of coupling agent treatments. The main properties required to the carbon black incorporation are colour and electrical conductivity[6].

Synthetic silica can be found as precipitated silica and fumed silica, different for production method, cost and thus application[7]. Precipitated silica is not expensive and it has been used mostly for rubber applications (tyres and footwear), while fumed silica is one of the most expensive fillers because it is produced by controlled combustion of compounds like silicon tetrachloride, so its use is restricted to silicone elastomer materials.

Precipitated calcium carbonate (PCC) is used mostly as "speciality" polymer filler, even if the main use is for paper production. Natural calcium carbonate is usually quite pure so the production of synthetic calcium carbonate is necessary when very fine sizes and narrow PSD are required.

Aluminium trihydroxide (ATH) is obtained by synthetic routes from gibbsite-containing rocks as bauxite. Bayer process is the first to be used and still the most important (about 60% of ATH fire retardant market by volume) for coarse form and fine precipitated grades[8]. The process consists of extraction of gibbsite from bauxite ores, followed by precipitation. The obtained ATH is a coarse form characterized by high particle size (up to 750 μm) and high presence of aggregates[5]. These are milled to produce finer size form of Bayer hydrate (0.25-3 μm of particle size), suitable for polymer application. The production of higher quality ATH products follows similar chemical steps of Bayer process with the use of purer reagents and controlled precipitation conditions in order to obtain directly required particle shape and size, avoiding milling step. It represents one of the principal polymer fillers (650000 tonnes a year): the main applicative uses of ATH are for flame retardant composites based on elastomeric, thermosetting and thermoplastic matrices (90% of the usage) and in solid surface because its composites are characterized by good performance and mostly desirable aesthetic quality.

Magnesium hydroxide can be commercially found as both natural and synthetic filler, but most of the filler grade product is synthetic, despite the high number of natural deposits of brucite in China and in North America. The two main synthetic process are hydropyrolysis and hydrothermal, which both go through a solution stage (magnesium chloride) for purification and then the treatment of purified solution by using different

methods. The main uses of magnesium hydroxide are for pharmaceuticals, water treatment and for conferring flame retardant properties to polymeric materials. Its performances are quite similar to ATH, but the synthetic production processes are significantly more expensive and so it is usually used only when more thermal stable filler is necessary.

Natural fillers

Natural fillers come from natural mineral sources[1, 5], which must be abundant, low cost, colourless, inert and easily convertible in filler with the required particle size. The raw materials are obtained by mining, followed by a variety of processes depending on the desired final properties, such as comminution, purification, classification, calcination, surface treatment and drying. The main problem is that the commercial form of fillers from natural sources may still contain significant quantities of other minerals as well as other constituents, so it must be considered if they can be deleterious for the intended application.

Carbonates, silicates, hydroxides, together with blends of them can be found in natural deposits and they represent most of the mineral fillers used for polymer applications.

Metal carbonates, in particular calcium carbonate, are the most common natural fillers. Ground calcium carbonate (GCC) is widely used in a variety of polymers and the main applications are in PVC, polypropylene, polyethylene, elastomers and unsaturated polyester. Due to the high purity at which it can be found in nature, it is generally very white and its price usually increases with whiteness. Calcite is the most used crystal form of calcium carbonate, with usually isotropic particle structure of the filler. It can be produced from three different mineral sources such as chalk, limestone and marble: the origin influences deeply the final properties of the filler because they are characterized by different hardness and purity.

Natural magnesium carbonate is natural magnesite, which is mostly used for refractory application. It is characterized by very high Mohs hardness (4) and specific gravity (2.9-3) (Table 1.1.1): these are often considered a disadvantage especially because of the high milling costs for production.

Huntite/hydromagnesite is a natural physical blend of magnesium calcium carbonate and magnesium hydroxy-carbonate: the ratios vary between 40 and 30% of huntite and 60-

70% hydromagnesite and specific gravity depends on the ratio. The main deposits are present in Turkey and Greece and the level of impurities is very low[9]. The blend has gained importance for flame retardant properties in polymer application, but it is mostly appreciated for reinforcing effect in rubber compounds due to their lamellar shape form and high surface area of particles.

A large amount of natural fillers are characterized by layered crystal structure, where sheets of different composition are stacked together by Van der Waal's forces. The main are talc, mica and clays (like kaolin), which are widely used especially as reinforcement agents for polymer application due to their general high aspect ratio, high specific surface of particles and the good dispersion can be achieved in compound. In particular in the last decades nanosized layered clays have gained interest: they are composed by silicate stacks, potentially able to separate down in sheets with a thickness on the order of nanometers. The incorporation of such fillers in polymers have been widely studied especially in order to maximize their dispersion in the matrix: it is reported that nanocomposites with good dispersion show improved stiffness, heat distorsion, gas barrier and flame retardancy of polymeric materials only with few percentage incorporated[10].

1.1.1. Natural magnesium hydroxide (Hy), magnesium carbonate (Mf) and calcium carbonate (SM)

The three natural fillers, which could be considered as the "main characters" of this PhD thesis research, are a magnesium hydroxide, magnesium carbonate and calcium carbonate, indicated as **Hy**, **Mf** and **SM** respectively as abbreviations of their commercial names. They are produced by the same industrial process by the italian company Nuova Sima, even if they come from different deposit areas. In fact the main difference among the fillers, in addition to the chemical composition, is their origin: Hy is a natural mineral brucite coming from far East of Asia (most from China), Mf is a natural magnesite coming from Turkey and only SM comes from Italy, taken from a limestone majolica quarry in the area close to the company plant.

The production process is reported in the scheme in Figure 1.1.1.1.

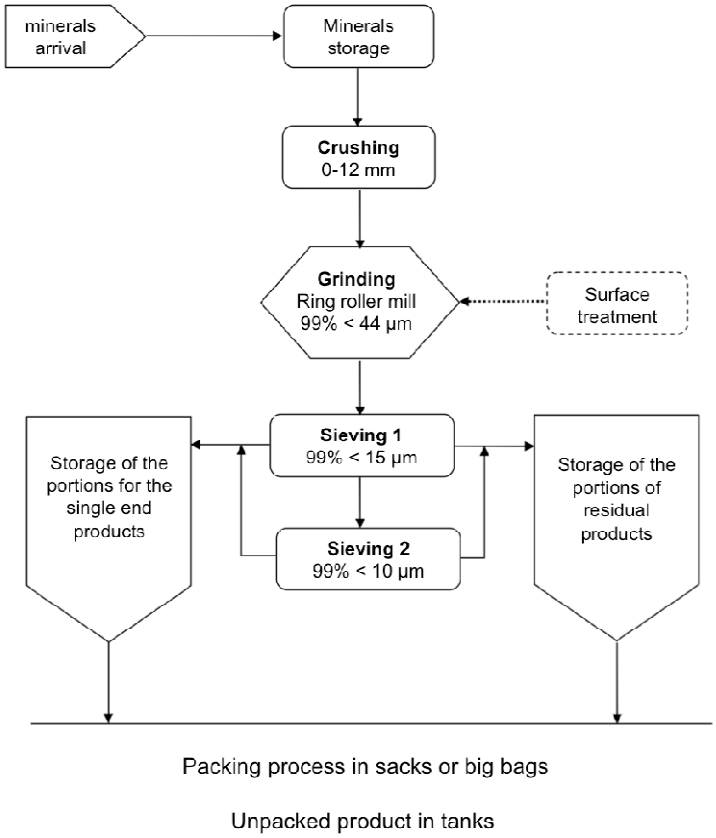

Figure 1.1.1.1: Scheme of the production process of Hy, Mf and SM fillers.

The mineral stones used as raw materials are first crushed down and then ground repeatedly; crushing/grinding step is followed by sieving process, which can be composed by two steps, depending on the desired mesh size of the filler. These steps are the most important for the properties of the final product, because they influence the particle size and its distribution: for each kind of filler it is possible to have different types of product due to the obtainable average particle size and this aspect deeply influences its final application. For example it is possible to find a range of natural magnesium hydroxide products from a D_{50} between 1.5-2 µm, which is the finest and most expensive, to a D_{50} around 15-20 µm. A further optional step in the productive process, mostly used on products for polymer applications, is the treatment of filler surface with organic compounds in order to improve the filler-matrix interfacial adhesion. The common coating applied on these natural fillers is stearic acid especially for magnesium hydroxide and calcium carbonate.

The main applications of these fillers are for varnish industries and plastic materials. Hy and Mf are used for improving flame retardant properties of compounds for electrical cables, roofing, buildings, transport, etc. In particular natural magnesium hydroxide (Hy) has been introduced in patented compositions for low-smoke self-extinguishing cables by Prysmian (former Pirelli Cavi e Sistemi)[11]: the use of some of Hy products (different average particle size and/or surface treatment) is indicated alone or in combination with synthetic magnesium hydroxide in order to guarantee flame retardant performance.

The common matrices for the incorporation of the natural flame retardant fillers are thermoplastic polyolefin materials like polypropylene and polyethylene, together with its copolymers, such as ethylene-vinyl acetate (EVA), ethylene-alkyl acrylate (EMA,EBA and EEA), metallocene copolymer ethylene-octene (mULDPE) and ethylene-propylene (EPR/EPDM). However magnesium hydroxide (Hy) and carbonate (Mf) have been suggested as flame retardant filler suitable also in rubber, thermosetting and PVC compounds: it has been found that Hy and Mf can be used in partial substitution of antimony trioxide (Sb_2O_3), the most popular flame retardant agent in PVC compounds, in order to maintain or improve the final flame retardant properties reducing the smoke toxicity during combustion.

1.2. Polyolefin highly filled composites

Polymeric composite materials are defined as polymers filled with solid particulate or fibrous fillers of organic and inorganic nature. They are heterophasic polymer systems, composed by two or more phases, which can interact each other. Lipatov[12] classified the polymeric composite materials in three main systems according to the types of the components introduced in the polymer matrix:

- polymers filled with particulate or fibrous mineral and organic fillers, such as talc, chalk, carbon black, silica, polymeric powders, etc;
- reinforced polymers with continuous reinforcing inorganic and organic fibers, which are distributed in definite way in the matrix;
- polymer blend of polymeric components which are not thermodynamically compatible and form different phases with definite distribution of the phase separation regions.

The final properties of composites are the result of the composition, structure and influence of single components properties together with the interphase phenomena. This means that introducing filler into a polymeric material cannot be considered only a method of modification of polymer, but it represents the creation of new material with different properties. In particular fillers introduced are chosen in order to obtain materials with improved specific properties, such as mechanical reinforcement, thermal stability and flame retardancy.

As reported in the previous paragraph, filler size and filler structure, together with the level of dispersion, are the main factors affecting the final properties of the composites. Even the amount of filler in the composites influences greatly the properties and it depends on filler characteristics and functionality: filler with very high specific surface area such as nanofiller can give the desired mechanical and gas barrier properties with very low percentage (usually less than 10 wt%) of dispersed filler[10], while for compounds with flame retardant fillers (microsize particles), such as hydroxides, high amounts are necessary for obtaining acceptable level (usually more than 50 wt%)[13].

Polyolefins are among the most interesting polymeric matrices for highly filled composites from the applicative point of view: especially polypropylene and polyethylene (and copolymers) based composites offer a variety of uses in different fields of application (construction, electric and electronic applications, transportation, etc) involving different types of functional filler.

The interactions, which take place in a particulate filled polymer, are particle-particle and particle-matrix interactions. Particle-particle interaction is of great importance in influencing the dispersion of the filler in highly filled composites, even if it is often neglected; this kind of interactions are mainly determined by the size and distribution of the filler particles. Usually more importance is given to particle-matrix interaction as interfacial adhesion between filler and polymeric phase. In fact it is considered the most influent factor responsible for mechanical behaviour of polymer composite. Leong et al.[14] studied the effect of talc, calcium carbonate and kaolin on the mechanical properties of PP composites. The results showed that strength and stiffness of talc/PP composites were higher than the others, while the elongation at break decreased more with increasing talc loading than with calcium carbonate and kaolin. The effects were evaluated in terms of interfacial interactions: as shown in Figure 1.2.1 for talc/PP sample, talc particles are

deeply embedded in the fracture surface, indicating good filler-matrix interaction, while $CaCO_3$ particles interact weakly with the matrix due to the evidence of cavities around filler. In the case of kaolin/PP the mechanical behaviour was mostly influenced by particle-particle interactions, which took to detrimental aggregates formations (circle in Figure 1.2.1 c).

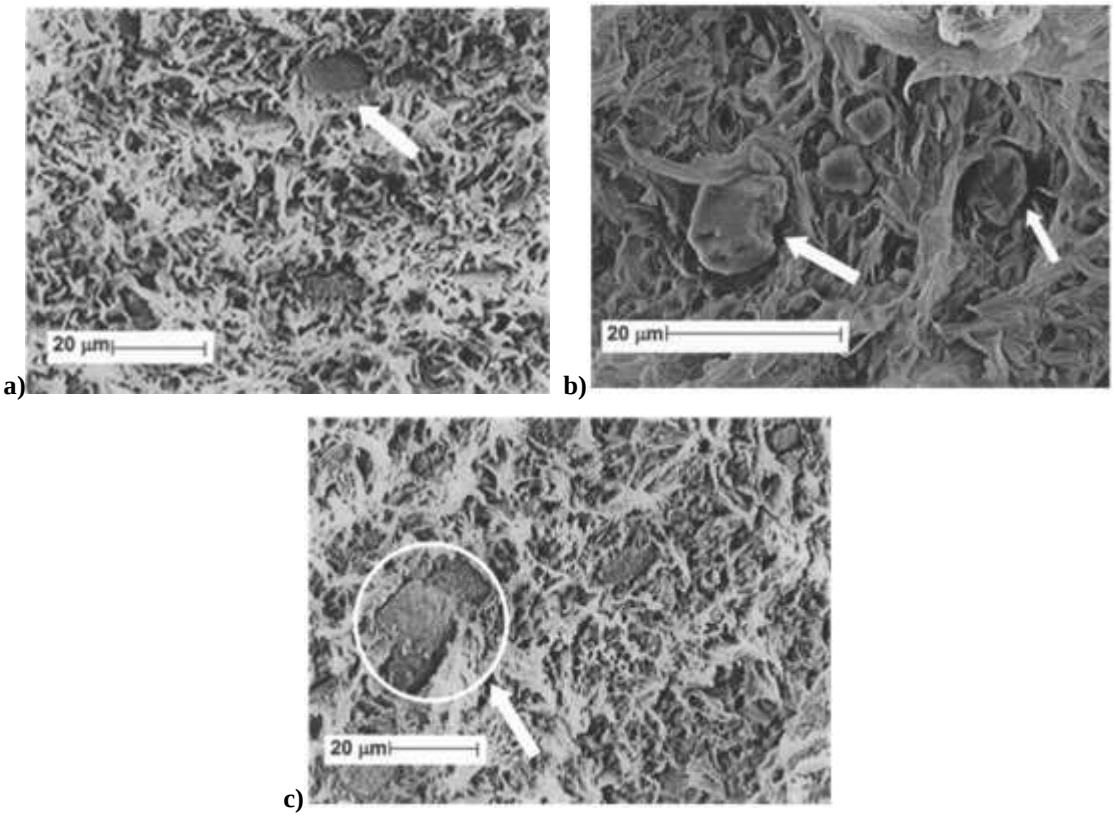

Figure 1.2.1: SEM micrographs of PP composites with 30 wt% of a) talc (filler embedded into the matrix), b) calcium carbonate (weak bonding of the filler to the matrix) and c) kaolin (presence of aggregates).

It is possible to highlight that both the types of interaction depend strongly on the nature of filler and of polymer matrix. The understanding of these interactions is crucial for the final properties of the composites as they can be really problematic: as reported, for example, in the case of carbon black[15], kaolin[14], etc, high particle-particle interactions can create strong aggregates of filler, which are difficult to destroy also at high shear of processing and that are detrimental especially for the mechanical properties of composites.

Filler-matrix interactions can also be determinant for the thermal behaviour of polyolefin composites, as it has been reported by a variety of studies[16-18] mainly on polypropylene composites. Polymer morphology and the structure aspects such as crystallinity, size of

crystallites and spherulites can be changes deeply by the incorporation of filler. This effect is due to the nucleating activity of fillers, which depends on many factors, including surface energy, ion spacing and state of aggregation. The incorporation of high amount of inorganic fillers takes to the strong increase of nucleating sites, which influence the crystallization level and so the internal morphology of the composite. Liauw et al.[19] studied the thermal effect of aluminium hydroxide in PP matrix by using dynamic differential scanning calorimetry: they found that ATH acted as nucleating agent and the effect increased by increasing the amount of filler (from 35 to 70 wt%) due to the higher viscosity induced to the system. The effect has been explained by the orientation of polymer chains in the melt and impingement of the aligned molecules against filler particle surface: higher is the filler content, higher is the stability of the crystalline structure[20].

The addition of rigid particles to polymers influences a number of mechanical effects[21], such as stiffness, stress, modulus, elongation, creep resistance and fracture toughness. Obviously all these parameters are dependent on the properties of the reinforcing particles and in literature it is possible to find a variety of theories and equations developed in order to describe how these parameters affect the macroscopic mechanical behaviour of filled polymers[22]. Polyethylene and polypropylene can be successfully toughened with the introduction of rigid particles, such as calcium carbonate. Fu et al.[23, 24] analysed the dependence of impact toughness of HDPE/$CaCO_3$ on concentration and particle size. They reported that both filler loading and size were really influent on impact strength of composites as shown in Figure 1.2.2 and in particular smaller was the average particle size and higher was the impact strength; furthermore they observed that the incorporation of calcium carbonate with narrow particle size distribution resulted more effective for toughening HDPE. The fine dispersion of $CaCO_3$ particles and the interphase adhesion have been indicated as crucial factors for the improvements of mechanical behaviour of composite.

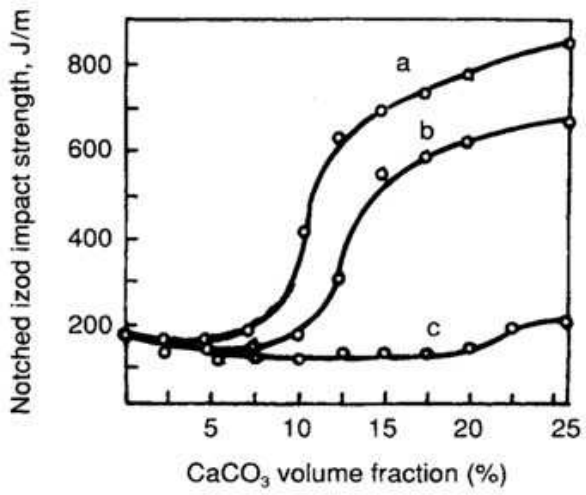

Figure 1.2.2: Impact strength of HDPE/$CaCO_3$ composites as a function of $CaCO_3$ loadings and size. $CaCO_3$ average particle diameter (μm) are a) 6.66; b) 7.44; c) 15.9.

Surface treatment is a common method for changing both particle-particle and particle-matrix interactions especially for polyolefin compounds. It takes to combined modification of composite properties and it is often used for evaluating the presence and the degree of interactions: the starting point is that hydrophilic feature of mineral fillers promotes difficulty to combine with most polyolefin materials, which are usually hydrophobic. The modification of filler surface with low molecular weight organic species contributes in preventing sedimentation and in reducing agglomeration (aid for dispersion), taking to the desired properties, especially for wire and cabling application systems[25]. Four main classes of modification can be recognized[26]:

1. non-reactive treatment by using amphoteric surfactants
2. reactive treatment such as coupling agents, mostly organosilanes;
3. compatibilizers based on functionalized polymers like maleic anhydride grafted polymers (polymer-*g*-MA);
4. encapsulation of filler with elastomers or use of functionalized elastomers during composite processing[27];

Stearic acid is one of the most used non-reactive treatment, especially for calcium carbonate and it has shown great contribute to mechanical properties of highly filled composites. Zuiderduin et al.[28] reported that calcium carbonate particles treated with stearic acid showed a larger increase in impact strength than the untreated in PP composites. They attributed the effect to the improved dispersion due to the lower particle-particle interaction induced by organic coating. Even the tensile properties were

modified and specifically in Figure 1.2.3 the reduction effect of stearic acid treated calcium carbonate on tensile strength of PP composites is reported: higher is the filler surface coverage and lower is the obtained strength.

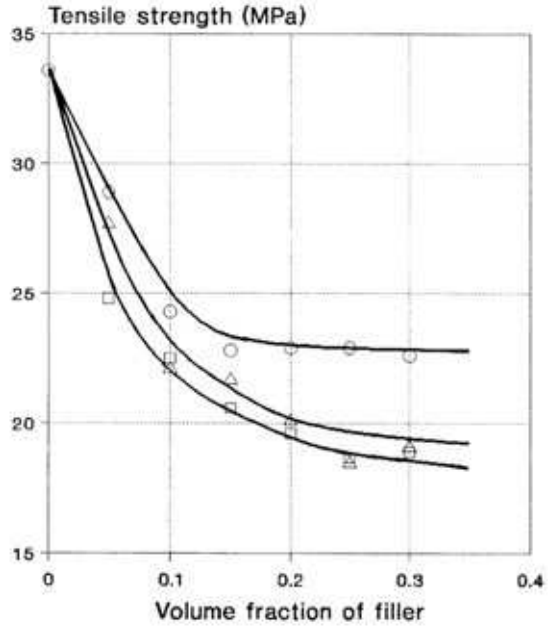

Figure 1.2.3: Effetc of non-reactive surface treatment of a $CaCO_3$ filler with stearic acid on the tensile strength of PP composites (circles: non-treated; triangles: 75% surface coverage; squares: 100% surface coverage).

Polymeric compatibilizers are also widely used for improving interfacial adhesion in composites, especially because they are of great practicalness in industrial compounding. Azizi et al.[29] analysed the effect of PP-*g*-MA on the mechanical properties of PP/$CaCO_3$, PP/talc and their mixture. They point out that the incorporation of compatibilizer took to the increase in tensile strength and in tensile modulus compared to the composites without compatibilizer. Moreover impact strength increased with compatibilizer in both the case of talc and carbonate, due to the better dispersion of the fillers, which allows the impact energy to be more uniformly distributed.

1.2.1. Rheological behaviour of highly filled composites

The study of the rheological properties of highly filled composites is of great importance due to the applicative consequences they have on processing: the rheological phenomena resulting from the high filler contents must be understood for an objective formulation design and process control.

The processability[30] of a material is sure to be altered by the addition of particulate fillers and it is usually measured by melt flow tests, such as Melt Flow Rate tests, which is the most practical and used in the industrial field, torque rheometer and capillary rheometer, which is adequate for characterization of continuous flow in well-defined tubes and it correlates directly with common production process. In the case of concentrated suspensions, another common method for flow properties evaluation is rotational rheometry, used both for continuous rotational flow and dynamic properties.

Highly filled composites are the most difficult systems to study from a rheological point of view and the existing theories remain enable to predict all the complex aspects of rheological properties of concentrated suspensions. Some of the perturbating effects can lead to misinterpretation of rheological data such as wall slip, entrance pressure, fracture, migration, edge effects, etc[31]: for this reason, when it is possible, many studies ignore and/or approximate some of these effects in order to obtain an indicative and faster evaluation of the filler properties influence.

Generally the rheological characterization of composites involves shear viscosity dependence on shear stress and shear rate, elongational viscosity behaviour depending on uniaxial extension and complex dynamic modulus dependence on applied frequency[32]. The introduction of high amount of filler is generally related to increased viscosity and moduli over the whole range of shear rates and frequencies, influencing deeply the factors (temperature, pressure, etc) necessary for processing such materials and thus the cost of production.

The flow behaviour of polymer suspensions containing rigid fillers is also strongly affected by filler properties, including particle size, morphology, surface chemistry and concentration. For this reason it is quite difficult to find general and absolute conclusions about rheological behaviour of composite filled with different types of filler due to the influence they have on the internal structure of the materials. A lot of works deal with the experimental analysis of rheology of highly filled system, but most of them consider "model fillers", which are synthetic and characterized by regular shape and narrow particle size distribution. Most of these studies concern with the use of carbon black[33] and calcium carbonate in elastomers and polyolefin materials (mostly PP and PE), due to their considerable use and diffusion especially for cable and wire production fields.

However in the last decades great interest for other types of fillers, such as nanofillers and flame retardant hydroxides has grown[4].

Kaully et al.[34, 35] analysed the effect of different content of natural calcium carbonate (until 70 wt%) and particle size distributions on the rheological behaviour of PDMS suspensions by using capillary rheometer and oscillatory rotational rheometer. They highlighted, beyond the general tendency of viscosity and shear moduli to increase with increasing filler loading, shear thickening effects at high filler content due to the tendency of structuring of the material; they also indicated particle size distribution as the most influent parameter on flow behaviour among filler properties (increase of PSD led to a decrease in viscosity). Yang et al.[36] studied the effects of particle size and content of PP composites filled with a mixture of magnesium and aluminium hydroxide by using a melt flow rate instrument and varying both load and temperature. They found out that apparent melt viscosity increased roughly linearly with the increase of flame retardant mixture content and that it was affected by particle size. As reported in Figure 1.2.1.1, when the average diameter of particle is smaller than 5 μm, viscosity increases with increasing particle size of fillers, while it reduces with a further increase of particle size at all the considered temperatures. They explained that when particle size exceeded a specific value, the distance among particles increased and consequently the flow resistance of polymer decreased.

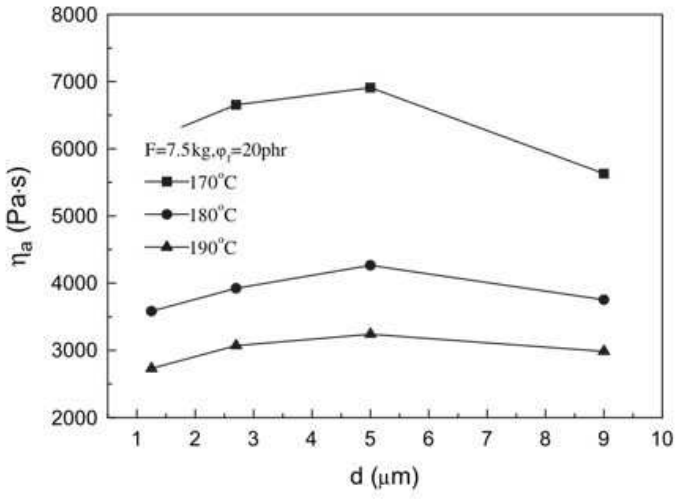

Figure 1.2.1.1: Influence of average particles diameter on viscosity of PP/$Al(OH)_3$/$Mg(OH)_2$ composite.

The considerable increase of melt viscosity with high filler content is mostly related to the hydrodynamic force effects caused by the presence of solid particles within the

system, which hinder the flow of the melt[37]. At high solid concentration the straining motion is concentrated on the small interstitials between particles, which are present in the composite structure. At low shear rates, viscosity can show an additional significant increase, which corresponds to the effect of yield stress. Yield stress is the applied stress necessary to exceed in order to make a structured fluid flowing and it strongly depends on particle-particle interactions forming a strong network: for this reason the presence of yield stress seems to be mainly associated with small particle fillers, that have higher specific surface and thus they can interact more. The yield stress effect is observed as unbounded viscosity at low shear stress for shear viscosity or as low frequency plateau in the dynamic moduli[38].

Generally the determination of shear yield stress comes out from direct measurements at very low shear stresses (frequencies) or by applying the extrapolation of capillary and dynamic viscosity measurements to zero shear rate, even if the latter usually leads to an overstimation of yield values. Osanaiye et al.[39] analysed the rheological properties of EPDM with the introduction of carbon black over a wide range of stresses. At low shear they highlighted the presence of yield stress from the lower concentration used (20%), as shown in Figure 1.2.1.2: it is possible to appreciate the sudden increase of viscosity corresponding only to the elastic deformation of the material.

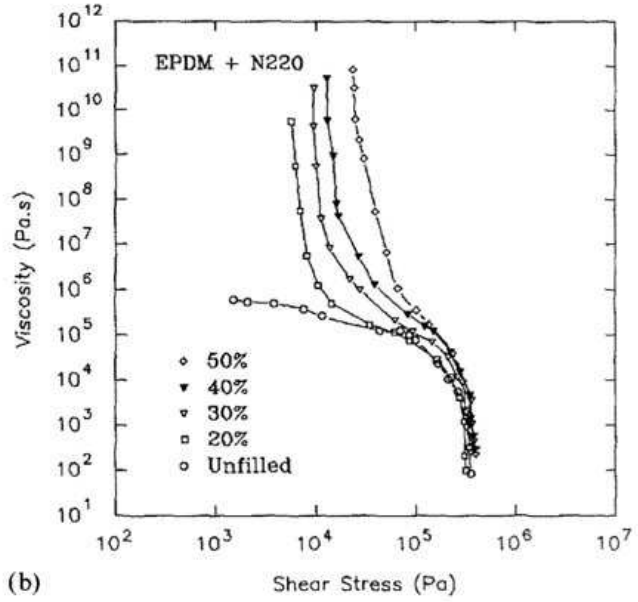

Figure 1.2.1.2: Shear viscosity versus shear stress for pure and filled compounds of EPDM at different filler loadings (at 100°C).

At higher shear rate values, the gel-like structure formed by particle-particle interactions is progressively destroyed and its influence on viscosity can be neglected: melt viscosity of particle filled polymer depends mostly on the already reported hydrodynamic behaviour[40].

Another important factor affecting the rheological properties is the presence of aggregates and/or agglomerates, which have been studied for their structure and their influence[41, 42]. In general for the filled composites, the phenomenon influences deeply the maximum volume loading of filler that the polymer can incorporate, commonly called maximum packing fraction. For equivalent volume fraction, the real packing will be lower for the system with aggregates and so embedded polymer than that without, indicating a lower capacity of the composite of accepting filler. In order to understand this kind of influence, in Figure 1.2.1.3 the reduction of maximum packing fraction as a function of the number of particles forming a spherical aggregate is reported[43]: the higher the number of particles forming a sphere, the lower the maximum packing fraction. The same effect can be achieved if the particle apparent volume fraction becomes higher due to the formation of linked polymer on the filler surface for the presence of strong matrix-filler interactions[40].

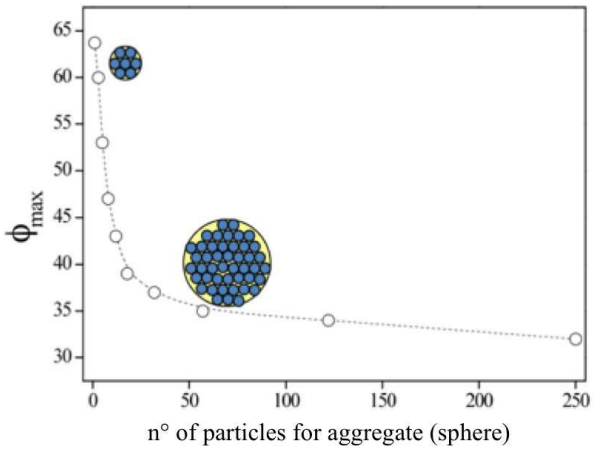

Figure 1.2.1.3: Effect of aggregation on maximum filler concentration.

As reported in the previous paragraph, the most used method for influencing and studying particle-particle and particle-polymer interactions is the surface treatment of fillers: it has a very strong influence on the rheological behaviour of highly filled composites and for this reason, together with the great applicative interest, there is a wide variety of works in literature[37, 44, 45]. The presence of an organic layer as coating on the

particles surface reduces the tendency to agglomeration of particles and the resulting rheological effects are the general reduction of viscosity and of the yield stress effect at lower shear[46].

1.2.1.1. Melt elasticity phenomena in extrusion

Melt elasticity behaviour is an important aspect of polymer processing connected to rheological properties of materials and it is evaluated by analysis of swelling tendency and of surface morphology of extrudated products. The occurrence of swelling and/or surface defects on extrudates over a certain critical shear rate can limit the use of high shear rate, thus indicating a reduced production in many practical polymer process, such as calendering, extrusion, film-blowing, wire coating, etc[47]. Furthermore the analysis of melt elasticity behaviour of polymeric materials is really determinant for the selection of shape-processing parameters and design of extrusion apparatus (screw, head, length-to diameter, etc). These phenomena are more evident in the processing of unfilled polymers (or blends) and in particular those with narrow molecular weight distribution and absence of long-chain branching. In particular, in the 1980s, when LLDPE production and consumption grew, melt fracture phenomena became one of the most important issue in polymer processing, because of its influence on both production rate and product appearance.

When a viscoelastic fluid leaves a die, the extrudate diameter becomes greater than the channel diameter: this is called die-swell phenomenon, extrudate swell or Barus effect, which is usually expressed by the swell ratio (B). Many interpretations on the origin of extrudate swell have been proposed, which take into account normal stress, elastic energy, entropy entanglements, orientation, memory[48]. However they are all related each other considering that in general the relevant stresses and strain of the macromolecules in the melt are produced during extension, shear and compression: when the fluid leaves from the die, if these stresses cannot be completely relaxed, they give origin to elastic deformation of the extrudate (Figure 1.2.1.1.1).

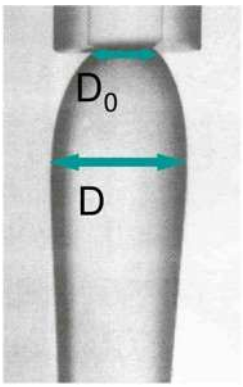

Figure 1.2.1.1: Die swell effect on an extrudate of polymer exiting from a die[49].

The introduction of filler usually decreases the extrudate swell behaviour of polymers. As expected the elasticity of the material decreases with increasing filler concentration, while filler content increases the rigidity of the polymer: these effects imply less mobility of the macromolecular chains under the influence of applied shear stress[50-52].

In case of highly filled composites, the most of the studies can be found in literature are on filled rubber[33, 53, 54] and for polyolefin matrices, PP composites have been widely analysed[55] due to the more evident effect. Liang et al.[56] analysed the die swelling behaviour of PP/$Al(OH)_3$/$Mg(OH)_2$ composites in order to evaluate the influence of condition parameters and filler properties. They found that swell ratio increased by increasing shear stress and by decreasing temperature at fixed concentration, while at fixed stress and T, swell ratio decreased linearly with filler concentration and by reducing particle size of $Al(OH)_3$/$Mg(OH)_2$ mixture.

Surface treatment of filler influences die swelling behaviour as reported by Samsudin et al.[57] on calcium carbonate and talc filled PP: they could evaluate that the presence of stearic acid on particle surface took to improvement in fluidity of composite, dispersion of particles with consequent reduction of die swell of extrudates (Figure 1.2.1.1.2).

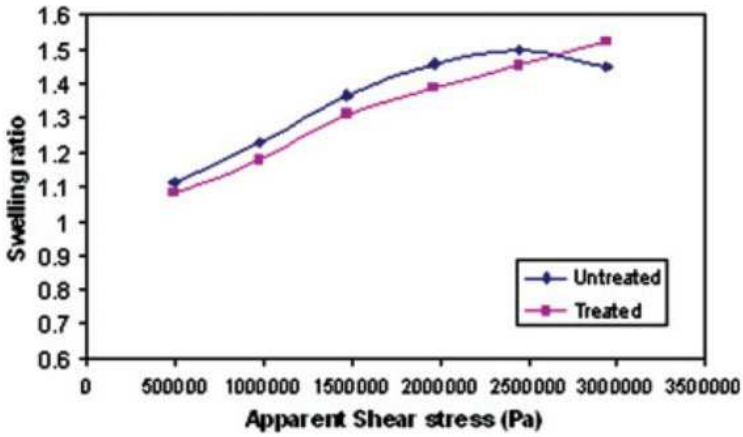

Figure 1.2.1.1.2: Swelling ratio versus shear stress for PP composites filled with 30 wt% of a treated and untreated mixture of talc and $CaCO_3$ (at 180°C).

The distorsion of the extrudate surface is called Melt Fracture and it has a ranging from the simple roughness to helical indentation of the surface. Generally during extrusion through a capillary die the polymer is smooth as it exits the die at sufficiently low rates of extrusion. The first instability that may occur at progressively higher rates is called *sharkskin melt fracture*, characterized by surface roughness. At higher rates there is an increase in oscillating *stick-slip transition*, which takes, at further higher rates, to *gross melt fracture*, characterized by an extremely irregular surface. Many authors have studied these extrusion effect and different theories[58, 59] have been proposed in order to explain the phenomenon: nowadays the most accepted theories associate instability to die exit effects, such as the stick-slip between the polymer melt and the metal die. Inn et al.[60] reported the visual observation of development of sharkskin on the surface of PBD extrudate, observed with a CCD camera focused on the exit of the die in order to study how the surface fracture was originated and to propose a qualitative model. In Figure 1.2.1.1.3 it can be clearly observed the phenomenological effect of fracture: the origin, the growth to a certain size and then the slippage of the ridge, which is immediately followed by another one.

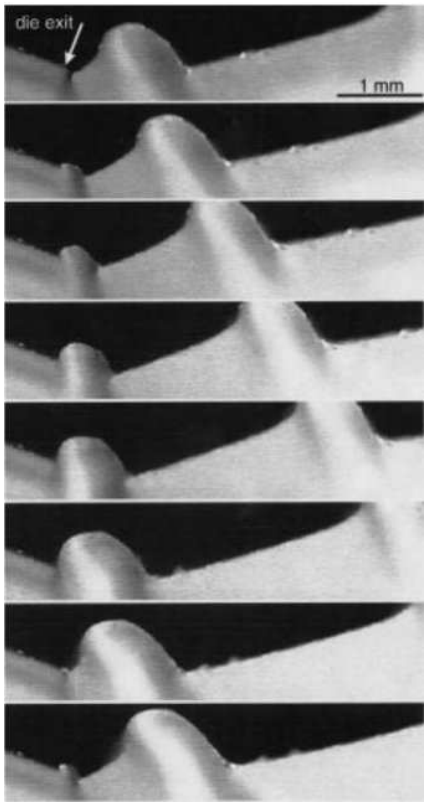

Figure 1.2.1.1.3: Pictures of sharkskin in profile taken every 1 second (at 150 kPa).

The introduction of fillers can improve the aesthetic quality of extrudate, but it does not completely eliminate the surface roughness. The fracture effect obtained for filled materials usually appears different respect to that of pure polymers due to the influence of the filler properties. Rahim et al.[61] studied the effects induced by introduction of high amount of kaolin on flow and melt elasticity behaviour of PP composites. At 30 wt% of filler loading the surface of composite extrudates was quite smooth at lower shear rates, while it became rough and irregular at higher rate of extrusion. They attributed the presence of periodic waviness on surface to the ability of the extrudate to emerge out of the die even at a semisolid state. This was possible for the high pressure applied, which caused the surface effect by following the stick-slip phenomenon.

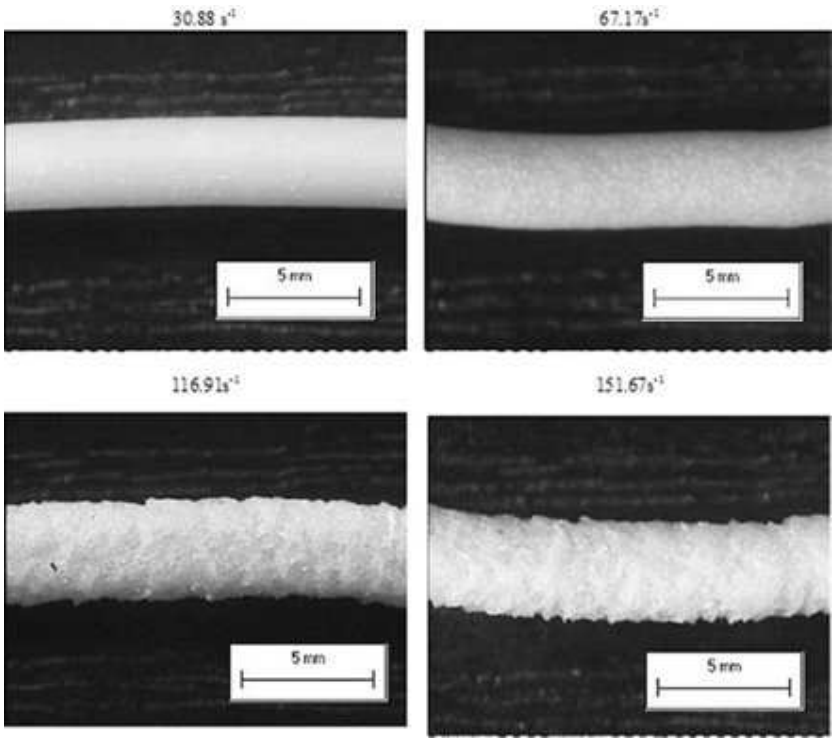

Figure 1.2.1.1.4: Extrudate surface morphologies for PP composite filled with 30 wt% of kaolin at different apparent shear rates.

1.3. Fire retardant fillers for composites

Nowadays the principal fire retardant fillers for composites of industrial application are aluminium hydroxide (ATH), magnesium hydroxide (MDH) and hydromagnesite/huntite mixture (H-U). As for the other composite properties, the relative fire retardant performance depends strongly on the nature of the filler, on its origin, on the chemical characteristics of the filler and of the host polymer, together with the polymer-filler interactions can be achieved. Hornsby[5, 62] reported that the inclusion of magnesium hydroxide in different polymers takes to different performances: in Figure 1.3.1 it is possible to appreciate, for example, that the effect of MDH at 50 wt% in nylon-6 (PA6) is strongly higher than that in polypropylene.

In general the addition to polymers of any particulate non-combustible filler affects the reaction to ignition and combustion due to various effects reported in the first column of Table 1.3.1. However these effects usually are not enough for passing the fire resistance tests, so further and more specific factors are required, as those reported in the second column of Table 1.3.1[1].

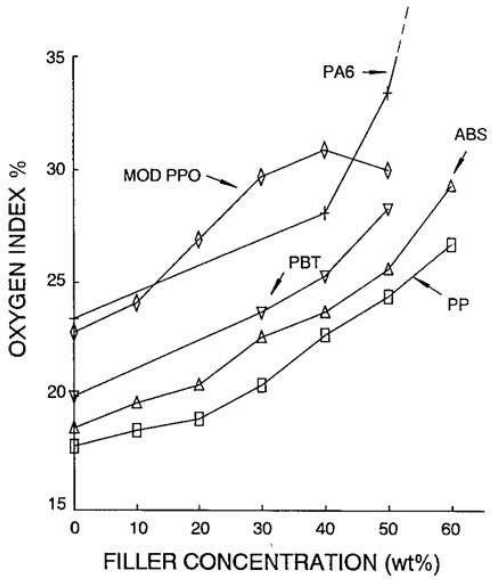

Figure 1.3.1: Influence of magnesium hydroxide loading on oxygen index of selected thermoplastics (PA6: polyamide 6; ABS: acrylonitrile-butadiene-styrene copolymer; MOD PPO: modified polyphenylene oxide; PBT: polybutylene terephthalate; PP: polypropylene).

Table 1.3.1: Resumptive table of the general effects on combustion of fillers and of flame retardant fillers.

General effects of fillers on polymer ignition and combustion:	Additional effects of Flame Retardant fillers:
a) *dilution, reducing the amount of fuel available for combustion;* ***b)*** *change of the heat capacity and thermal conductivity of material;* ***c)*** *thermal effects such as reflectivity and emissivity;* ***d)*** *formation of solid residue;* ***e)*** *slowing down the rate of diffusion of oxygen and pyrolysis products;* ***f)*** *influence on polymer melt rheology (reduction of dripping).*	***a)*** *solid state effects depending the chemistry, surface or shape of the additive (strong charring effect);* ***b)*** *heat adsorption due to endothermic decompositions;* ***c)*** *release of gases, providing a significant dilution and cooling of pyrolysis products, together with insulation of substrate from radiative energy transfer.*

Among the products of decomposition of flame retardant fillers, the main are non-flammable molecules, such as H_2O and CO_2, which dilute combustible gases: the flame requires a critical concentration and temperature of pyrolysis gases to be self-sustaining, so the emission of water or carbon dioxide makes the combustible gases concentration and temperature fall down, taking to flame extinction. In addition the release of water from hydroxides takes to a further absorption of energy as latent heat, than the release of carbon dioxide from carbonates.

Beyond the gaseous products, the decomposition of fillers takes to the formation of oxides: they create a barrier on the surface of the material that avoids the oxygen reaching the fuel, pyrolysis products reaching gas phase and the feedback of the radiant heat, coming from the flame, to decomposing polymer surface. Furthermore the presence of oxides, rather than hydroxides, decreases the heat capacity of the material.

Another effect is the smoke suppression, which is really important because smoke is the main reason of death during real fire due to the obstruction of the escape for the victims. The process is indicated as a consequence of the deposition of carbon residues onto the oxide surface and subsequent oxidation: the formation of carbonaceous residue as carbon oxides does not create the common obscuration effect of the smoke[5].

The decomposition temperature of the fillers must be less than the processing temperature of the composite and it must be around (or before) the polymer decomposition temperature: the suitability of decomposition temperature, together with the energy absorbed by the filler during and after decomposition are important parameters in the choice of the most performing flame retardant filler for a specific polymer. For example calcium carbonate cannot be considered a flame retardant filler: it has a very high decomposition temperature (>750°C), which allow the processing of almost all the polymeric composites, but usually it is too high for acting during polymer decomposition. In Figure 1.3.2 the effect of ATH loading on LOI of PE is compared with that of $CaCO_3$: calcium carbonate gives a small increase of LOI, while ATH shows a much greater effect[1].

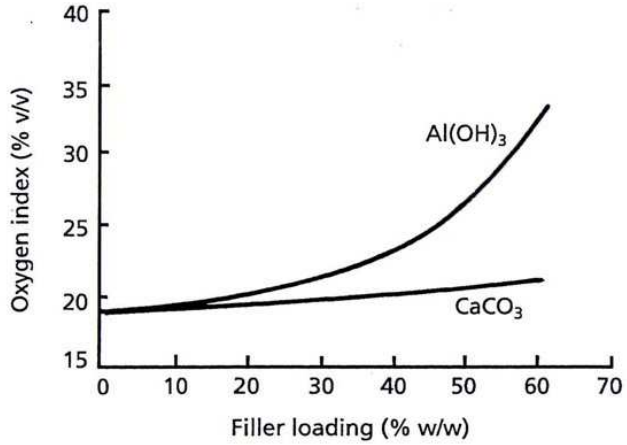

Figure 1.3.2: Comparison between the effect of calcium carbonate and aluminium hydroxide fillers on the oxygen index of a filled polyethylene.

However, despite all the reported effects, if the use of flame retardant fillers is compared with that of other additives, they appear less effective, requiring high level of content (usually more than 50 wt%) in order to achieve acceptable flame retardant properties. This is the main disadvantage of fillers as flame retardant because the high amount required has a strong influence on rheological and mechanical properties of composites (paragraph 1.2).

The decomposition of aluminium trihydroxide occurs between 180 and 200°C and follows the reaction:

$$2Al(OH)_{3\,(s)} \xrightarrow{180\text{-}200°C} Al_2O_{3\,(s)} + 3H_2O_{(g)} \qquad \Delta H = +1.3\ kJ\ g^{-1}$$

with formation of water (39% w/w) and alumina. ATH finds wide application mostly in LDPE and EVA matrix, due to the lower processing temperature than other polymers, like PP, and due to the similar decomposition temperature of polymer and filler.

Magnesium dihydroxide follows the same decomposition reaction of ATH, but it occurs at higher temperature and with lower water release (31% w/w):

$$Mg(OH)_{2\,(s)} \xrightarrow{300\text{-}320°C} MgO_{(s)} + H_2O_{(g)} \qquad \Delta H = +1.45\ kJ\ g^{-1}$$

It starts decomposing at around 300°C, so it can be incorporated in polymer matrix, which needs high temperature to be processed. Some of the main examples of used matrices are polypropylene, polyamides such as nylon-6 and nylon-6,6[63] , polyethylene[64] and its copolymer, especially ethylene vinyl acetate where magnesium hydroxide shows a special synergistic effect expressed by high LOI values[65]. Comparing the efficiency of MDH and ATH in polyethylene at equivalent filler loading, they take almost to the same LOI result, while when they are dispersed in EVA (30 wt% of vinyl acetate content) MDH is more effective in LOI than ATH, taking to a value of 46% compared with that of 37% of EVA/ATH[66].

One of the problems of aluminium and magnesium hydroxide use (especially MDH) is the catalytic effect they have on the combustion of carbonized residues. This was reported as solid state afterglow effect due to oxidation of carbonaceous residues, that can explain the incandescence phenomena visible during flame retardant tests[67]. This highly exothermic phenomenon represents a potential risk because it may reignite the polymer some time after the extinction of the flame.

The influence of physical properties of the fillers on flame retardant behaviour of the composites has been reported for ATH and MDH, even if the effects are less evident than those on rheological and mechanical properties[2]. In particular the particle size and morphology of filler can influence the thermal stability of hydroxides, with the consequence of flame retardant effects: usually smaller is the particle size, higher is the thermal stability and better are the flame retardant properties. Fine grades ATH has been indicated as more thermal stable than the coarse grade and with higher limiting oxygen index when dispersed in PMMA[68] (Figure 1.3.3). Magnesium hydroxide particle size has been reported to influence flame retardancy of EVA composites: despite the effect is not linear, Huang et al.[69] suggested to use, at 55 wt% of filling level, MDH with smaller size due to the better dispersion can be achieved, which assures better FR performance.

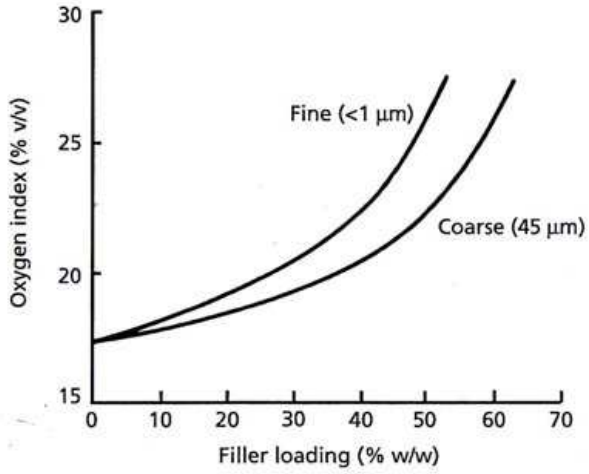

Figure 1.3.3: Effect of filler particle size on the oxygen index of PMMA filled with aluminium hydroxide.

Natural mixture of hydromagnesite-huntite and the synthetic hydromagnesite[70] are quite recent flame retardant fillers, introduced as possible alternative to ATH and MDH and they have found wide industrial interest as they offer good cost/performance ratio[9] . The use of the natural mixture has been reported for many polymeric materials, giving good flame retardant effect mostly in polypropylene, polyethylene, EVA, where it gives a LOI value of 35-36%[71]. Atay and Celik[9] studied the flame retardant behaviour of Turkish huntite/hydromagnesite mineral in EVA, pointing out that the mixture was somewhat more effective than ATH by LOI results and that particle features were influent also in the case of the mineral mixture: as reported in Figure 1.3.4, the flame retardancy of the composite, expressed by LOI, increases with decreasing the size of filler particles.

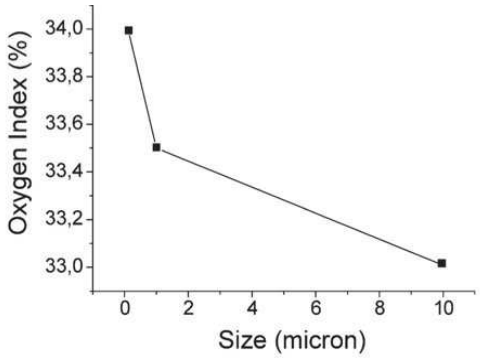

Figure 1.3.4: Oxygen index as a function of particle size for huntite/hydromagnesite reinforced plastic composite materials.

1.3.1. Halogen Free flame retardant additives in combination with inorganic fillers

Researches dealing with the development of synergistic agents for metal hydroxides have become the main topic of numerous papers in the last years[72] due to the necessity of decreasing the total amount of filler in composites.

Usually synergy is associated with the idea that the whole is greater than the sum of its parts. In the field of fire retardancy, combination of additives, which can show synergistic effects, are required in order to improve the performance of materials or, especially in the case of fillers, in order to decrease the loading of FR components, maintaining the performance[73]. For the toxicological and environmental concerns, the latest research trends are mostly focused on the development of Halogen Free flame retardant systems (HFFR), where no additives containing halogen are introduced.

The combination of different kinds of fillers have shown improved effects as fire retardancy. Aluminium and magnesium hydroxide when used together can give improved properties mainly due to the increased range of temperature for endothermic reaction of dehydration. Haurie et al.[70] studied the effect of mixing a synthetic hydromagnesite, compared to magnesium hydroxide and mineral hydromagnesite-huntite, with aluminium hydroxide in LDPE/EVA blends; it was pointed out that the use of hydromagnesite in combination with ATH could take to the highest LOI value, time to ignition (TTI) and Flame Performance Index (FPI). They also studied the effects of incorporation of montmorillonite in the system[74], which led to reduction of peak of heat release (pkRHR), increase of TTI and to higher residue stability as reported in Figure

1.3.1.1: the introduction of nanofillers has seen to take to a foamed structure with limited expansion and better residue cohesion during combustion.

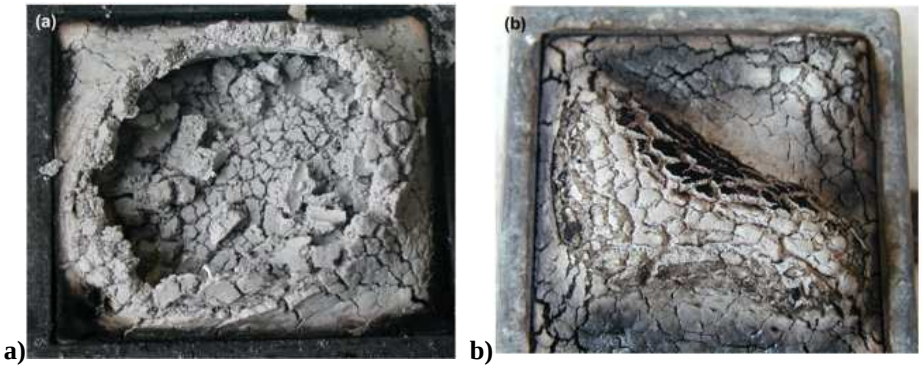

Figure 1.3.1.1: Pictures of LDPE/EVA filled samples after cone calorimeter test: a) Hydromagnesite/ATH (30/30); b) Hydromagnesite/ATH/Montmorillonite (15/30/5).

Many other studies deal with the use of nanofillers as synergistic additives in combination with fillers (especially hydroxides) due to their physical effect in the condensed phase[75]: the reinforcement of the surface structure, with the formation of strong and protective layer, leads to the inhibition of the heat and mass transfer and so to better fire retardant performance. Boron and silicon containing compounds are other common additives, which can improve the surface structure in combination with hydroxides.

Boron containing additives are smoke suppressant, afterglow suppressant (due to the B_2O_3 moiety), anti-arcing agent and char forming[76]: there are various compounds, such as zinc or calcium borates, boric acid and relative esters, etc, but the most frequently used as commercial products are zinc borates. In particular in HFFR systems zinc borates have been used in combination with ATH or MDH in EVA[77], where they showed improvements on LOI value (Figure 1.3.1.2) with a maximum at 5 wt% in the composition (with total amount of filler of 60 wt% for MDH and 65 wt% for ATH); they also caused the delay in TTI, a significant reduction of peak of HRR and delay of the second pkRHR, together with the formation of a stronger char on the surface (glassy protective layer), which can avoid that volatile gases reach the combustion zone. The increased physical rigidity of the protective layer on the surface of the sample during combustion was confirmed even by rheological studies at high temperature[78].

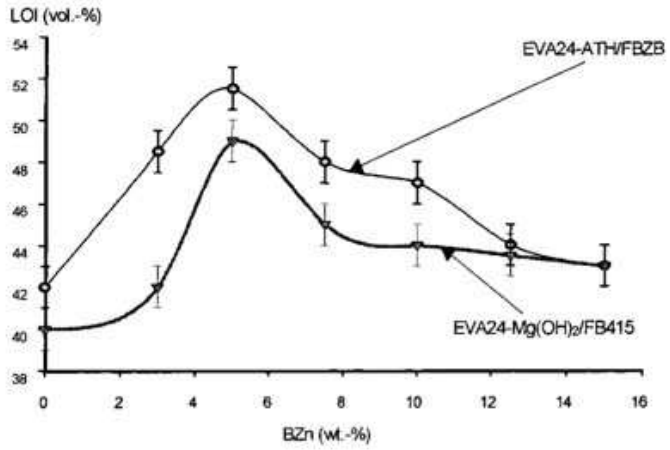

Figure 1.3.1.2: LOI values versus the amount of zinc borates (FBZB and FB415) in substitution of aluminium (ATH) and magnesium ($Mg(OH)_2$) hydroxides filled EVA composites (total loading constant).

It has been reported by different studies that zinc borate and metal hydroxide interaction can be further enhanced by using co-additives such as silicone[79], melamime phosphate, red phosphorus[80], talc[81], silica, kaolin and nanoclays.

The combination of fillers with various formulations of silicon containing compounds have been widely used to achieve the required flame retardant efficiency in a variety of polymers including polyolefins. Among the most common silicon-based fire retardants it is possible to find organic silicon compounds, such as polyorganisiloxane, silane, POSS, borosiloxane[82], etc and inorganic silicon compounds, such as fumed silica and silicate minerals[83]. The organic compounds used in combination with metal hydroxide can be non-reactive, usually those with high molecular weight and higher stability, and reactive, such as alkoxy silanes used as surface coatings for hydroxides and mineral fillers, silanes grafted on polymeric systems and silanes used as coupling agent, which promote flame retardancy by modifying rheology of the system[84]. Huang et al.[85] compared the use of different silicon additives in EVA/MDH composites and they found that silicon rubber took to better results on LOI and horizontal fire rating in respect to silicon powder, silica and different clays (MMT, attapulgite, etc); the beneficial effects of silicon rubber, silicon powder and organic MMT was pointed out also in cone calorimeter test by the increase of TTI and decrease of pkRHR (Figure 1.3.1.3).

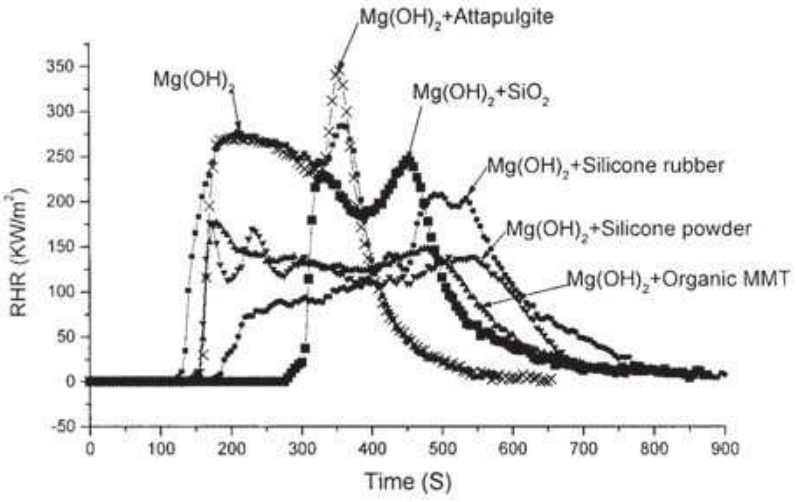

Figure 1.3.1.3: Rate of Heat Released (RHR) versus time for EVA composites filled with magnesium hydroxide in combination with different silicon compounds.

Other important classes of synergistic additives studied in combination with fillers are phosphorus and/ or nitrogen containing, but also transition metal oxides (nickel oxide, zinc oxide, etc) and organic compounds, such as novolak, polyaromatic phenols, etc.

Among the nitrogen and phosphorus additives the most frequently encountered are the commercially available such as melamine (and its thermally more stable salts, like melamine cyanurate, phosphate, borate, etc), ammonium polyphosphate (APP), red phosphorous and other phosphorated compounds.

Zilberman et al.[86] reported that the use of melamine in combination with ATH in EVA could impart flame retardant effects due to the increase of TTI, the slight smoke suppression and CO reduction, even if it caused higher rate of heat release during combustion. They also studied the effect of partial substitution of ATH with ammonium polyphosphate, finding out that APP took to a noticeable reduction of HRR presumably due to the formation of aluminophosphates from the reaction of alumina and APP, which formed a cohesive protective intumescent char.

Red phosphorus is considered a very good flame retardant especially in polymers that contain hydroxyl groups, but it shows also a slow flame retardant effect in polymers like polyethylene and EVA. Its action is reported in both gas and condensed phase and it is claimed as good synergist for hydrate fillers[87], where it contributes by enhancing charring of the polymer surface. Burns et al.[88] studied the effect on LOI of red phosphorus in combination with magnesium and aluminium hydroxide in polymers and blends, such as EVA, PVB, LDPE and EVOH: specifically for EVA, they found that in

the absence of hydrated fillers, the addition of up to 5 wt% of red phosphorus did not improve limiting oxygen index, while, in combination with magnesium hydroxide, even a small amount of red phosphorus (3 wt%) caused a significant increase in LOI.

1.4. Objectives of the work

In the previous paragraphs of this chapter it has been extensively explained how the incorporation of fillers can modify polymer properties and how the effects can be enhanced and/or changed in highly filled composites due to the large amount of filler. In particular it has been underlined that the macroscopic effects depend on the specific filler and polymer properties, which can influence particle-particle and particle-polymer interactions.

As already reported in the paragraph 1.1.1, the "main characters" of this PhD thesis are three natural fillers: magnesium hydroxide, magnesium carbonate and calcium carbonate, indicated respectively as Hy, Mf and SM. The study of the influence of the natural fillers on the properties of polyolefin highly filled composites is the aim of this research. Particular attention will be given to Hy due to the widespread application of magnesium hydroxide as flame retardant additive: the incorporation of high amount of Hy as alternative flame retardant filler to synthetic magnesium hydroxide in composites highlights some positive and negative aspects on rheological, mechanical, thermal degradation and flame retardant behaviour of composites that will be analysed. The polyolefin matrix chosen for the composites preparation is poly(ethylene-co-vinyl acetate) (EVA), which is widely used especially for cable and wire application.

In particular the first part of the PhD thesis will be devoted to the study of how the main filler characteristics can positively or negatively affect rheological, mechanical and thermal properties of EVA composite. In order to highlight the most important effects and influent filler properties, a comparative study will be carried out on the use of the three natural fillers Hy, Mf and SM and the synthetic magnesium (H5) and aluminium hydroxide (ATH), which are the reference fillers commonly used for application of highly filled composites. The selected fillers will be analysed in order to compare their physical and chemical properties.

The rheological behaviour of EVA composites will be studied in order to point out the main effects of filler concentration and properties on composite processing. In particular a theoretical approach will be applied to the results of the rheological characterization as an attempt of rationalizing the filler properties influence on rheological behaviour of composite. Moreover great attention will be given to melt elasticity properties, in the

form of swelling behaviour and surface roughness of extrudates, in order to evaluate how the filler characteristics can modify these polymer phenomena.

The mechanical properties of composites will be analysed due to the predictable strong effect of the different properties of fillers on modulus, yield strength and elongation behaviour.

The evaluation of filler properties effects will be carried out also on the thermal properties of the composites and specifically the thermal degradation behaviour of pure EVA will be compared with the degradation behaviour of the composites, in order to point out differences induced by filler presence.

The second part of the PhD thesis will be focused on the study of the flame retardant properties of EVA composite filled with the natural magnesium hydroxide Hy. Due to the high amount of hydroxide necessary to obtain acceptable flame retardant performance of the material, the combination of other additives with Hy will be performed in order to improve or maintain the flame retardancy of the composites reducing the total amount of filler incorporated. Specifically the determination of a method for screening a variety of flame retardant additives, parameterize the flame retardant behaviour of formulations in vertical burning test and so evaluate the performance of different combinations of additives with Hy will be carried out.

Subsequently particular attention will be focused on a specific formulation of flame retardant additives combination. In this case, one silicon and one boron containing additives have been selected and the flame retardant properties of the quaternary system, which they form together with Hy and EVA matrix, will be studied by means of chemometric approach. The analysis of a variety of flame retardant parameters coming from different tests will be performed in order to rationalize, by determining valid models and performing analysis of the responses, the behaviour of the flame retardant system, together with the effects of the components, and so tailor formulations with the desired performance (high applicative interest). The indications, which will emerge from the mathematical models, will be correlated to the phenomenological aspects (charring behaviour, thermal properties, etc) of the system in order to find physical validations of the statistical results.

2. Experimental part

2.1. Materials

Polymers

- Poly(ethylene-*co*-vinyl acetate) (EVA): cable grade Escorene Ultra UL00328, ExxonMobil Chemical. (Vinyl Acetate: 27.5 wt%; Melt Index 3 g/10 min @190°C, 2.16 kg; Density: 0.951 g/cm^3; Melting point: 71°C).

- Ultra low density poly(ethylene) with grafted maleic anhydride (ULDPE-g-MAH): Compoline COUL-MH, Auserpolimeri. (Grafting: 0.5-1 wt%; Melt Index 1 g/10 min @190°C, 2.16 kg; Density: <0.88 g/cm^3).

Fillers

- Magnesium hydroxide: (Hy) Hydrofy G2.5, Nuova Sima;
  (H5) Magnifin H-5 , Martinswerk Albermarle.
- Aluminium hydroxide: (ATH) Martinal OL-104, Martinswerk Albermarle.
- Magnesium carbonate: (Mf) Magfy, Nuova Sima.
- Calcium carbonate: (SM) Microcarb SM, Nuova Sima.

Property	**Hydrofy G2.5**	**Magnifin H-5**	**Martinal OL-104**	**Magfy**	**Microcarb SM**
Principal component	$Mg(OH)_2$	$Mg(OH)_2$	$Al(OH)_3$	$MgCO_3$	$CaCO_3$
Origin	natural	synthetic	synthetic	natural	natural
Indicative purity (%)	>90%	≈99.8%	≈99.4%	>90%	>95%

Additives

- Poly(dimethylsiloxane) (PDMS): UHMW siloxane polymer (65%) and fumed silica, Genioplast Pellet S, Wacker Chemie.
- Zinc borate (ZB): Zinborel, Società Chimica Larderello.

- Calcium borate (CaB): hydrated borate mineral, Portabor A13, Ankerpoort NV.
- Boric Acid (BA): technical grade, Società Chimica Larderello.
- Tributyl borate (Tbb): purity 98%, Aldrich.
- Triphenyl phosphite (Tpp): purity 99%, Acros Organics.
- Red phosphorous (RP): masterbatch of microencapsuleted red phosphorus (70%), Masteret 40470, Italmatch Chemicals.
- Melamine cyanurate (MC): Plastisan S, 3V Sigma.
- Poly[(6-(4-morpholinyl)-1,3,5-triazine-2,4-diyl)-1,4-piperazinediyl (PPMt): PPM-Triazine, Jurgen Schmidt.

2.2. Instruments and methods

Filler properties analyses (tap density, particle size distribution and specific surface), polymer compounding and pressing processes, mechanical analysis and most of the fire tests (Limiting Oxygen Index, DIN 4102 B2 test and cone calorimeter) have been carried out at Nuova Sima S.r.l. laboratory. The rheological properties, together with most of the melt elasticity analyses of extrudates, and the thermogravimetric analyses have been carried out at Mixer S.p.A. laboratory.

Tap density

Tap density (or *apparent density*) was determined by putting the filler in a 250 ml measuring cylinder (volume of 150 ml). The weight of the sample was recorded and the cylinder was tapped by an automatic *forcer down* for 1500 times. The tap density (d_{tap}) was given by the ratio of the weight and the occupied volume at the end of the measurement. Free volume (X_v) could also be calculated based on tap density and real density of the filler (d_{real}) using the following equation:

$$X_v = 1 - (d_{tap} / d_{real})$$

Particle size distribution

The particle size distribution of the fillers (PSD) was determined using a Micromeritics Sedigraph 5100 instrument. The method of analysis is based on the sedimentation theory (Stokes law), which correlates particle size to the sedimentation rate in a viscous

medium. The sample was prepared as a suspension of the filler (the amount depends on the type of filler) in water solution of sodium hexametaphosphate (0.5 wt%). The concentration determination of particles in the suspension during analysis is based on transmittance (X-rays).

Specific surface

The specific surface measurements were carried out by using a Micromeritics Flowsorb II 2300 instrument. The analysis follows the B.E.T. method: the total surface area of the filler was calculated based on the amount of gas, which is necessary to cover the particles with a monomolecular layer. The used gaseous flow was a mixture of 30% nitrogen and 70% helium. The filler was degassed before the measurement and cooled by liquid nitrogen to allow gas adsorption.

Polymer compounding

All the composites were melt mixed via twin-roll mill (Vi_Mach) at the constant temperature of 140°C for 15 min. At first the polymer matrix was melted for 1 minute and then the fillers and the flame retardant additives were added as a mixture.
Before mixing the fillers were heated at 100°C for 8 h in order to get them dried.

The specimens for each kind of measurement were hot-pressed (Vi_Mach) under 150 bar for 5 min at 150°C using suitable steel masks.

Rheological and swelling behaviour analyses

The shear viscosity of EVA and the filled compounds was determined using capillary rheometer (Gottfert Rheograph 2002). A round hole die of length-to-diameter ratio (L/D) of 30 with a die diameter of 1 mm and entrance angle of 180°, was used. Compounded samples were cut into suitable size pellets, they were loaded into the cylinder and preheated for 4 min. The flow properties of specimens were measured over a range of apparent shear rates of 18-2304 s^{-1} and over a temperature range of 110-150°C. The rheological data were calculated directly on the rheometer.
The shear stress and apparent shear rate are expressed as:

$$\tau = \frac{RP}{2L} \qquad \gamma_{app} = \frac{4Q}{\pi R^3}$$

where R is the die radius; P is the pressure difference; L is the die length and Q is the flow rate.

The apparent shear viscosity is given by the relation as follows:

$$\eta = \frac{\tau}{\gamma_{app}}$$

where η is the viscosity; τ is the shear stress and γ_{app} is the shear rate.

The Rabinowitsch correction was applied in order to obtain the real shear rate. The relation is as follows:

$$\gamma = \left(\frac{3n'+1}{4n'}\right)\gamma_{app}$$

where n' is the flow behaviour index, determined as the slope of the plot of log τ versus log γ_{app} and it is computed by application of regression analysis.

Entrance pressure losses were negligible for such a long capillary die and no Bagley correction was applied.

Extrudate swell was indicated by Swell ratio (B) and it was calculated as the ratio of diameter of extrudate to that of capillary, using the following expression:

$$B = \frac{D_e}{D_c}$$

where D_e is the extrudate diameter and D_c is the capillary diameter.

The extrudates were carefully collected as they came out from the die. The diameter was measured at five places using a micrometer that avoids any deformation of the surface morphology.

Dynamic mechanical measurements were performed at 150°C using a rotational rheometer (Rheometrics RMS800) equipped with the parallel plate geometry (gaps ranging from 0.8 to 1.1 mm). The samples were compression-moulded at 150°C and recovered as 25 mm diameter disks. Frequency sweep tests were performed in the range 0.1-100 rad/s under a N_2 atmosphere using strain values low enough to keep the measurements within the linear viscoelastic region (strain around 5%). The temperature

was stable within 0.2°C over the range used in this study. The analysis has been supplied by the rheology laboratory of Polimeri Europa S.p.A. (Mantova).

Mechanical analysis

The tensile properties were determined by using a Galdabini Sun 500 dynamometer at a crosshead speed of 250 mm/min. The width and thickness of the tensile test specimens were respectively 6 and 1-1,2 mm, and the stretched length was 40 mm. Five samples for each test were usually analysed in order to obtain reproducible results and determine average values. Young's modulus was calculated as the slope at the beginning of the stress/strain curve by using the software interfaced with the instrument.

Morphological analysis

The particle morphology of the fillers was evaluated using scanning electron microscopy (SEM). The analyses were carried out using a Jeol JSM microscope T-300 model supplied by the Laboratories of Metals Science at Engineering department (Università di Pisa). They also provided the chemical characterization of the fillers by energy-dispersive X ray spectroscopy analytical technique (EDS).

The micrographs, reported in Figure 3.1.2.1.3, have been supplied by the Chemical Institute of University of Campinas, Brazil.

The surface characteristics of the extrudates were observed by using optical microscope and SEM analyses were performed in order to point out morphological properties.

The optical microscope is a ZEISS STEMI 1000 model and pictures were captured by using a HP Photosmart E337 model (5 megapixel) camera.

For the SEM analysis of morphological properties along the cross section, cryogenic fracture was used, obtained by fracture of composites under liquid nitrogen.

Thermal degradation analysis

Thermogravimetric analyses were carried out using a TGA Pyris 6, Perkin Elmer, coupled with an infrared spectrometer Spectrum 100, Perkin Elmer by a balance flow transfer line BFHTL - TG6 TL8000, Perkin Elmer. Samples of 10-15 mg were placed in Al_2O_3 crucibles and the runs carried out in high purity N_2, flowing at 70 cm^3/min. The used heating rates were 10 and 20°C/min over the range 50-1000°C. The gas flow was

transferred to the FTIR gas analysis cell through the transfer tube. The transfer line was kept constant at 270°C and the cell at 250°C.

The IR-spectrometer was equipped with a DTGS KBr detector, which operates with an optical resolution of 4 cm^{-1}. FTIR spectra were recorded over the wavenumber range of 4000-400 cm^{-1}.

The TG analysis reported in Figure 3.2.3.2.6 and 3.2.3.2.9 have been carried out at Silma S.r.l. laboratory by using a Mettler Toledo (TGA/DSC 1 model) almost at the same experimental conditions.

Fire tests

The fire tests used for all the investigated formulations are Limiting Oxygen Index (LOI), vertical burning tests and Cone Calorimeter test.

- *Limiting Oxygen Index* (ASTM D2863): the instrument used is a ATS-FAAR Critical Oxygen Index apparatus. A burner flame was applied on the top of a vertically oriented bar, which was in a test column with a mixture of oxygen and nitrogen flow. LOI value represents the minimum concentration of oxygen (%) in the gas mixture necessary to support the combustion of the material, which was initially at room temperature. Initial concentration of oxygen is chosen arbitrarily. The used specimens were cut by bar shaped hollow die punch with dimension of $125 \times 6.5 \times 3$ mm.

- *DIN 4102 B2 test*: the measurements were carried out on samples with dimension of 190×100×1.5 mm, with a graduation line at 150 mm. The specimen was fixed at a specimen holder and a Bunsen burner flame was applied at the bottom of the sample for 15 seconds. The time necessary for the top of the flame to reach the graduation line was recorded (t_a). The burning droplets were observed by means of a paper under the specimen. According to the standards, a material can be classified as B2 if the flame reaches the graduation line before 20 seconds, if the paper doesn't ignite and the droplets are not burning for more than 2 seconds. A specially modified set up of this test was used for determination of characteristic

burning time parameters and for evaluation of the physical stability of the materials during combustion (dripping, unstable residue, stable residue).

- *UL94-V test*: flammability measurements were carried out by using AMSE equipment. The gas flux of the burner was regulated by a pressure controller. The flame was calibrated by using a thermocouple (temperature increases from 100 to 700°C in 44±2 seconds). The samples with dimensions of 125×12.5×1.6 mm were exposed to a Bunsen flame for 10 seconds. In the case of self-extinguishing behaviour, the flame was applied for further 10 seconds. Five replicates for each sample were tested. According to the standards for vertical rating, if none of the samples burns for more than 10 seconds and the drops do not ignite the cotton, the material is classified as V-0. If none of the samples burns for more than 30 seconds and the drops do not ignite the cotton, the material is classified as V-1. If the cotton gets ignited and burning stops before 30 seconds, the material is classified as V-2. The vertical type of the test has been performed in order to measure the time necessary for the specimen to burn completely or to self-extinguish considering the first flame application. The considered parameter was the calculated average burn rate (cm/min).

- *Cone calorimeter test*: the main instrument used is a Stanton Redcroft Cone Calorimeter (Polymer Laboratories), based on the principle of oxygen consumption. The principle states that the heat released during combustion of a burning specimen is proportional to the total amount of oxygen consumed during combustion, considering the heat of combustion for a broad range of materials basically constant (average value of 13.1 MJ/kg). For some tests, a Fire Testing Technology (FTT) Mass Loss Calorimeter (at the Department of Organic Chemistry and Technology Department of Budapest University of Technology and Economics) was used: the equipment was similar to the used oxygen consumption cone calorimeter. In the mass loss calorimeter, the heat release is calculated based on the temperature of smoke measured by a thermopile in the flue, which is calibrated by burning methane with known gas flow rates. In the case of both the instruments, during the measurement, the samples got ignited and

mass reduction was continuously recorded during burning. The specimen (100×100×3 mm) fixed in an aluminium tray was exposed to an external heat flux of 50kW/m^2 during the whole test. The heating element was a radiant electrical heater with the shape of a truncated cone. An electric intermittent spark located above the sample was used to start the ignition on the pyrolysis gaseous products. In the case of cone calorimeter, a stainless steel grid placed on the test sample was used to restrict deformation and to retain constant distance between sample surface and cone resistance. The collected data were the time to ignition (TTI), the peak of rate of heat release (pkRHR), the time at which there was the peak of rate of heat release (pkRHR$_{time}$), the average effective heat of combustion (avEHC), the average rate of heat release in the first 180 seconds after ignition (avRHR$_{180}$), the total heat release (THR), the peak of smoke temperature (Tsmoke) and the time at which there was the peak of smoke temperature (Tsmoke$_{time}$).

Statistical analyses

The statistical analysis for the screening method (Multivariate Linear Regression, MLR, and Variable Importance in Projection, VIP) and for the chosen D-optimal mixture design were performed respectively by PLS Toolbox (Eigenvectors Research Inc) and by Design Expert (Stat-Ease-Corp., Minneapolis MN 55413-9827 USA). The statistical elaboration and the statistical results on the data from fire tests reported in this PhD thesis have been planned and provided by Dr. Marco Calderisi, Ph.D. (www.chemiometria.it).

3. Results and discussion

3.1. Use of natural fillers in highly filled EVA composites for cable application: rheological, morphological, mechanical and thermal properties

The incorporation of several types of filler in polyolefin matrix has been widely used to improve the compound performance. As reported in the Introduction, the presence of fillers completely changes the rheological and mechanical properties of polymer matrix. Even if several papers have tried to correlate filler-matrix interactions with the composite properties in order to propose methods for improving them[89-93] just a few of these deal with the use of natural fillers[5, 45] due to the difficulty of rationalizing the behaviour of the composite system.

The first part of this PhD study is mostly focused on the use of natural magnesium hydroxide (**Hy**) and other natural fillers produced with the same industrial plant, which are magnesium carbonate (**Mf**) and calcium carbonate (**SM**). The research deals with filler properties impact on the rheological, morphological, mechanical and thermal degradation behaviour of their compound with poly(ethylene-*co*-vinyl acetate) as matrix (EVA). A comparative study is presented using EVA composites with different fillers in order to point out the positive and negative aspects of natural fillers use.

3.1.1. Morphological, physicochemical and thermal degradation properties of fillers

In this section the properties of natural magnesium hydroxide (Hy) are analysed together with the properties of other fillers. The chosen inorganic fillers are reported in Table 3.1.1.

Table 3.1.1: Chosen inorganic fillers.

Sample	Principal component	Origin	Ore type
Hy	$Mg(OH)_2$	natural	brucite
H5	$Mg(OH)_2$	synthetic	-
ATH	$Al(OH)_3$	synthetic	-
Mf	$MgCO_3$	natural	magnesite
SM	$CaCO_3$	natural	majolica limestone

Among them synthetic magnesium hydroxide (H5) and synthetic aluminium hydroxide (ATH) have been chosen in order to have a comparison with natural hydroxide in terms of filler and composite properties, especially rheological and mechanical.

Figure 3.1.1 shows the morphology of the filler particles as observed by SEM.

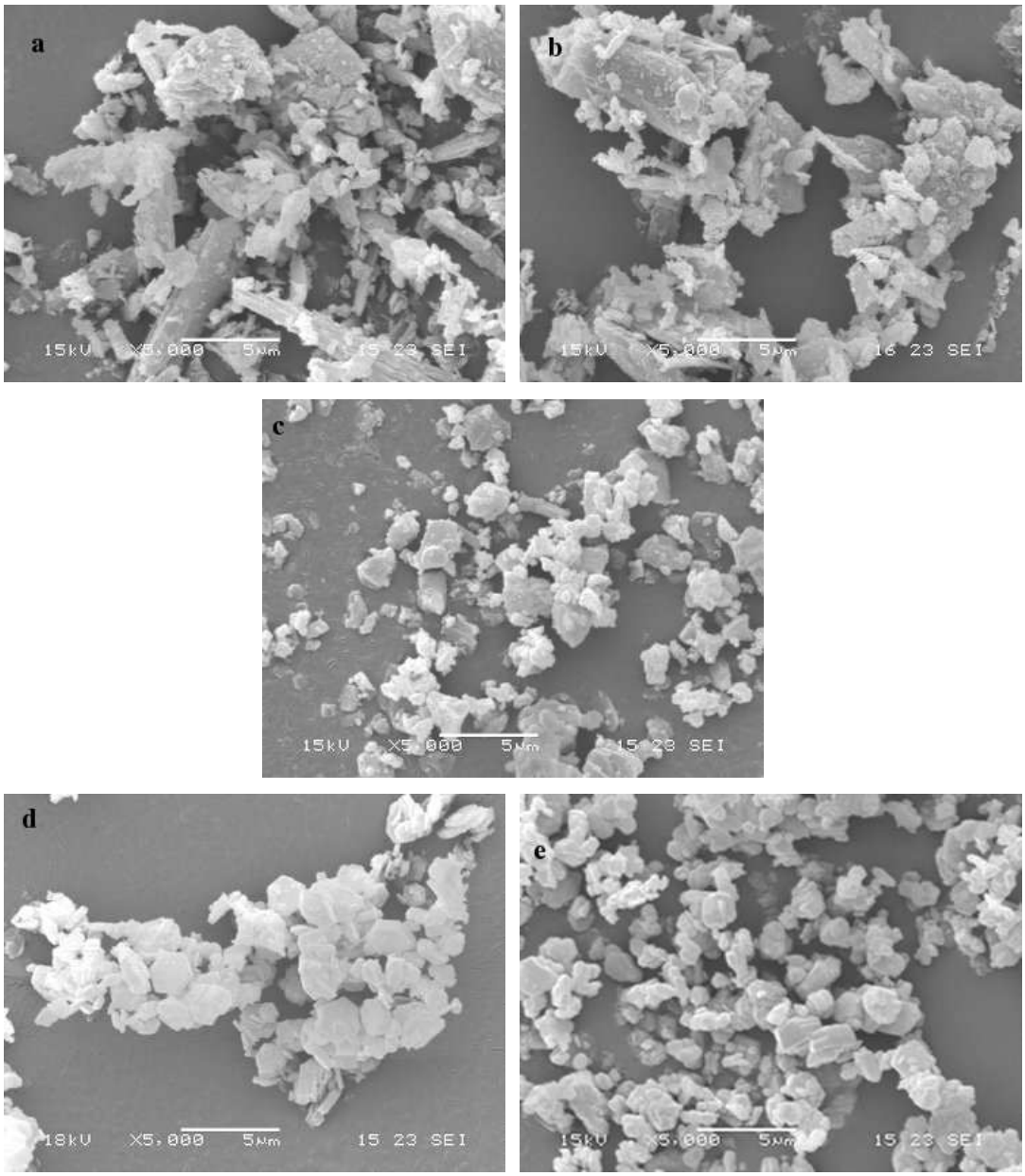

Figure 3.1.1: SEM micrographs of the analysed fillers: Hy (a), Mf (b), SM (c), H5 (d) and ATH (e).

The micrographs show that natural magnesium hydroxide particles are characterized by irregular shape, which could be approximately considered needle-like for most of the particles. Magnesium carbonate shows also irregular shape of particles, but more

rounded. From the micrographs it is also possible to evaluate the presence of particles with very different sizes for these natural fillers.

The analysis of the synthetic fillers points out the regular shape of the particles together with size uniformity: in particular magnesium hydroxide shows plate-like particle with hexagonal base, while aluminium hydroxide particles are almost similar to spheres.

Calcium carbonate is the natural filler with morphological properties similar to those of synthetic fillers, in fact the particles are well-formed and rounded. Observing the morphologies of the three natural fillers chosen for this study it should be possible to appreciate that the micrometric size particles of each filler have different shape and this is almost similar to the shape of the stones which are used as raw material for the production (Figure 3.1.2). It seems that during the milling production the break of the stones in order to obtain micrometric particles follows specific points and faults determined by the microcrystalline structure[4].

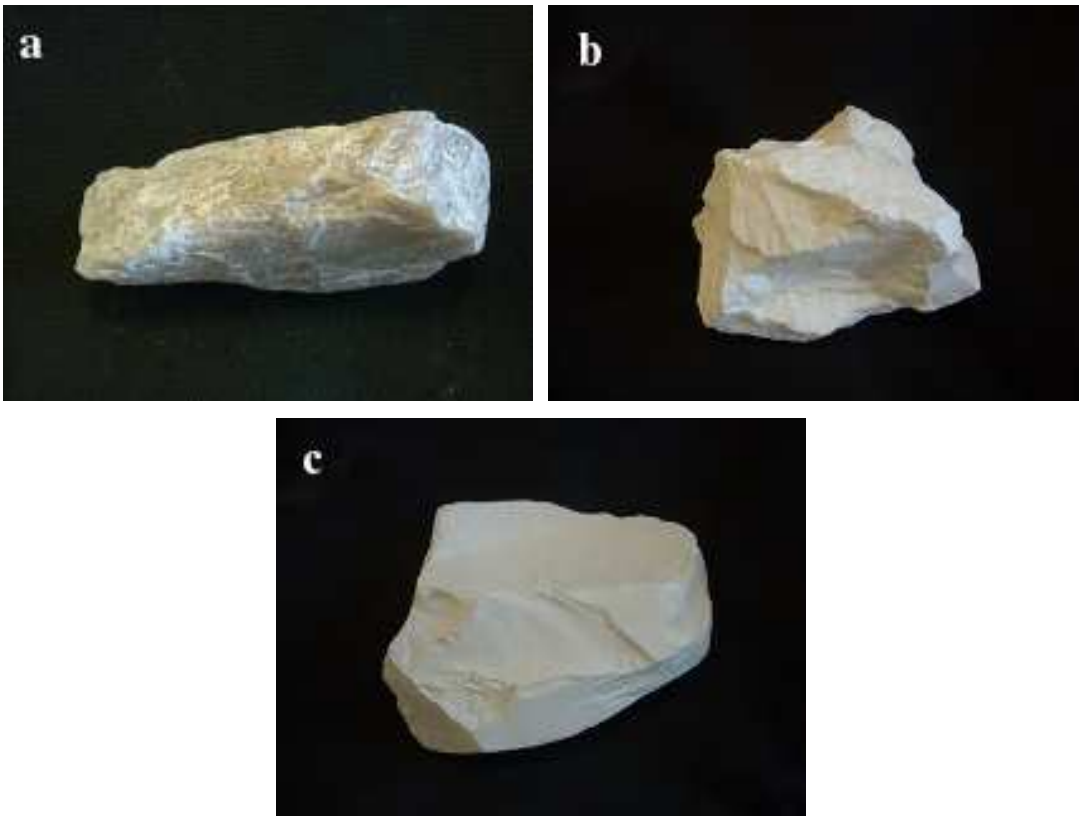

Figure 3.1.2: Photos of the stones used as raw material for natural fillers production: brucite (a), magnesite (b) and limestone (c).

The analysed physical properties of the fillers are reported in Table 3.1.2, among which their size distribution, with the main points of analysis (D_{90}, D_{50} and D_{10}), the specific

surface area measured by BET method, the tap density and the free volume calculated using tap density and the real density obtained from the literature.

Table 3.1.2: Properties of the inorganic fillers.

Filler	Size distribution (μm)			Specific surface (BET)	Tap density	Free volume
	D_{90}	D_{50}	D_{10}	(m^2/g)	(g/cc)	(u.a.)
ATH	3.43	2.22	1.30	3.56	0.62	0.73
H5	2.73	1.62	1.00	4.67	0.81	0.65
Hy	10.23	3.38	0.78	6.71	0.59	0.74
Mf	10.20	2.76	0.52	8.68	0.94	0.68
SM	3.95	1.65	0.67	4.09	0.85	0.69

Size distribution data confirm the qualitative information obtained by the micrographs of the fillers. The natural fillers show a wider distribution of the particle size than the synthetic fillers. This result was expected due to the different production method of the fillers. The synthetic ones are obtained by precipitation method, where almost the same growth of the particles can be reached regulating all the parameters (temperature, time, etc). The narrow particle distribution of ATH and H5 can be observed also in Figure 3.1.3, where the size curves, expressed by mass fraction versus particle diameter, are reported.

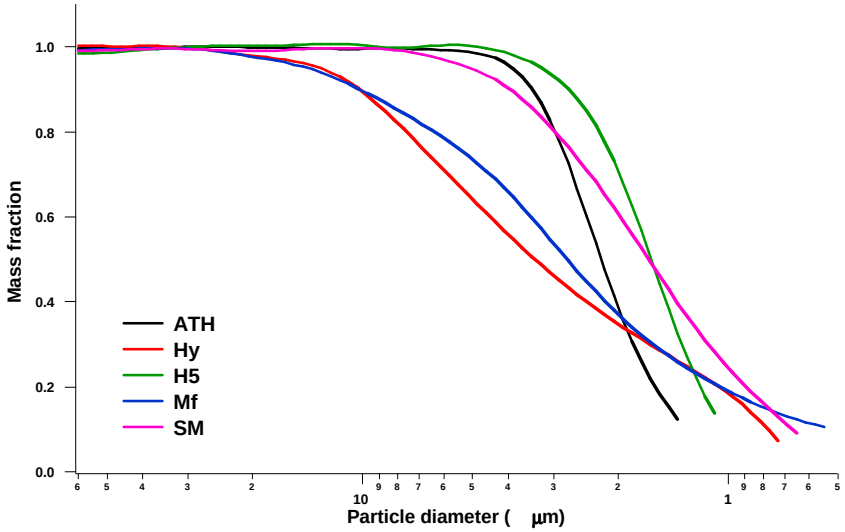

Figure 3.1.3: Size distribution curves of the fillers.

The natural fillers are produced by milling method starting from big stones as raw material and the crucial step is the "sieving process", which can really determine the final average size and the distribution. In particular among the natural fillers, Hy and Mf show

a very wide particle size distribution, while the calcium carbonate shows a curve more similar to those of synthetic fillers. Natural calcium carbonate is characterized by a lower hardness than that of magnesite and brucite and so the same milling process conditions can take to smaller particles with almost narrow size distribution.

Among the analysed fillers, Hy and Mf show the highest values of specific surface area, while even for this aspect the natural calcium carbonate shows a result quite similar to those of the synthetic hydroxides (around 4 m^2/g). The high values obtained for the natural magnesium hydroxide and carbonate can be justified by the presence of a portion of very small particles, especially in the case of Mf, and by the high particle porosity of these fillers, especially for the brucite.

In a previous work[94] on the same natural magnesium hydroxide filler with smaller average particle size (Hydrofy G1.5 with D_{50} = 6.60 μm) it was found that the application of an organic treatment on the particles didn't change the size distribution and the tap density but it caused a significant decrease of the specific surface area (from 8.80 to 5.80 m^2/g) , without the formation of particles aggregates. The reduction of the surface area was assigned to the occlusion of the huge amount of pores, which characterize the brucite structure.

Other interesting parameters from an industrial point of view are the tap density and the free volume, cause they give information about the particle behaviour in space occupation, in particular as an indication of the "storage characteristics" of the fillers. In fact the application of more than 1500 taps, as required by the standards, would like to simulate the transport and storage condition of the filler, where they are subjected to gravity and other stresses. The natural magnesium hydroxide shows the lowest tap density value, which is quite close to ATH one, while H5, Mf and SM show higher tap density values, corresponding to lower free volume results. The obtained data point out that Hy particles tend to pack in worse way than the other fillers, leaving high free volume, that is almost the same of ATH. However this result could be a positive indication from applicative point of view, because one of the problems of the synthetic magnesium hydroxide is the tendency to aggregate (becoming like cement), when stored as raw material for long time or delivered on roads. The natural magnesium hydroxide seems to show lower tendency of particles aggregation indicating a better storage capacity.

The chemical composition of the fillers has been determined by using EDS analysis (Energy dispersive X-ray analysis) and the results are reported in Table 3.1.3 as percentages by weight of the elements.

Table 3.1.3 : EDS analysis results expressed as weight percentage of element for the studied fillers.

Element	Filler composition				
(wt%)	ATH	H5	Hy	Mf	SM
O	61.9	56.4	57.1	55.9	46.2
C	-	-	1.2	12.6	9.7
Mg	-	43.6	37.9	25.6	0.4
Al	38.1	-	0.4	0.9	0.3
Ca	-	-	1.8	2.8	42.7
Si	-	-	1.6	1.8	0.7
Fe	-	-	-	0.4	-

As it would be expected, the synthetic fillers don't show any relevant impurity: they are composed by oxygen and by the respective metal in the right proportions. It could be noted just a small shortcoming in the oxygen content compare with the theoretical composition: this can be due to the presence of small amount of other crystalline forms.
Among the natural fillers, calcium carbonate seems to be the purest, with small percentages of magnesium, aluminium and silicon. Magnesite and brucite are the most impure fillers among those that have been analysed. In particular they both seem to contain calcium carbonate, silica and a small amount of aluminium impurities and magnesite shows also iron impurities.
The presence of the impurities is related mostly to the origin of the natural fillers and sometime it could change depending on the raw materials, even if they are taken from the same area. This is one of the main problems for the industrial use of natural fillers[5].

The thermal behaviour of the fillers has been studied using thermogravimetric analysis in the range of temperature from 50 to 1000°C, because of the high decomposition temperature of the fillers. Figure 3.1.4 and Figure 3.1.5 show the thermogravimetric curves and their derivatives, while the obtained data are reported in the Table 3.1.4.

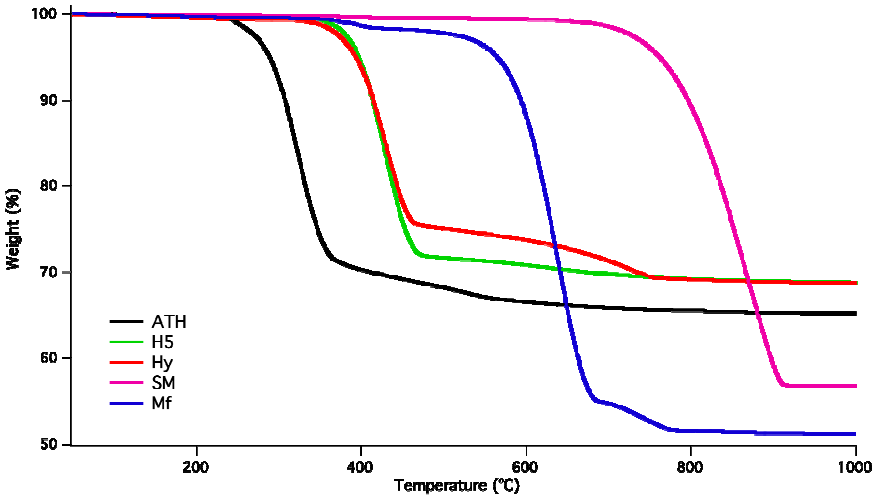

Figure 3.1.4: TGA curve of the inorganic fillers (N_2 flow, range 50-1000°C, rate 20°C/min).

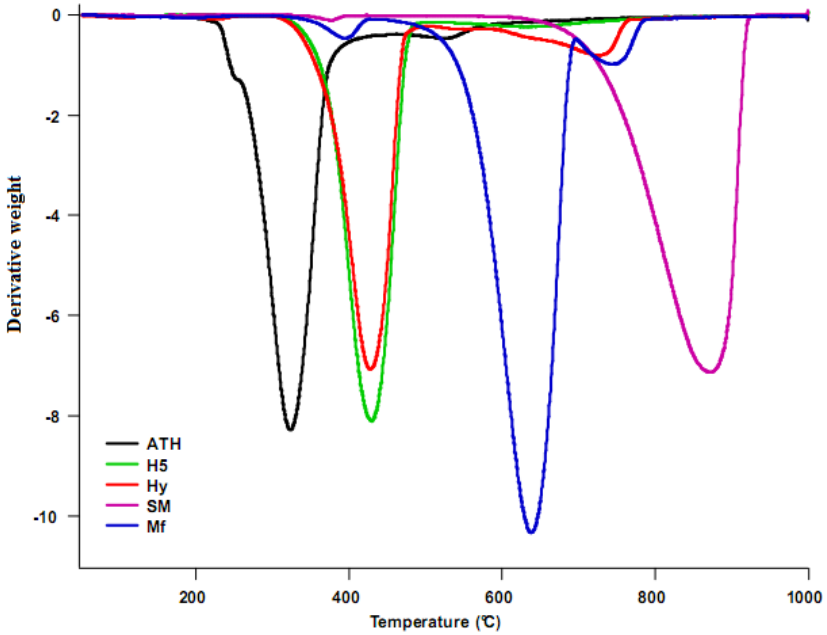

Figure 3.1.5: Derivative TGA curve of the inorganic fillers (N_2 flow, range 50-1000°C, rate 20°C/min).

Table 3.1.4: TGA data for the inorganic fillers.

Filler	T_{onset}* (°C)	$T_{main\ rate\ max}$ (°C)	% weight loss (50-200°C) **	% weight residue (1000°C)
ATH	277	324	0.2	65.2
H5	374	430	0.1	68.8
Hy	375	427	0.4	68.7
SM	734	870	0.1	56.8
Mf	571	638	0.3	51.2

*determination based on the tangents intercept point method.
**corresponding to the absorbed water on filler surface.

The analysed fillers are thermo-reactive because they decompose endothermically releasing water and/or carbonic anhydride as main gaseous products[13], as reported in the Scheme 3.1.1.

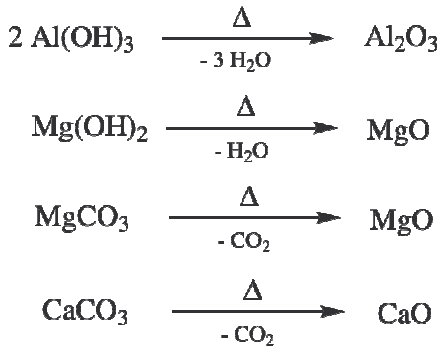

Scheme 3.1.1: Main decomposition reactions of the inorganic fillers.

The onset temperature (T_{onset}), the temperature of maximum rate of decomposition ($T_{main\ rate\ max}$) and the residue at the end of the analysis (1000°C) are in agreement with those reported in literature for almost all the fillers[95, 96]. The weight loss data obtained between 50-200°C (Table 3.1.4) show that the fillers with the highest specific surface, Hy and Mf, are also more hygroscopic than the others.

Synthetic aluminium and magnesium hydroxide decompose in a single step between 190-380°C and 320-480°C with a mass loss of 35% and 31% respectively.

Decomposition of natural magnesium hydroxide Hy takes place in two main stages in the ranges of 310-480°C and 480-780°C. The first step corresponds to the decomposition of magnesium hydroxide, while the second to magnesium and calcium carbonate thermal decomposition, which are the main impurities of the natural brucite. The decomposition mechanism is confirmed by the FTIR map of the evolved gas reported in the Figure 3.1.6, where the release of water in the first step and of CO_2 is highlighted. This result points out that the effective content of magnesium hydroxide is less than in the synthetic hydroxide because of the presence of carbonates corresponding to a weight loss of 7% of carbonic anhydride. This difference in $Mg(OH)_2$ content influences the effect of the filler when used as flame retardant additive.

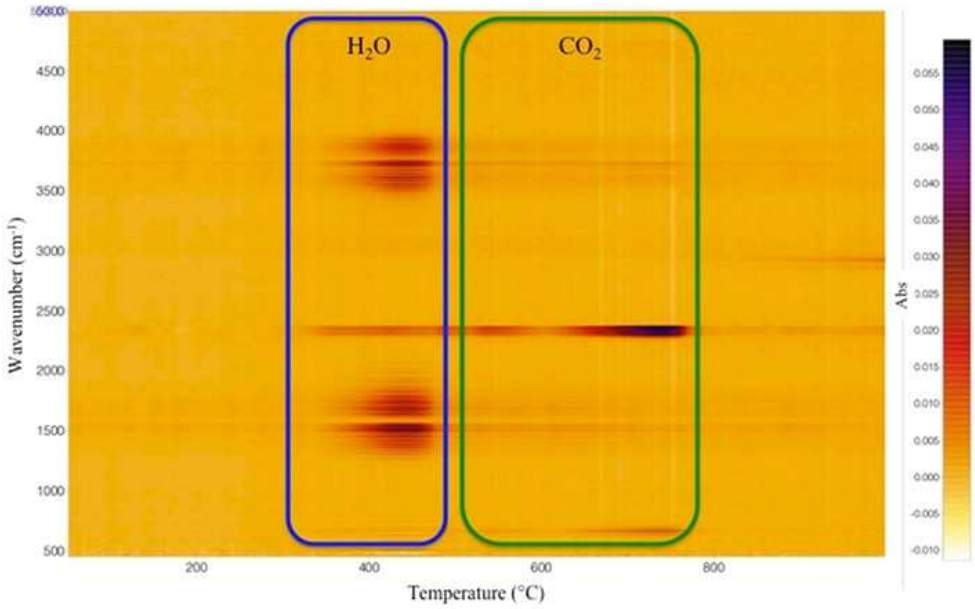

Figure 3.1.6: FTIR map of the evolved gases during the main steps of thermal degradation of natural magnesium hydroxide.

Magnesium carbonate degrades in two main steps between 460-690°C and 700-790°C, which correspond to the decarbonation reactions of magnesium and impurity of calcium carbonate. In particular the amount of calcium carbonate corresponds to a weight loss of 4% as CO_2 and this cause a higher residue value than that calculated for pure magnesium carbonate (around 48 wt%).

Thermal decomposition of calcium carbonate SM takes place as a single stage at temperature range between 650-910°C. By using thermogravimetric analysis, there are no particular impurities that can be found in the filler: even the thermal analysis confirms that SM shows almost the same characteristics of the synthetic fillers, in spite of its natural origin.

3.1.2. Rheological properties of the highly filled EVA compounds: effect of shear rate, filler type, temperature and filler loading

The chosen polymer matrix of the compounds is poly(ethylene-*co*-vinyl acetate) (EVA) with a content of 28 wt% of vinyl acetate groups and a melt flow index of 3 g/10 min. This copolymer has been chosen for its wide use, alone or in blend, especially for cable production. In this PhD Thesis no polymer blends or additives have been used for the

rheological, morphological and mechanical analyses in order to evaluate the effects of filler incorporation on pristine EVA.

The analysis of the melt rheological properties of EVA based composites, highly filled with natural magnesium hydroxide in comparison with the other natural and synthetic fillers, has been carried out using a piston-type capillary rheometer.

The evaluation of the main factors, which should influence the rheological behaviour of composites, has been carried out: the effect of shear rate ($\dot{\gamma}$), filler loading (ϕ) and temperature on rheological properties of natural magnesium hydroxide filled EVA composite are evaluated in comparison with the use of the other chosen fillers.

The composition of the analysed composites is reported in Table 3.1.2.1.

Table 3.1.2.1: Composition of the analysed composites, reported as volume and corresponding weight percentage.

Filler type	% by volume				% by weight*			
Hy	0	20	30	40	0	37.7	50.9	61.7
ATH	0	20	30	40	0	37.7	50.9	61.7
H5	0	20	30	40	0	37.7	50.9	61.7
Mf	0	20	30	40	0	43.3	56.7	67.1
SM	0	20	30	40	0	41.5	54.9	65.5

* Calculated using specific density values: 0.95 for EVA28, 2.3 for ATH, H5 and Hy, 2.9 for Mf and 2.7 for SM.

All the composites with different fillers have been prepared with the same volume percentage of filler because usually the rheological and mechanical properties of composite are studied taking into account the filler loading as volume percentage or volume fraction[34, 97]. In Table 3.1.2.1 the corresponding calculated weight percentage of filler, used for each sample preparation, are reported. Composite names are composed by the filler name abbreviation followed by the specific volume percentage (e.g. Hy_30 is the composite with 30 vol% of natural magnesium hydroxide). The compositions are characterized by high amount of filler which are almost the same used by cable industry or other applications (range of 35-65% by weight) in order to guarantee flame retardant and/or mechanical properties, together with the low total cost of the final product.

Effect of shear rate and filler type

Figure 3.1.2.1 shows the dependence of shear viscosity on shear rate for EVA and composites with the different fillers at 150°C at the same volume loadings (40 vol%).

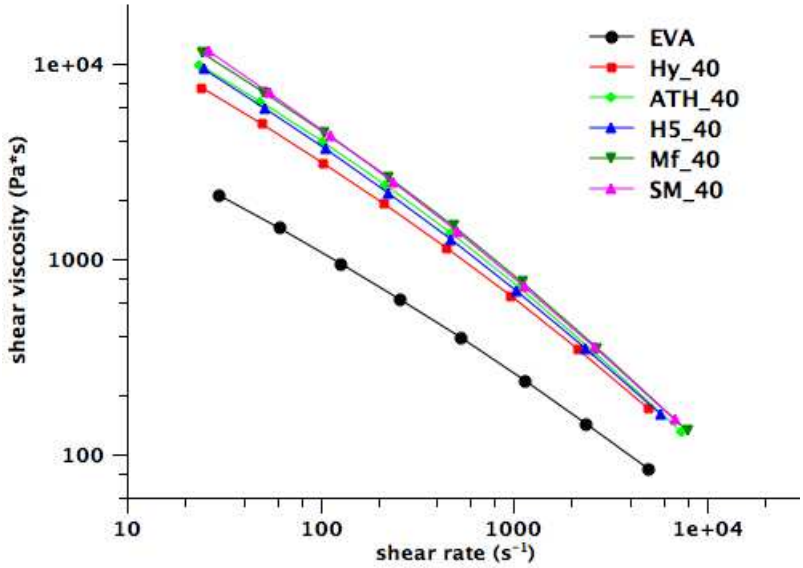

Figure 3.1.2.1: Shear viscosity of EVA and filled composite vs shear rate at 150°C.

The difference in viscosity among the materials is higher at low shear rates, while at high shear rates all the systems show nearly the same value, pointing out shear thinning effect. All the studied composites exhibit the typical behaviour of pseudoplastic materials, where shearing causes a reversible process of disentanglement as reported by other researchers [50, 52, 98]. In particular for filled polymer at high shear rates, the properties of the fillers provide lower effect on viscosity, because it is mostly dominated by the hydrodynamic interaction[57].

Two main explanations for this effect are reported by Bhagawan et al.[53]:

- under shear molecular chains become oriented, the entanglements are reduced and the viscosity decreases; at very high shear rate the orientation can be complete and the material can show a near-Newtonian behaviour (influence on polymer entanglements);
- where highly solvated molecules or particles are present, the solvated layers can be shared away increasing the shear rate, resulting in decreased viscosity (influence on particle-polymer interaction at interface).

It is possible to hypothesize the combination of these effects even in the studied composites.

In Figure 3.1.2.2 the melt flow curves for the matrix and for the composites filled with 40 vol% of different fillers are reported.

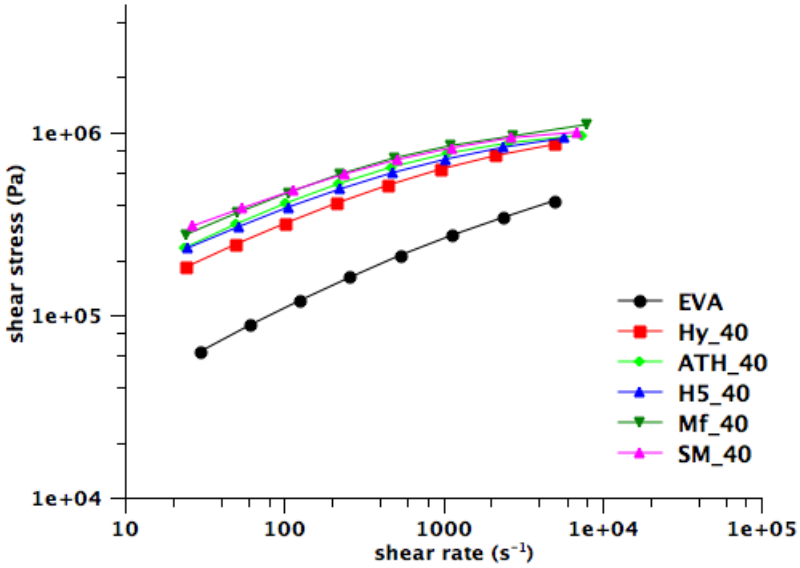

Figure 3.1.2.2: Flow curves for EVA matrix and for the composites with different fillers (40 vol% 150°C).

As shown in the graph, the incorporation of all the types of filler in the polymer matrix causes the increase of shear stress and so shear viscosity of the materials. Among them both magnesium and calcium carbonate filled composites show the highest values of shear stress, the curves of synthetic hydroxides composites are almost coinciding and they are higher than the flow curve related to Hy composite. The lowest shear viscosity of composite filled with natural magnesium hydroxide could be due to the combination of a variety of factors, where the most influent seems to be the morphology of Hy particles (at comparable chemical interaction). The term "morphology" includes particle shape, particle size and the distribution: particle size distribution and shape should be related to the packing capacity of filler and they influence strongly the melt viscosity behaviour of the composites. These effects will be deeply analysed in the following paragraph. However it is possible to underline that, even if Hy particles have irregular shape, the majority of them show "needle-like" shape, with an average aspect ratio higher than "1" (the value for "sphere-like" shape). During the capillary measurements, in the melt composite, Hy particles should orientate along the flux direction, taking to lower obstructing effect of the filler on the plastic flow than the other studied fillers.

The different behaviour of isotropic and anisotropic particles in composites during melt flowing is explained in the scheme in Figure 3.1.2.3 taken from Kim et al.[99] for calcite

(isotropic particle) and talc (anisotropic particle) composites, where it is also highlighted that this behaviour increases at higher shear rates.

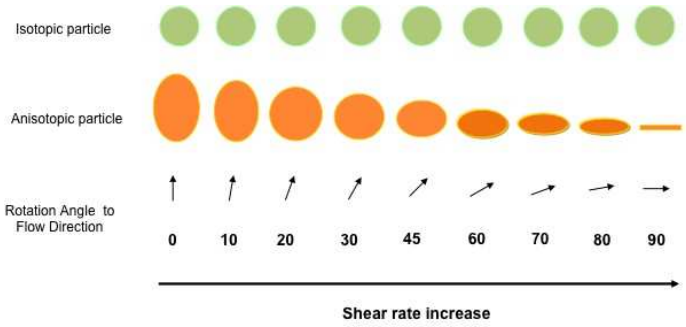

Figure 3.1.2.3 : Scheme of the orientation for the isotropic and anisotropic particles depending on the applied shear stress[99].

The lower shear viscosity of natural magnesium hydroxide composites especially in comparison with the synthetic hydroxides at the same volume percentage is a useful indication of the less expensive processing behaviour of the Hy filled material.

Effect of temperature

Temperature has an incisive influence on shear viscosity and the analysis of its effect is extremely useful in choosing the best experimental conditions to use during extrusion, calendering or injection molding processes. The introduction of filler in a polymer matrix could influence the temperature dependence of the shear viscosity especially because of the interactions that could be formed between filler and matrix.

Figure 3.1.2.4 illustrates the dependence of the melt shear viscosity on shear rate for the EVA matrix and for Hy_40 composite at different processing temperatures (110, 130 and 150°C).

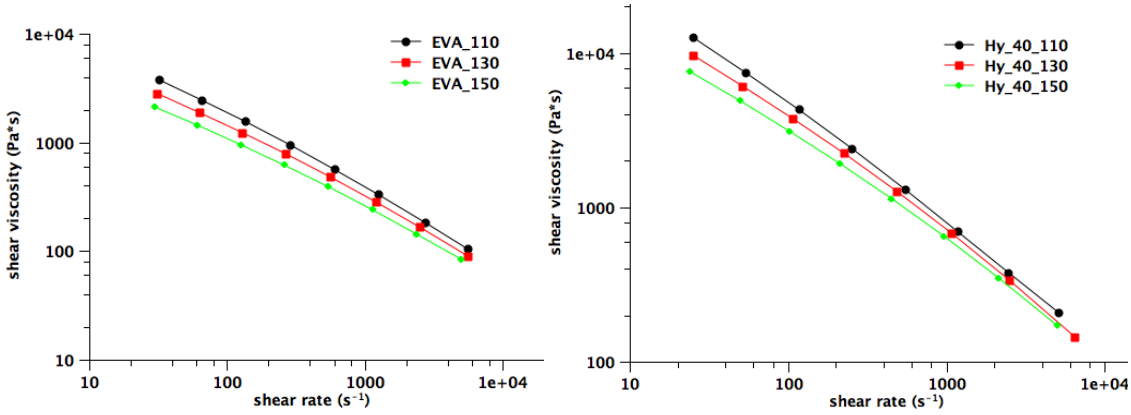

Figure 3.1.2.4: Flow curves for the EVA matrix and for the Hy composites with 40 vol% of filler at different temperatures (110, 130 and 150°C).

In general the viscosity of a polymer decreases with increasing temperature due to the greater free volume and less friction force available for molecular chain motion at higher temperature. This behaviour can be seen in EVA matrix, but it is the same also for the composites, as it is shown in Figure 3.1.2.4 for Hy_40 as an example.

The evaluation of the specific filler effect on the temperature dependence of the viscosity has been done by using the method based on the time-temperature superposition principle, TTS. This method allows the determination of the master curve from the flow curves at different temperatures by multiplying the data for specific factors and consequently causing a horizontal and vertical shift of the curves (Appendix I). TTS can be applied to the systems investigated in the present work, as an approximation: if satisfactory master curves could thus be constructed, it should be possible to capture the specific effect related to the different filler properties.

In Figure 3.1.2.5 the obtained master curves for EVA matrix and for Hy_40 are reported.

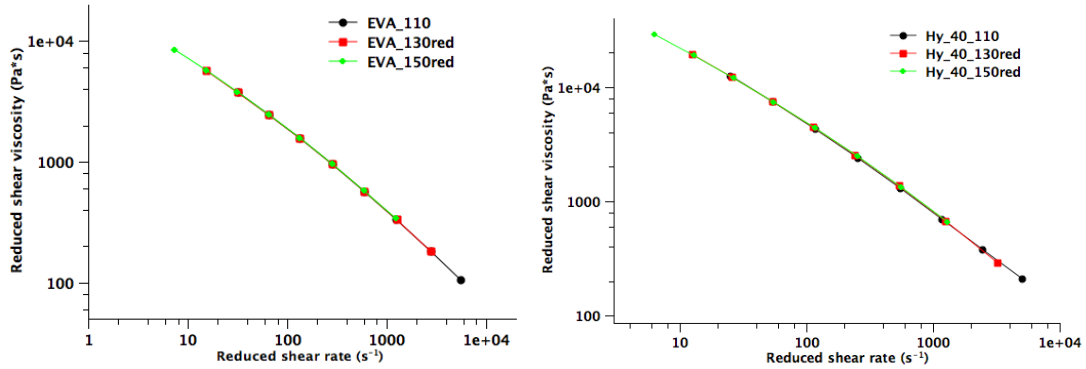

Figure 3.1.2.5: Master curves for the EVA matrix and for the Hy composites with 40 vol% of filler.

The possible effect of the filler on the temperature dependence of viscosity for the composites could be evaluated by shift factor analysis: the viscosity curves at 130°C and 150°C have been shifted on that at 110°C, obtaining the reduced curves (indicated as 130red and 150red). The shift factors calculated for EVA curves at 130°C (130red) and 150°C (150red) are 0.5 and 0.25 respectively. Table 3.1.2.2 lists the shift factor values obtained by shifting the reduced flow curves at 130°C and 150°C for all the studied composites.

Table 3.1.2.2: Shift factors relative to the flow curves of the composites at 130°C (130red) and 150°C (150red).

vol%	Hy		ATH		H5		Mf		SM	
	130red	150red	130red	150red	130red	150red	130red	150red	130red	150red
20	0.50	0.25	0.50	0.25	0.50	0.25	0.50	0.25	0.50	0.25
30	0.44	0.26	0.50	0.25	0.50	0.25	0.47	0.26	0.50	0.25
40	0.50	0.26	0.50	0.25	0.50	0.25	0.49	0.26	0.50	0.25

Looking at the shift factor data it is possible to appreciate that they do not change with changing filler type and filler loading and they keep almost the same values obtained for EVA matrix. This results points out that the introduction of the fillers does not influence the temperature dependence of shear viscosity for EVA. It can be concluded that temperature influences just the matrix rheological behaviour for the analysed EVA composites, without any significant effect on polymer-filler interactions.

Effect of filler loading

The shear viscosity of the Hy composites at different filler loadings as a function of shear rate is reported in the Figure 3.1.2.6.

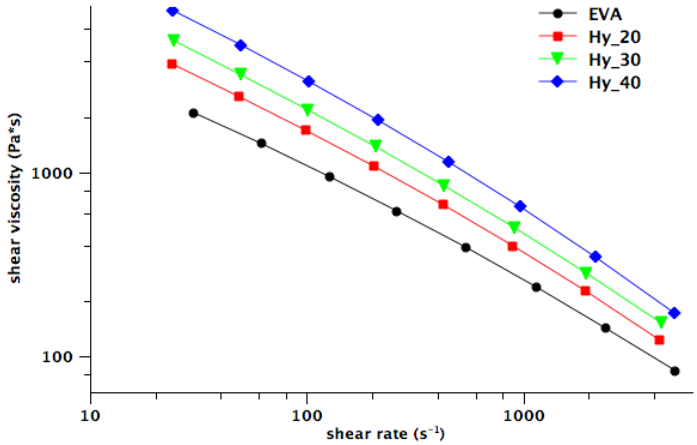

Figure 3.1.2.6: Shear viscosity versus shear rate for EVA matrix and Hy composites at different filler volume percentage.

The viscosity of the compound increases progressively with the increase of the Hy content, from 20 to 40 vol%. This behaviour is true for all the analysed systems and for all the shear rates: in general the presence of the filler-polymer interaction perturbs the normal flow of the polymer and hinder the mobility of the chain segments in the direction flow[30, 36]. Higher is the filler amount, stronger is this effect.

Among the composites the increase of viscosity with increasing filler loading could be different, due to the various effects that can influence the composite rheological properties. In Figure 3.1.2.7 it is possible to evaluate qualitatively the effect of filler content on the apparent shear viscosity of the studied composites at 150°C and 18 s^{-1} as apparent shear rate.

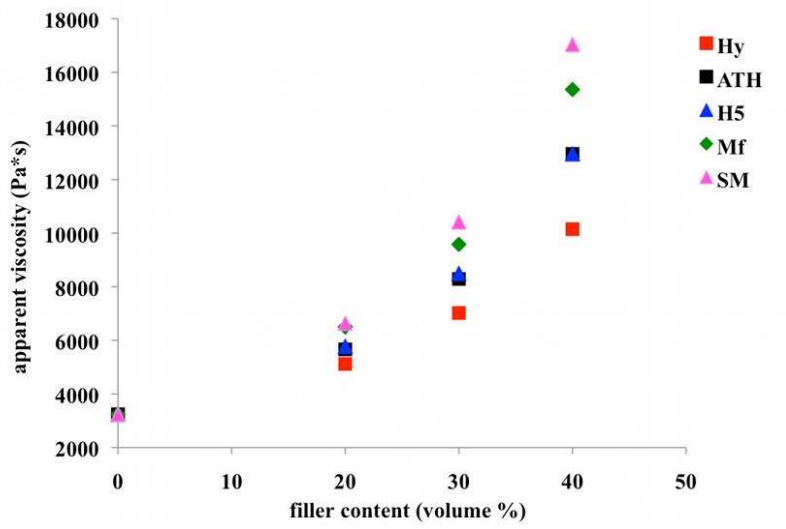

Figure 3.1.2.7: Apparent viscosity vs filler volume percentage for the composites at temperature of 150°C and apparent shear rate of 18 s^{-1}.

Shear viscosity of Hy composite seems to be the less influenced by the filler concentration. This result indicates preferable process conditions of natural magnesium hydroxide composites even at the very high filler concentrations required by industrial application.

3.1.2.1. Theoretical approach for evaluation of filler volume fraction and properties influence on rheological behaviour of Hy filled EVA composite

A deeper study has been done on the relation between viscosity and concentration for Hy composite together with the filler properties influence on rheological behaviour. Essentially a theoretical approach has been applied on the compounds filled with hydroxides in order to evaluate which are the main filler factors influencing the rheology of the composite and to estimate the quality of filler dispersion. This approach introduces particle correlations by taking into account hydrodynamic interactions and provides a

conceptual framework that explains how the microstructure of the system modifies the viscosity as a function of volume fraction[31, 100].

The analysis has been carried out on the compounds with natural magnesium hydroxide in comparison with the synthetic hydroxides. The restriction of the studied samples to the hydroxides (Hy, H5 and ATH) allowed us to overlook the effect due to the different chemical composition of carbonates, which could deeply influence the particle-matrix and particle-particle interactions, hiding the other effects. In Figure 3.1.2.1.1 the experimental viscosity curves as a function of shear stress are reported for the composites at different filler volume fraction (T=150°C). The experimental curves are compared with the predicted curves, which are calculated by applying an empirical model starting from viscosity values of the matrix. The chosen model[101] (Maron-Pierce) takes into account the only hydrodynamic interactions influence and considers the filler constituted by randomly close packed spheres (RCP, ϕ_m=64%). The theoretical curves predict the rheological behaviour of composites characterized by perfectly dispersed and non-interacting filler particles, in case of hydrodynamic interactions regime.

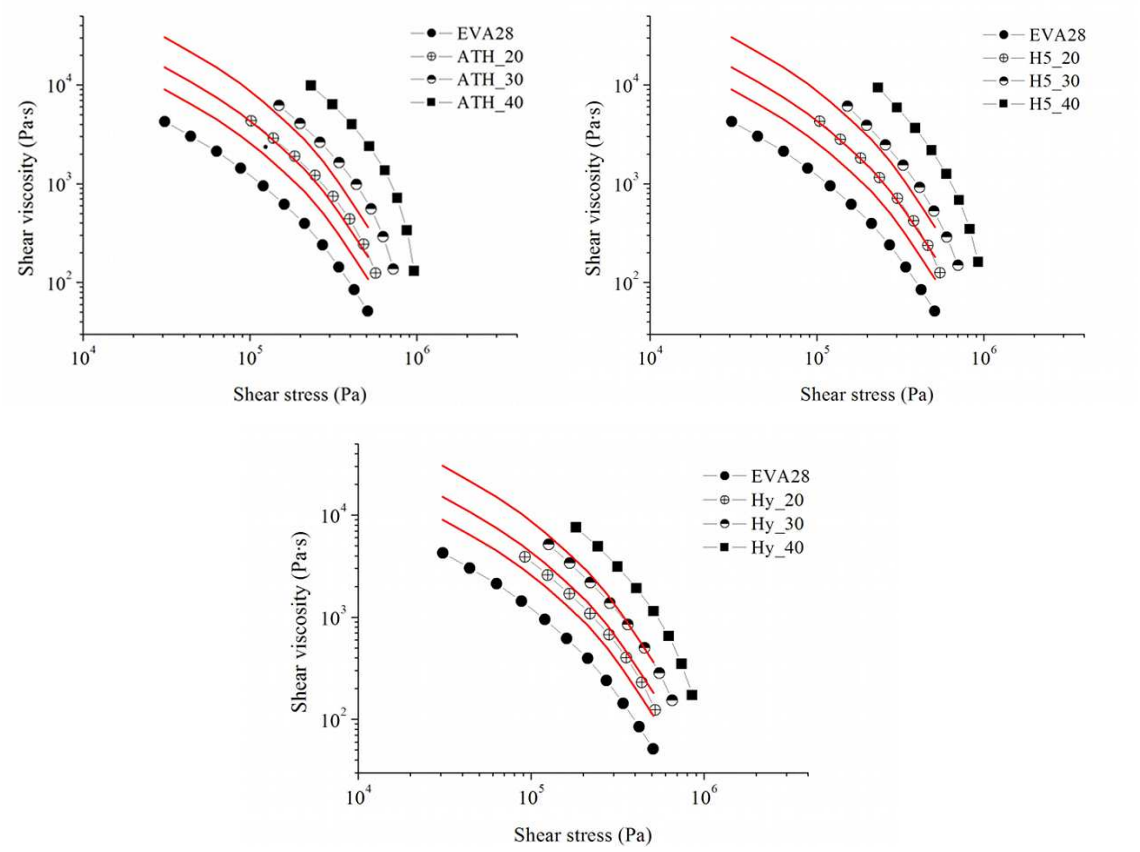

Figure 3.1.2.1.1: Comparison between the experimental and the predicted (red curves) flow curves for the hydroxides composites, taking into account rigid spherical particles with only hydrodynamic interactions.

For all the composites, the experimental curves are underestimated by the prediction, but Hy composite series show real curves, which are closer to the theoretical ones than ATH and H5 composites. In particular it is possible to observe that the average numerical distances between the predicted and experimental curves of synthetic hydroxides are almost the same, while for Hy composite the distance between the curves is half of the synthetic ones. This result suggests the presence of a variety of effects, which could influence the rheological behaviour of the composites in connection with the filler properties[34, 102-104]. Among them it is possible to underline the particle anisotropy, the particle size distribution, the yield stress effect and the dispersion degree of the particles inside the composite.

By considering the particle shape, the results seem to be in contradiction with the chosen hydroxides properties: generally at the same volume fraction, the particles, with an aspect ratio higher than 1, show relative viscosity higher than that of spherical particles due to the different maximum packing tendency. Hy composite gives real curves closer to the ideal ones, even if the average aspect ratio of its particles is very different with respect to the spherical particle ones. However, as reported in the previous paragraph, the average needle-like shape of Hy particles could be considered a factor of the lower viscosity due to the orientation during flow.

The trend of the particle size distribution is in agreement with the obtained results in fact the presence of particles with a wide variety of dimensions allows a better packing capacity of the filler and then the viscosity reduction of the composite.

The yield stress effect mostly depends on particle-particle interaction and it is usually appreciated at lower shear stresses than those explored by the capillary rheometer. For this reason the evaluation of yield stress has been carried out by means of a rotational rheometer: the complex viscosity dependence on the complex modulus is reported in Figure 3.1.2.1.2 for Hy_40 composite.

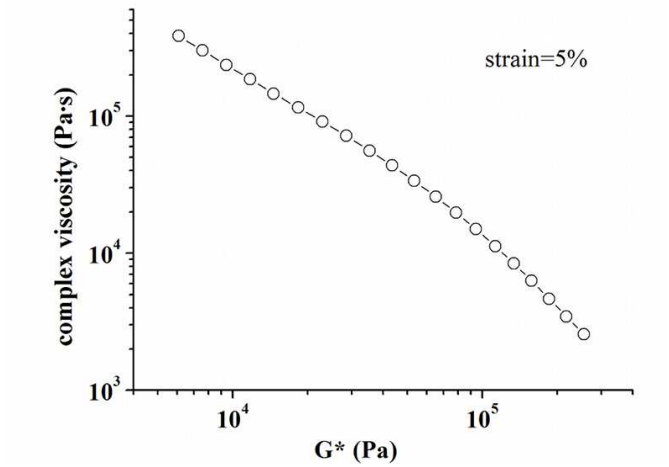

Figure 3.1.2.1.2: Complex viscosity of Hy_40 composite.

It is clear from the absence of upturns of the viscosity curve that the yield stress value, if there is any, is very low (less than 1000 Pa). For this reason, due to the high shear stress values measured in the capillary and the high difference between the experimental and the predicted curves, the yield stress effect can be ignored in the discussion of the viscosity behaviour at high shear rates. An investigation of the failure of the Cox-Merz rule, whose breakdown is well documented for highly concentrated suspensions[38, 105], is far from the scope of the present work.

The last important factor, which should influence the rheological behaviour of the composites, is the filler dispersion degree in the materials. In the studied system the viscosity trends for the natural magnesium hydroxide compound indicate a better dispersion of the filler compare to that of the synthetic fillers. In Figure 3.1.2.1.3 the SEM micrographs of Hy_20 and ATH_20 are reported.

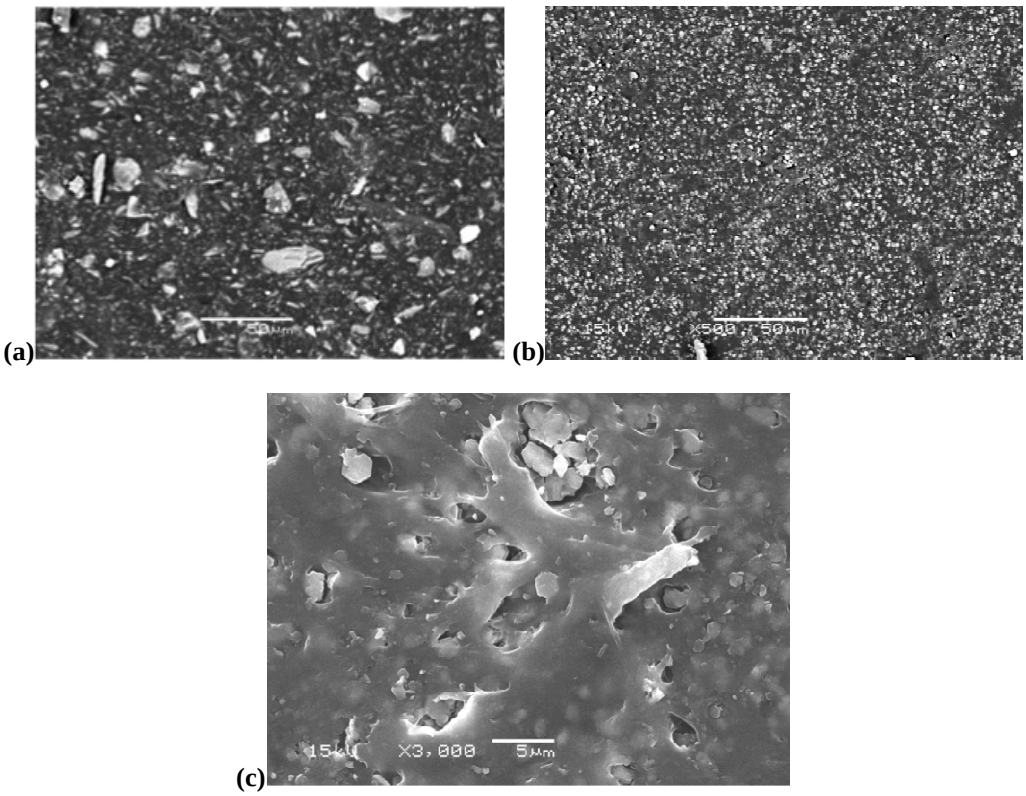

Figure 3.1.2.1.3: SEM micrographs of the cryogenic fractures of a) Hy_20, b) ATH_20 and c) a zoomed part of ATH_20.

.

Despite the difficulties of verifying the dispersion degree in such high filled materials, in the reported images it is possible to observe higher aggregation of particles in ATH composite (as in the zoomed image) that is less diffused in the Hy composite. The better dispersion of natural magnesium hydroxide due to the presence of different particle dimensions can be also appreciated.

A deeper analysis of the rheological results has been carried out calculating the relative viscosity for the composites filled with the hydroxides. The relative viscosity, η_r, is expressed as:

$$\eta_r = \eta_c / \eta_m$$

where η_c and η_m are respectively the viscosity of the composite and the matrix.

The relative viscosity is a function of shear stress and filler volume fraction. For this reason it is necessary to select and fix a specific shear stress in order to evaluate the effect of volume fraction of filler. The chosen shear stress value is around 300 kPa, which guarantees that the system regime is mostly dominated by hydrodynamic

interactions. This could be an acceptable approximation taking into account that an overlapping of other effects would be possible.

In the graphs of Figure 3.1.2.1.4 the relative viscosity versus the volume fraction for all the composites are reported together with the application of three different mathematical models, which try to fit the relative viscosity data. In literature there are many efforts done to describe the flow behaviour of highly filled systems in terms of relative viscosity-volume fraction of solid relationship[106]. They are useful for understanding the systems and for the prediction of the maximum packing fraction (ϕ_m), which is a best-fit parameter corresponding to the maximum loading level for a given compound, very important for the estimation of optimal filler loading[107].

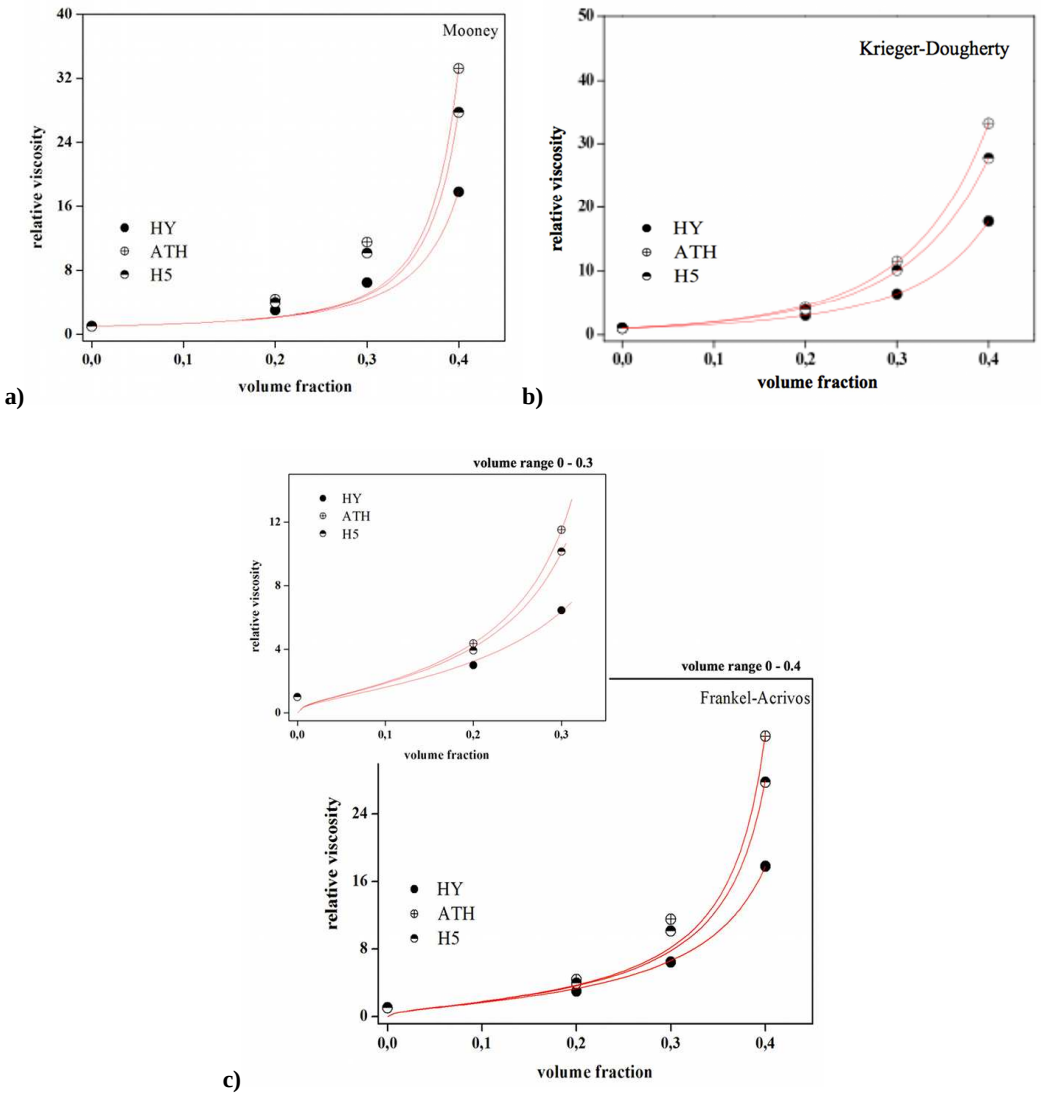

Figure 3.1.2.1.4: Relative viscosity versus volume fraction for Hy, H5 and ATH composites and application of a) Mooney, b) Krieger-Dougherty and c) Frankel-Acrivos models.

Three different models have been chosen for fitting the composites relative viscosity data: Mooney, Frankel-Acrivos and Krieger-Dougherty. The maximum packing fraction results for the hydroxide composites are listed in Table 3.1.2.1.1.

Table 3.1.2.1.1: Maximum packing fraction values obtained by different models fitting of relative viscosity data.

Samples	ϕ_m (Mooney)	ϕ_m (Frankel-Acrivos)	ϕ_m (Frankel-Acrivos, 3 points)	ϕ_m (Krieger-Dougherty)
ATH_composite	0.56	0.44	0.40	0.96 ([η]=6.8)
H5_composite	0.57	0.45	0.42	0.94 ([η]= 6.4)
Hy_composite	0.61	0.48	0.49	0.65 ([η]=4.6)

Mooney and Frankel-Acrivos models expressions are as follows:

$$\ln \eta_r = \frac{5}{2}\left(\frac{\phi}{1-\phi/\phi_m}\right)$$

$$\eta_r = \frac{9}{8}\left[\frac{(\phi/\phi_m)^{1/3}}{1-(\phi/\phi_m)^{1/3}}\right]$$

They are characterized by a maximum packing fraction as the only best-fit parameter. Even if these models do not fit very well the relative viscosity data of the synthetic hydroxide composites (whilst the fitting is good for Hy), they could indicate the relative maximum limit of loading level for our compounds. The maximum packing fraction values obtained for the composites are quite similar (Table 3.1.2.1.1), but ϕ_m for Hy composite is the highest both for Mooney and Frankel-Acrivos models. The lower ϕ_m values for ATH and H5 composites could be related to the presence of a greater number of agglomerates in the composite structure.

Furthermore these results point out that the particle size distribution can be considered the most influent Hy characteristic on the rheological behaviour and dispersion level of the composite in comparison with the used synthetic hydroxides, cause size distribution is strictly related to ϕ_m.

An attempt of Frankel-Acrivos fitting has been done also on three points of relative viscosity, deleting the highest volume fraction (ϕ = 0.4). In this restrict range the fittings seem better also for ATH and H5 compounds and the maximum packing fraction values are not so different from those obtained on the whole volume fraction range (0-0.4). This behaviour could point out that in such highly filled systems the dispersion of the filler could be changed by the flow effects, with the possible formation of bigger particles agglomerates. The effect is more pronounced in ATH and H5 composites.

This hypothesis is also supported by the trends of relative viscosity against the shear stress reported in Figure 3.1.2.1.5.

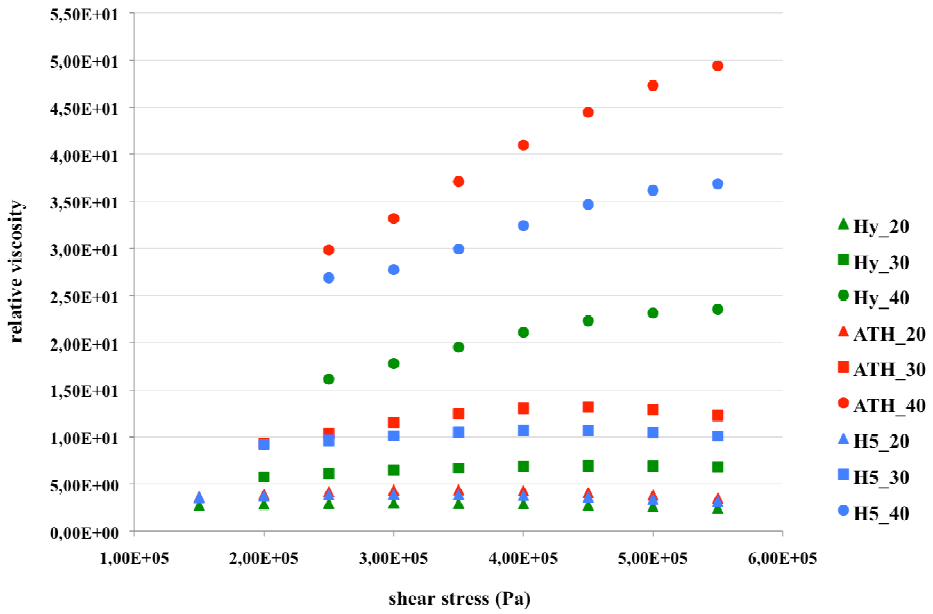

Figure 3.1.2.1.5: Relative viscosity versus shear stress for the hydroxides filled composites at different volume fractions (T = 150°C).

The increase of η_r at high stress only for the composite with 40 vol% of filler (circle markers) points out a shear thickening effect at this loading, which is caused by re-organization of filler particles in the material (*clustering*). The effect is more evident for synthetic filler composites, especially ATH. The cluster formation could influence the composite rheological behaviour more than the only hydrodynamic interactions[42, 108] leading to a difficult theoretical analysis of the system containing this high filler amount.

Krieger-Dougherty is a semi-empirical and more flexible model and its expression is as follows:

$$\eta_r = \left(1 - \frac{\phi}{\phi_m}\right)^{-[\eta]\phi_m}$$

It is possible to observe that in this case there are two best-fit parameters, ϕ_m and $[\eta]$, which correspond respectively to the maximum packing fraction and to the intrinsic viscosity of the material. For this reason the Krieger-Dougherty equation gives a better fitting of the relative viscosity data of the studied composites (Figure 3.1.2.1.4 c), but this does not prove that the best-fit parameters have real physical meaning. In general the existing models are too simplified for describing completely the complex behaviour that these highly filled composites exhibit. Among them the simplest models, with ϕ_m as the only best-fit parameter could give the most indicative information.

The general considerations, which come out from this theoretical study is that Hy composite should show higher maximum loading tendency than the synthetic hydroxide composites, as proved by the lower relative viscosity values at the same solids volume fraction. Among all the filler properties, the particle size distribution seems to be the most influent on rheological properties and dispersion. In fact a larger size distribution guarantees a better packing effect because of the possibility for the smaller particles to fill the interstices left by the bigger particles. For this reason Hy composite should be characterized by a better dispersion of the filler and a lower tendency of clustering at higher shear.

3.1.3. Extrudate swell and surface aesthetic quality of highly filled EVA composites with natural magnesium hydroxide (Hy)

Melt elastic property of polymers has been proved by many studies to be the most important characteristic determining the morphology and surface of extrudate. It is of great concern to many researchers due to the capability of the elastic part in the system to promote defects on a polymeric extrudates[60, 109]. This has a strong effect on the quality of end product for applicative interest.

The main common defects occurring in polymer extrusion are:

- swelling phenomenon, when the diameter of the extrudate product is larger than that of the capillary diameter (Extrudate Swell);
- flow instability and melt fracture, when deformations and/or surface roughness take place on the extrudate (Extrudate Morphology).

Extrudate Swell

The die swell ratio (*Barus effect*) is an indication of dimensional stability of the materials during processing. In fact it depends on the reorientation and recovery of the deformed molecules as the melt emerges from the die. The swelling behaviour is highly affected by a number of factors, such as shear rate, temperature, L/D ratio, filler content, etc. In the composites, filler and polymer exhibit unequal retroactive forces that lead to the redistribution of fillers and recoiling effect of the polymer chains[110].

The specific study deals with the effect of natural magnesium hydroxide on swelling behaviour of EVA compounds. A comparison has been carried out also with the introduction of synthetic aluminium hydroxide, which represents the reference for melt elastic properties because it is the most used flame retardant filler in highly filled EVA composites.

The swell ratio values of EVA matrix are characterized by high error range, because of the difficult determination of average values due to the irregular morphology of the extrudates, as shown in Figure 3.1.3.1(a). In particular it was impossible to determine extrudate swell data for matrix at the highest shear rates and higher temperature, cause the melt that emerged from the die was too hot and it stuck with the material already out (Figure 3.1.3.1(b)).

a)  **b)** 

Figure 3.1.3.1: Photos of a) extrudate of EVA obtained at 130°C and at shear rate of 2304 s^{-1} and b) the whole EVA extrudate sample obtained at 150°C.

Figure 3.1.3.2 shows the swell ratio versus apparent shear rate for the matrix EVA and Hy composites with different filler loading at temperature of 130°C.

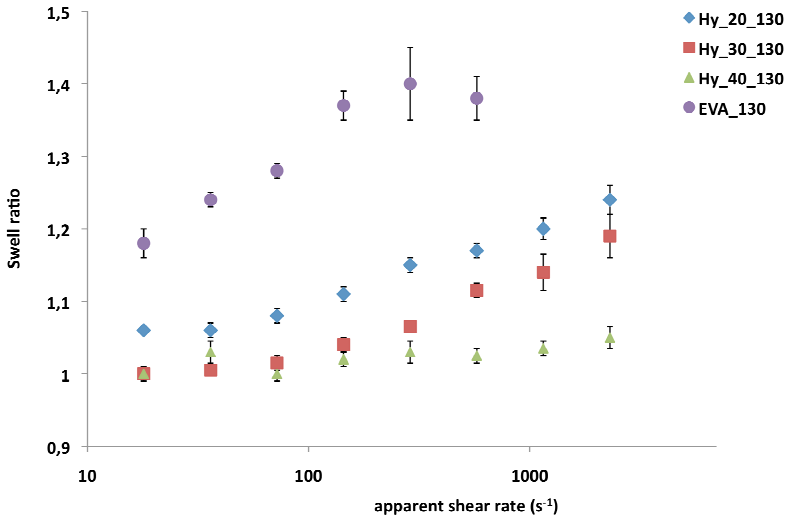

Figure 3.1.3.2: Swell ratio data vs shear rate of EVA matrix and Hy composites at different filler loadings at temperature of 130°C.

By observing the reported data it is possible to evaluate that the swell ratio increases by increasing shear rate for EVA and Hy composite extrudates. This result is in agreement with previous research works[57, 111]. At higher shear rates the elastic energy stored in the polymer melt flow is higher and the extrudate swell values increase. Physically the macromolecules, which are disentangled and oriented inside the die, become entangled again: higher is the shear rate, stronger is the elastic recovery after the die exit (higher swelling effect).

The results point out also that more is the filler content, lower is the increase of the swell ratio with increasing shear rate, indicating more stable dimensions of the extrudate due to the presence of very high loading of filler (almost 60% by weight). It is verified that not only the polymeric molecules but also filler particles could orientate under shear[50]. In particular, the latter are difficult to turn back to their original state when the melt leaves the capillary die. The presence of the filler increases energy dissipation, so the elasticity recovery is less for a filled polymer than for an unfilled one. Furthermore the presence of filler can limit the elastic recovery of the macromolecular chains, which are confined along the extrusion direction in the capillary die (Figure 3.1.3.3). This phenomenon can explain the lower extrudate swell values we have observed for filled polymer than the unfilled one at different filler volume percentages and at the studied temperatures.

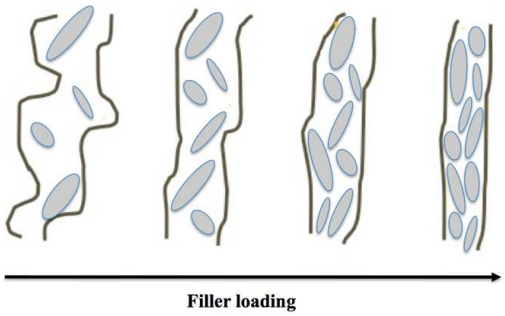

Figure 3.1.3.3: Schematic representation of the decrease in swelling of extrudate with increasing filler loading (at fixed shear rate).

In the Figure 3.1.3.4 the swell ratio trend of Hy_20 is compared with the ATH_20 one at 150°C of temperature extrusion.

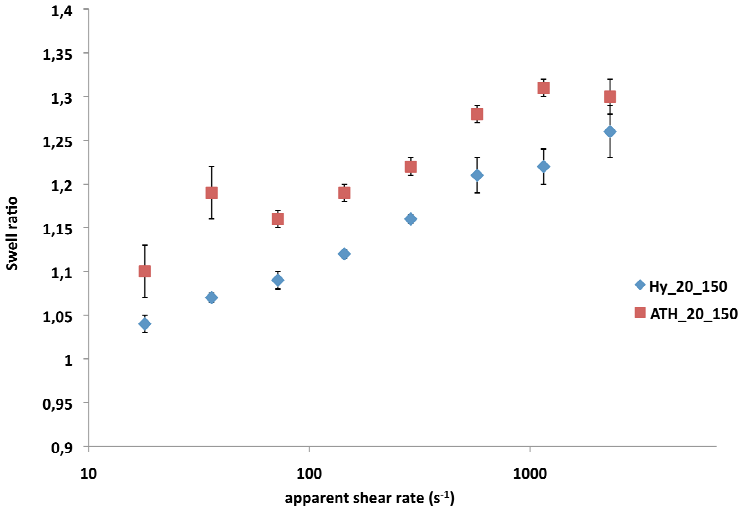

Figure 3.1.3.4: Swell ratio data vs shear rate of Hy_20 and ATH_20 composites at temperature of 150°C.

The Hy composites exhibit lower die swell than the ATH composites at all the analysed compositions and the differences are not so much influenced by the filler contents. This suggests that natural magnesium hydroxide Hy is more efficient in reducing the deformation rate of the system than the synthetic aluminium hydroxide ATH.

The difference in die swell ratio between the two filler composites can be explained by the analysis of the particle structure, the packing factor and filler-matrix interaction[3]. Hy particles are characterized by higher average aspect ratio than ATH particles, which can be considered spherical. At relatively high stress, polymer chains and solid particles could orientate themselves according to flow direction, which Hy particles can perform, while ATH cannot do because of their spherical shape. As the melt flows out of the die

the aligned polymer chain try to recover to the original configuration, but the elastic rearrangement is more restricted by the presence of Hy particles than ATH, due to the compact cage structure (Figure 3.1.3.5), which is more efficient in creating a less deformable extrudate.

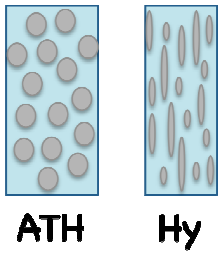

Figure 3.1.3.5: Schematic representation of the internal cage structure of the ATH and Hy composites.

ATH particles are characterized by narrow particle size distribution and spherical shape, which allows the formation of more micro-voids in the composites packing structure. This scenario leads to a denser packing structure for Hy composite than ATH composite and consequently to a lower swelling effect.

The stronger capacity of Hy filler in maintaining a cage structure with the polymer could depend also on filler-matrix interaction. Average shape, size distribution and larger specific surface of the particles indicate that Hy have higher possibility of interacting with polymer than ATH and of enhancing melt strength of the system, which cooperates in stabilizing the internal structure of the composite.

Extrudate morphology

Melt flow instabilities and extrudate distortion have been known to occur during extrusion of polymers. They lead to formation of roughness and tearing on the extrudate surface upon emerging from the die. The capillary rheometer allows the analysis of the extrudate morphology, cause it is possible to select on the extrudate sample different portions corresponding to different shear rate of extrusion. Here, the most indicative portions are reported in order to evaluate the surface morphology of EVA and composites extrudates, pointing out the effects of natural magnesium hydroxide incorporation in comparison with the other fillers.

The analysis of the surface roughness has been evaluated by optical microscope and SEM micrographs to appreciate also the smallest differences. The study is only

qualitative, because it is difficult to quantify the system and to determine by far the most influent factors on surface morphology for this kind of materials.

In Figure 3.1.3.6 the extrudates at the lowest and the highest apparent shear rate of pure EVA at 150°C are reported.

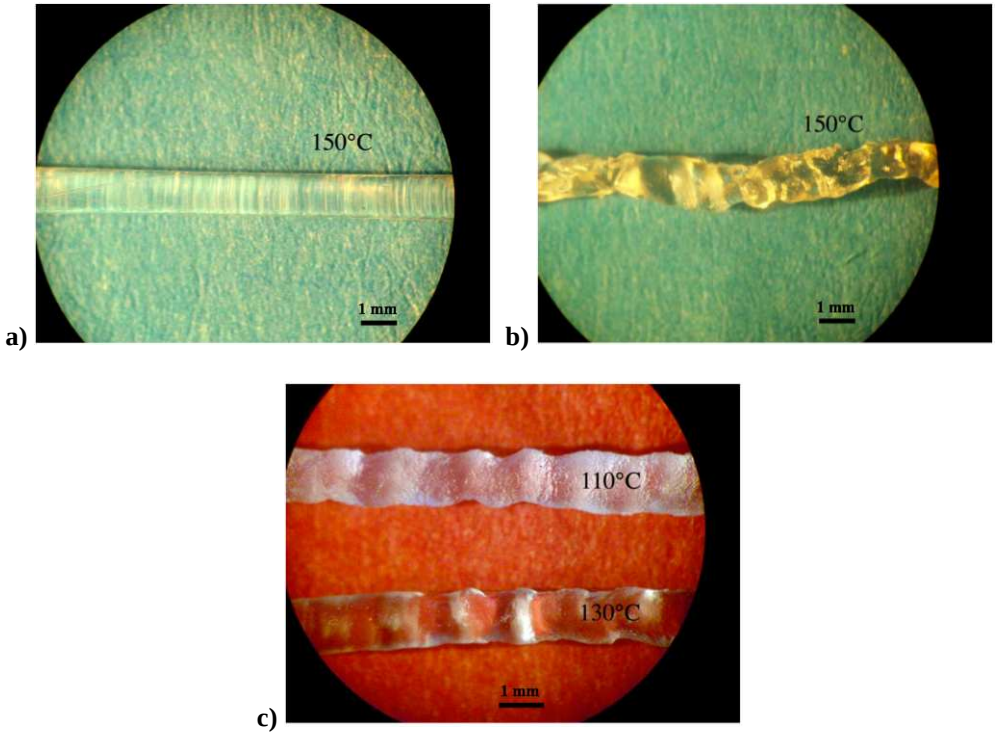

Figure 3.1.3.6: EVA extrudates at apparent shear rate of a) 18 s^{-1} and b) 2304 s^{-1} and temperature of 150°C and c) at 2304 s^{-1} with temperature of 130 and 110°C.

While the extrudate at low shear rate shows a very smooth and regular product, at higher shear rate the morphology is very irregular and it shows also the sticky effect of the melt with the previous emerged material. Almost the same tendency can be seen at lower temperature (130 and 110°C), where, even if the sticky effect is lower, the morphology of the extrudate is characterized by deformation at higher shear rate. This kind of deformation could be due to the strong effect of shear stress at higher extrusion rate, which causes flow instability[112]. It is possible to observe in EVA that there are not any effects of sharkskin both at lower and higher shear rate, with the exception of the extrudate at 110°C, where the slight roughness would be caused by the local friction of the surface material during slippage at the capillary wall (common at lower temperature). The absence of evident sharkskin on EVA extrudates is in agreement with what is known about polyolefin extrusion, because usually the sharkskin phenomenon influences

polyolefin materials composed by linear macromolecules[112], as those obtained by Z-N catalysts and metallocene, while EVA is produced by radical polymerization and it is composed by branched macromolecules.

In Figure 3.1.3.7 the effect of incorporation of natural magnesium hydroxide in EVA at 40 vol% on surface morphology is shown.

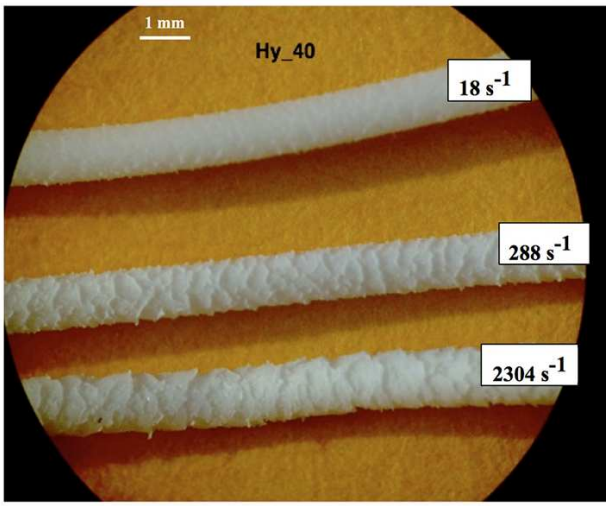

Figure 3.1.3.7: Hy_40 extrudates at different shear rates.

It is believed that the introduction of a filler in a polymeric matrix takes to the reduction of deformation[110]: this is true also for Hy composite, where the incorporation of filler makes the extrudates more compact and without the flow instability effects of EVA extrudates at high stress, as it has been shown also in the scheme of Figure 3.1.3.4. However it is possible to observe that the introduction of 40 vol% of Hy gives rough surface of the extrudate and this effect is enhanced with increasing the shear rate. The same shear rate effect is obtained for the other fillers, both synthetic and natural ones. At high shear stress, the phenomenon can be classified as melt fracture due to the evident periodic defects, while it is difficult to classify clearly the Hy_40 surface fracture at low shear rates as sharkskin. For this reason the surface of the extrudates is analysed and compared in terms of surface roughness and aesthetic quality.

The synthetic aluminium hydroxide effects on its composite extrudate morphology can be seen in Figure 3.1.3.8.

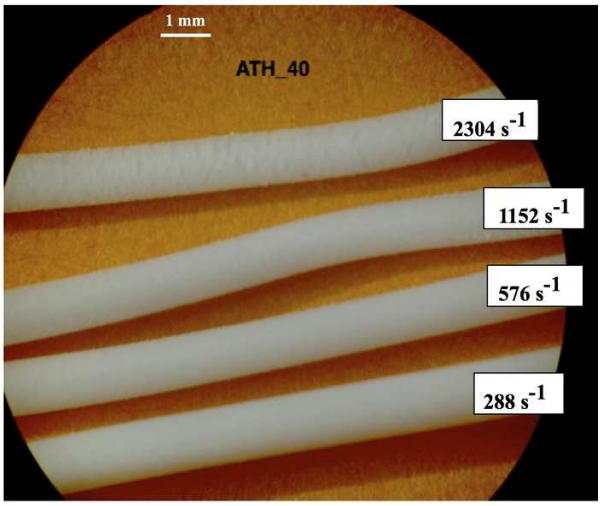

Figure 3.1.3.8: ATH_40 extrudates at different shear rates.

Even for ATH_40 composite, which could be considered the "reference material" for surface morphological quality of extrudated composite, the surface becomes rough at the highest used shear rates (2304 and 1152 s^{-1}). However, ATH_40 compound shows smooth surface of extrudate at quite high shear rate (576 s^{-1}) confirming its better aesthetic properties than Hy_40.

In Figure 3.1.3.9 the extrudates of all the studied composites at 40 vol% are reported in order to appreciate the main differences among them. It has been chosen to study the morphology of the extrudates at the lowest shear rates because the extrusion rates used for cable production as industrial reference are from 10-20 s^{-1} until 200-300 s^{-1}, depending on the cable part and type[113]. Furthermore, the main differences in morphology caused by filler properties could be observed at the lowest shear rates, where the flow and hydrodynamic interaction are less effective than the intrinsic composite properties.

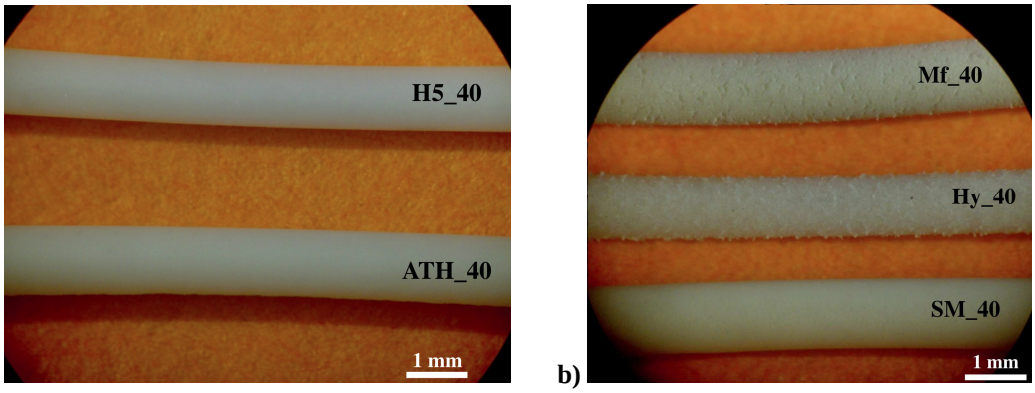

Figure 3.1.3.9: Extrudates of composites with a) synthetic fillers and b) natural fillers obtained at 18 s^{-1} apparent shear rate and T=150°C.

The incorporation of synthetic fillers and calcium carbonate leads to regular and smooth external morphology, confirming that the regularity of the shape and particle size distribution of the filler are very influent also on the extrudate surface properties.

Observing Hy_40 extrudate the main evidence is that it is rough even at the lowest shear rate used in this study. A similar behaviour could be found for Mf_40. In SEM backscattering micrographs of Figure 3.1.3.10 it is possible to see that, even if the extrudate are both rough and they take almost to the same tactile sensation, the nature of roughness is not the same: Hy_40 shows "waves" deformation on the surface, while Mf_40 looks less warped but with holes and ruptures on the skin.

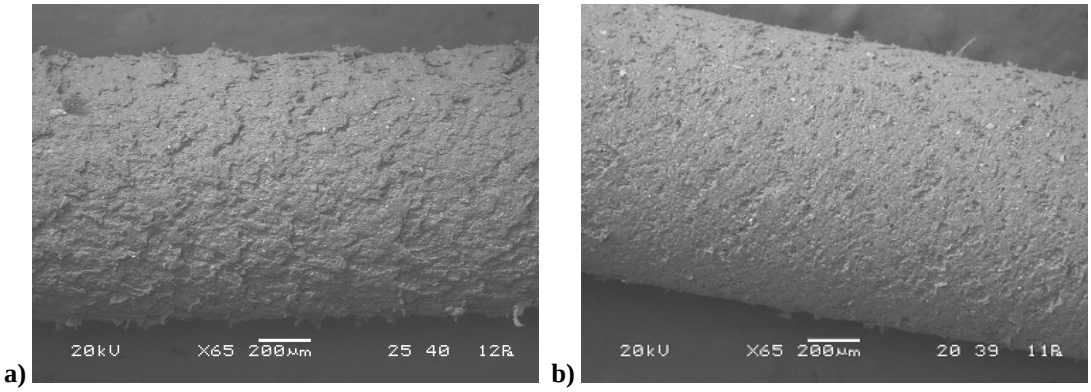

Figure 3.1.3.10: SEM backscattering micrographs (×65) of extrudates obtained at 18 s^{-1} apparent shear rate e T=150°C of a) Hy_40 and b) Mf_40.

In Figure 3.1.3.11 the SEM backscattering micrographs of the same surfaces are reported at higher zoom values for a deeper evaluation of the filler effect.

a) 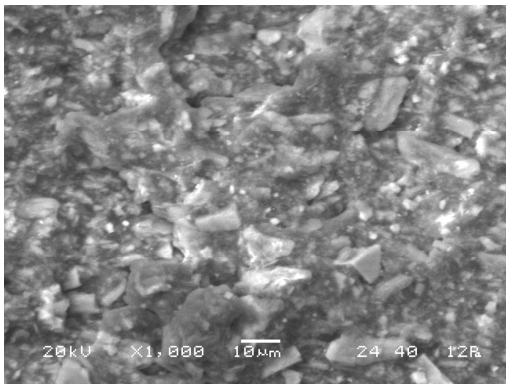

b) 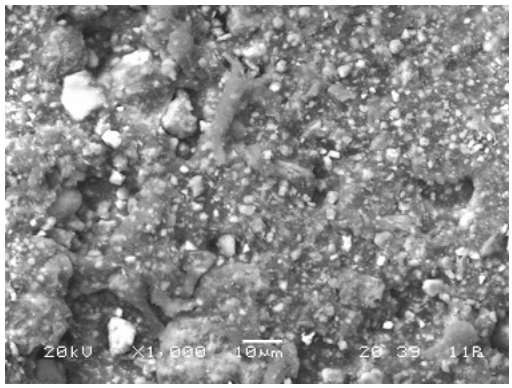

Figure 3.1.3.11: SEM backscattering micrographs (×1000) of extrudates obtained at 18 s^{-1} apparent shear rate e T=150°C of a) Hy_40 and b) Mf_40.

It should be observed that in Hy_40 the filler-matrix adhesion is strong and the material looks homogeneous, while in Mf_40 the adhesion between filler and matrix is not complete especially with the biggest particles, creating defect points on the surface. Ariffin et al.[110] studied the effects of talc and calcium carbonate on PP melt elasticity phenomenon and they found that talc (aspect ratio > 1) could orientate along the melt flow together with the polymer chains, improving filler-matrix interaction and creating a less deformable extrudate than $CaCO_3$ (aspect ratio ≈ 1). In our case, natural magnesium hydroxide could interact more strongly with EVA matrix than Mf especially due to its particle shape (average "needle-like" shape) and, as in the case of talc, it can create a more compact surface on the extrudate than magnesium carbonate.

The main different aspect between talc used by Ariffin et al. and natural magnesium hydroxide of this work is the irregularity of Hy particles, which could make the difference on surface morphology. In fact talc incorporation in PP composite took to better aesthetic quality of extrudate than $CaCO_3$, whilst in our case Hy composite shows the worst surface almost in the same condition (γ, T, ϕ, etc). The particle shape irregularity seems to be the most influent factor on the surface roughness of Hy composite extrudates, which could be considered a problematic feature of its industrial use for cable application.

Control of surface aesthetic quality for Hy composite

In order to find how the surface of Hy composite extrudates could be better, the changes on the surface morphology have been verified by modifying the following conditions: temperature, filler loading and mixing with another filler. No attempt to change the filler

surface or to use interfacial additives has been carried out, because it does not concern this PhD thesis research.

In Figure 3.1.3.12 the extrudates of Hy_40 obtained at the lowest shear rate at different temperatures are reported in comparison with those of Mf_40 because they represent the composites with the problematic extrudate morphology.

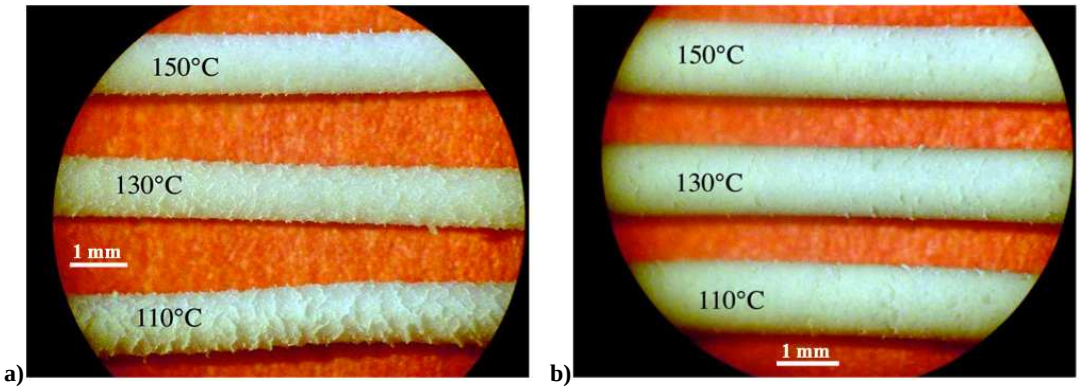

Figure 3.1.3.12: Extrudates at 18 s^{-1} at different temperatures of a) Hy_40 and b) Mf_40.

It can be observed that the surface of Mf_40 does not change so much with decreasing temperature, showing almost the same fracture effect; Hy_40 composite shows, instead, small cracks on surface at 150°C, which increase in amplitude at 110°C pointing out that surface morphology of Hy composite becomes better by increasing temperature. The improvement of surface quality on Hy sample can be due to the relative low elastic recovery and the high mechanical restraint of the material at higher temperature, which reduce its surface roughness at the exit of the die. This kind of effect could be more definite in Hy_40 than in Mf_40 because of the lower polymer-filler adhesion noticed for magnesium carbonate composite.

The effect of Hy loading has been also evaluated and the extrudates at different volume percentage of filler are shown in Figure 3.1.3.13.

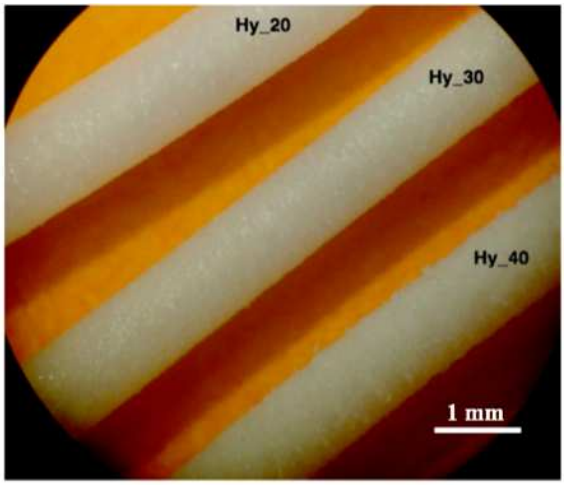

Figure 3.1.3.13: Extrudates of Hy composites at different volume percentage of filler (150°C and 18 s^{-1}).

Decreasing Hy amount in the composite, the surface of extrudate appears smoother and more coherent. However it does not reach the aesthetic quality of the synthetic filler composites (Figure 3.1.3.9). As it is possible to appreciate comparing the SEM backscattering micrographs in Figure 3.1.3.14, the irregular shape of Hy particles influence deeply the surface aspect of the extrudates, even at lower filler total amount (20 vol%).

a) 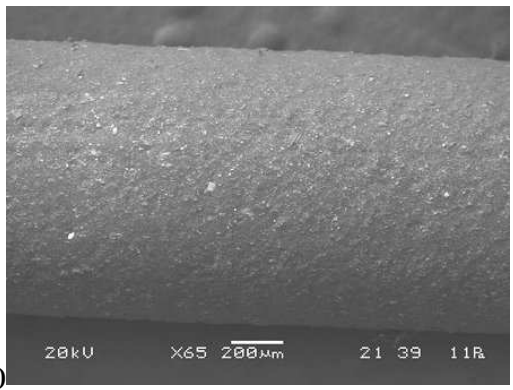

b) 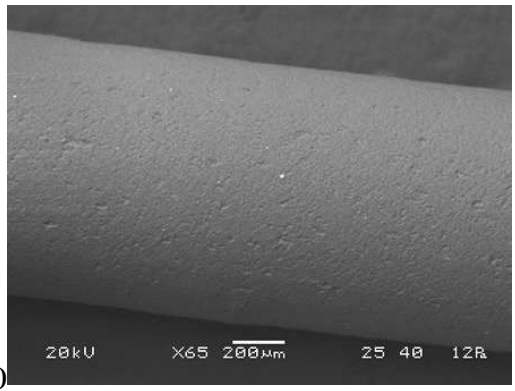

Figure 3.1.3.14: SEM backscattering micrographs (×65) of extrudates obtained at 18 s^{-1} apparent shear rate e T=150°C of a) Hy_20 and b) ATH_40.

The last attempt regards with the mixing of different percentage of Hy with the synthetic aluminium hydroxide in order to evaluate how the natural filler influences the surface morphology in combination with the reference filler for extrudate surface quality. Mixtures of magnesium and aluminium hydroxide used as filler (for composite) has also great applicative interest because they are already used in combination due to their synergistic flame retardant effects[114, 115].

In Figure 3.1.3.15 the photos of the extrudates at different ratio of Hy/ATH (with 40 vol% as total volume percentage of filler) are reported.

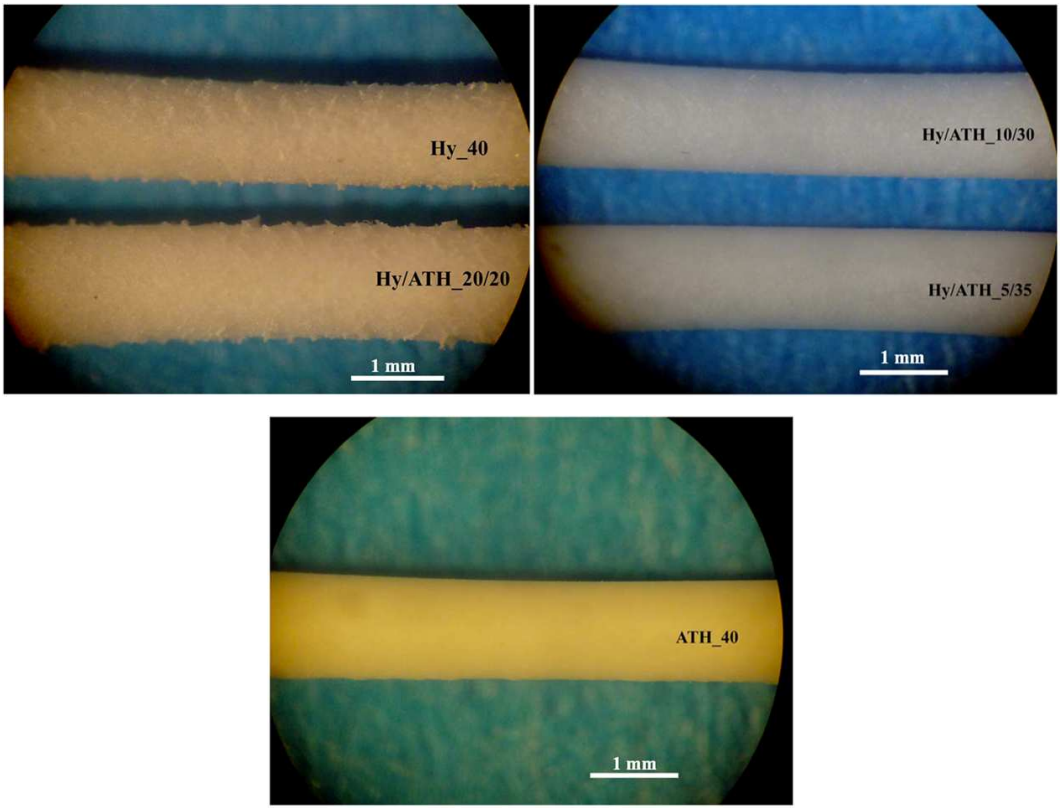

Figure 3.1.3.15: Extrudates of composites filled with 40 vol% of mixture of Hy and ATH at different ratio (150°C and 18 s^{-1}).

The influence of Hy incorporation is very low at small percentage (composition with ratios 5/35 and 10/30), while a rough and inhomogeneous surface can be appreciated in the composition with ratio 20/20 as a result of Hy presence. At percentage lower than 50% as filler mixture the synthetic hydroxide could hinder the natural Hy effect. It is possible to deduce that the combination of Hy with fillers, whose composites are characterized by good aesthetic quality, can take to acceptable results in terms of extrudate morphology if the Hy amount is less than half of the total amount of filler (around 60 wt%). This could be considered a possible stratagem for the applications, which need good surface of products allowing the mixing of different fillers and so decreasing the cost of materials.

3.1.4. Mechanical properties of the highly filled EVA compounds

The analysis of mechanical properties of composites has been carried out in order to evaluate the main influences of natural magnesium hydroxide properties Hy in comparison with the use of the other synthetic and natural fillers (H5, ATH, Mf and SM). Despite the high amount and the irregular properties of the studied natural fillers (wide size distribution, irregular particle shapes, etc) some attempts of results rationalization have been done according to previous works on mechanical behaviour of composites.

The representative stress-strain curves of EVA matrix and related composites at different Hy content are depicted in Figure 3.1.4.1.

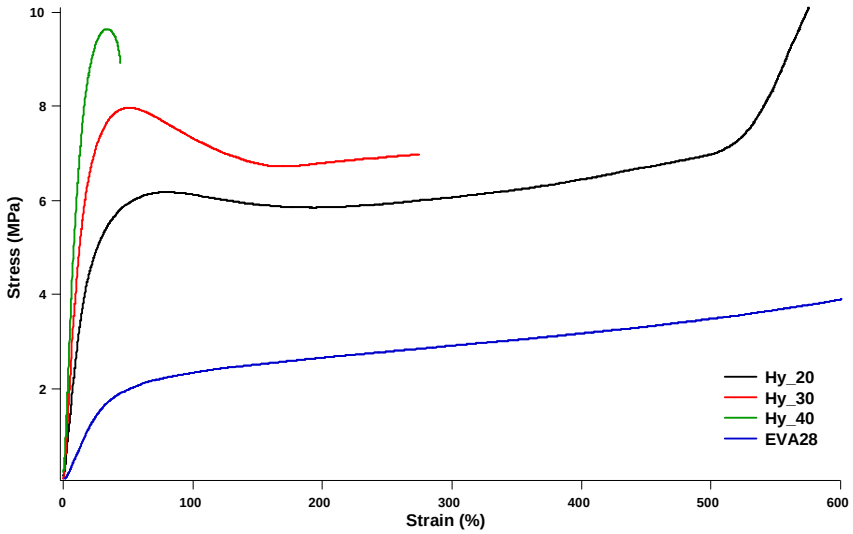

Figure 3.1.4.1: Stress-strain curves of EVA and Hy composites at different filler loading.

In agreement with what is already reported[12, 116], the introduction of filler, like natural magnesium hydroxide, leads to an increase of Young's modulus, yield strength and a decrease of elongation at break with increasing filler content. In particular the elongation at break seems to remain quite high also at 30 vol%, but when the filler loading becomes higher its reduction is really drastic.

In Figure 3.1.4.2 representative stress-strain curves of the composites filled with 40 vol% are reported: Hy composite shows different trend, corresponding to different tensile behaviour compare to the other composites. For a better comprehension of differences and properties, Young's modulus, tensile strength and elongation at break results have been analysed.

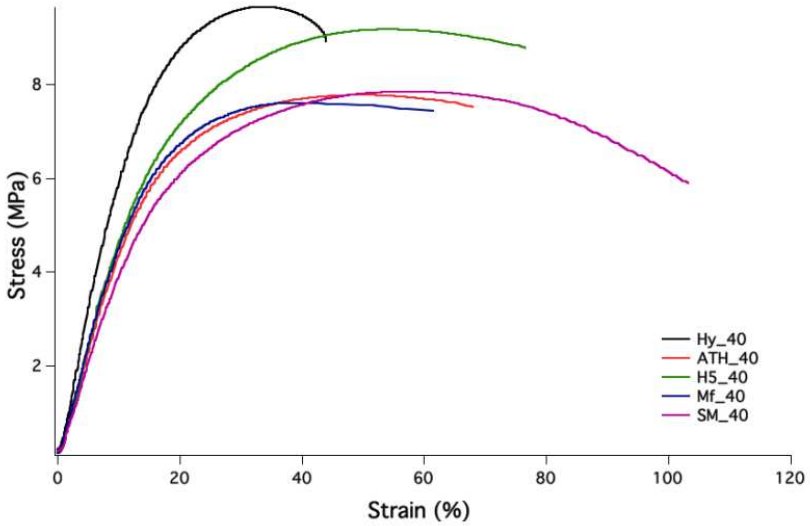

Figure 3.1.4.2: Stress-strain curves of the composites with 40 vol% of different fillers.

The dependence of Young's modulus of all the chosen composites on volume fraction of the filler is shown in Figure 3.1.4.3. The relative Young's modulus is used for describing Young's modulus dependence on the filler content and it can be expressed as:

$$E_{rel} = E_c / E_m$$

where E_c and E_m are respectively the Young's modulus of the composite and the matrix.

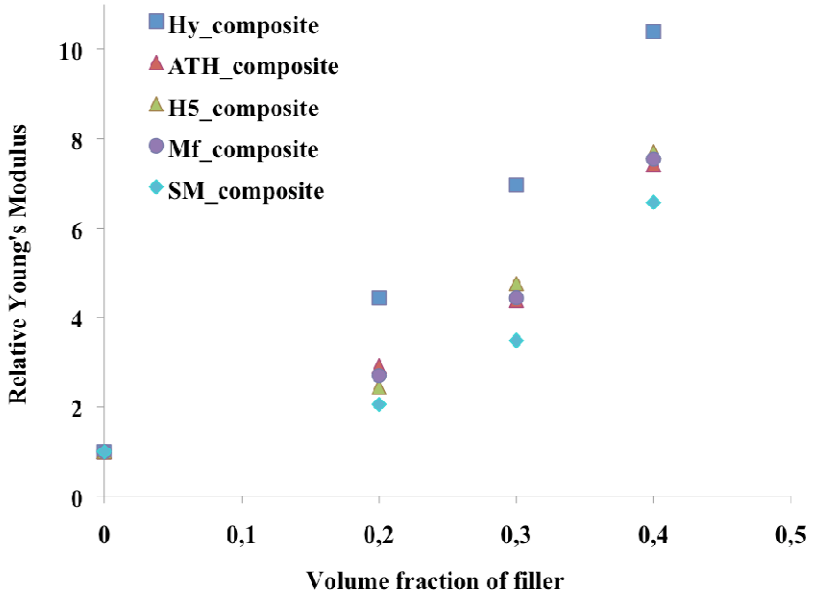

Figure 3.1.4.3: Dependence of the relative Young's modulus of the EVA composites on the filler content.

The obtained results are in agreement with what has been indicated by previous work[117], cause in general relative Young's modulus increases with increasing filler content and this is attributed to the higher modulus and stiffness of inorganic particles in respect to polymer matrix. Among the analysed samples, Hy composite exhibits the highest increase with filler loading.

In Figure 3.1.4.4 tensile yield strength results obtained for the analysed composites are shown. The tensile yield strength obtained for EVA matrix as reference is 2.2 ± 0.1 MPa.

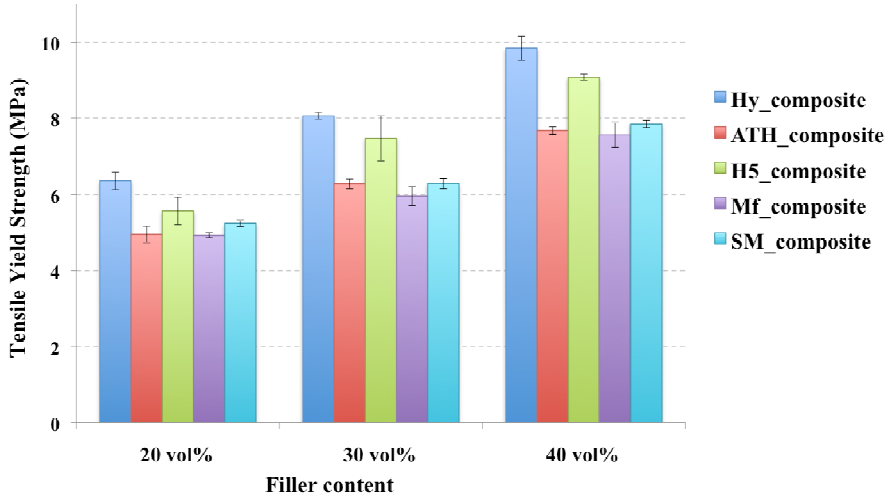

Figure 3.1.4.4: Dependence of the tensile yield strength of the highly filled EVA composites on filler volume content.

Even tensile yield strength data for all the composites increase with increasing filler loading and in particular both natural and synthetic magnesium hydroxide filled compounds show the highest values.

The different tensile yield strength values could be correlated to interfacial interaction between polymer matrix and filler. Pukanszky and coworkers[26] reported a semi-empirical correlation as an attempt for estimating the matrix-filler interfacial adhesion:

$$\sigma_c = \sigma_m \left(\frac{1-\phi_f}{1+2.5\phi_f} \right) \exp(B_y \phi_f)$$

where σ_c and σ_m are respectively the yield stress of the composites and the polymer matrix, ϕ_f is the volume fraction of the filler and B_y is the empirical parameter related to the stress transfer and proportional to the interfacial adhesion. The equation is based on volume fraction dependence of the tensile yield strength in heterogeneous polymer materials.

The correlation has been applied on the obtained results for EVA composites as an attempt to have an indication of the modification of matrix-filler interaction by introducing the different fillers. In Figure 3.1.4.5 the linear plots of ln(x), which corresponds to $\ln\left[\sigma_c(1+2.5\phi_f)/\sigma_m(1-\phi_f)\right]$, versus the filler volume fraction are reported for Hy and ATH composites as examples.

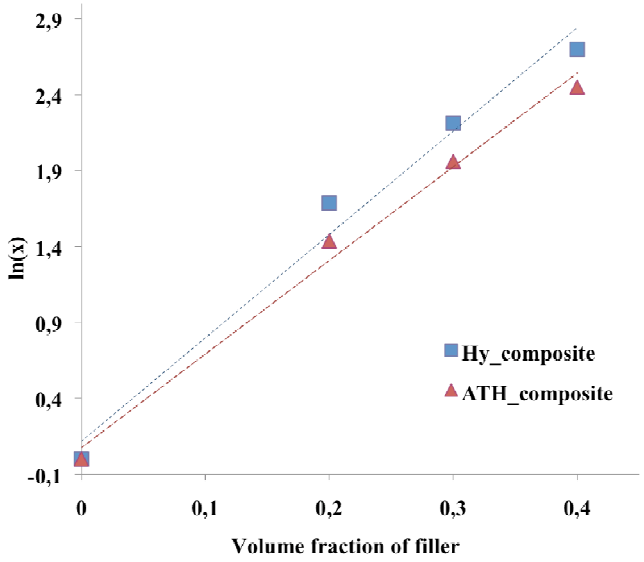

Figure 3.1.4.5: Dependence of the relative tensile strength of the EVA composites on the filler volume content.

B_y parameter for all the composites has been calculated as the slope of the linear curves and the values are reported in Table 3.1.4.1.

Table 3.1.4.1: Results for the empirical parameter B_y and the corresponding R^2 of the linear fitting.

Sample	B_y	R^2
Hy_composite	6.81	0.981
ATH_composite	6.17	0.991
H5_composite	6.62	0.988
Mf_composite	6.10	0.991
SM_composite	6.20	0.987

Even if the values are close each other, the results indicate that the interfacial adhesion of magnesium hydroxide fillers are stronger than the others, and in particular the natural magnesium hydroxide shows the highest B_y value.

These results give an indication of the overall highest interfacial tension and filler-matrix interaction of the natural Hy, which could be due to combination of high specific surface area, high particle size distribution and average shape of the particles. For this reason Hy seems to be the most reinforcing filler among those used for samples preparation.

The application of this model to the composites indicates also that SM composite should have almost the same interfacial interaction of ATH composite. This is an opposite indication in respect to the Young's modulus analysis, higher for ATH than for SM composites. This result could be clarified by considering the different trend of the stress-strain curve (Figure 3.1.4.2): SM_40 has the lowest stress in the first part of the curve and it reaches higher elongation at yield than ATH_40, where the tensile strength values of these two compounds become almost the same.

The limit data[118] of maximum elongation at break for the composites depending on the filler volume fraction are reported in Table 3.1.4.2. The obtained result of elongation at break for EVA matrix is around 1000%.

Table 3.1.4.2: Elongation at break of the composites expressed as limit data*.

Volume fraction	Hy composite	ATH composite	H5 composite	Mf composite	SM composite
0.2	> 600 %	> 800 %	> 800 %	> 800 %	> 800 %
0.3	> 200 %	> 400 %	> 400 %	> 400 %	> 600 %
0.4	≈ 40 %	≈ 80 %	≈ 70 %	≈ 70 %	≈ 90 %

* The elongation at break values for highly filled composites are affected by high error values and the limit data are used to give the indicative idea of elongation behaviour of the samples.

The general trend of the results is the decrease of the maximum elongation with increasing filler loading for all the composites. It is also interesting to underline the significant reduction of the elongation capacity when the composition of 40 vol% is reached.

As it could be expected, Hy composite shows the lowest limit data of elongation at break for all the compositions. Even at 20 vol% of filler content, while all the other composites could get elongation results higher than 800%, Hy_20 reaches a lower elongation limit (600%). The reduced deformability of EVA matrix in Hy composite is probably due to filler-matrix interaction: adsorbed polymer chains on particles surface lead to higher

rigidity (as indicated also by the higher Young's modulus for these compositions), which leads to earlier fracture initiation and propagation[117, 119].

Figure 3.1.4.6 shows SEM micrographs of fracture surface section of the composites Hy_20 and H5_20 after tensile measurement. They are reported for a comparison between the different fracture morphologies that the chosen natural and synthetic magnesium hydroxides can create inside the composites.

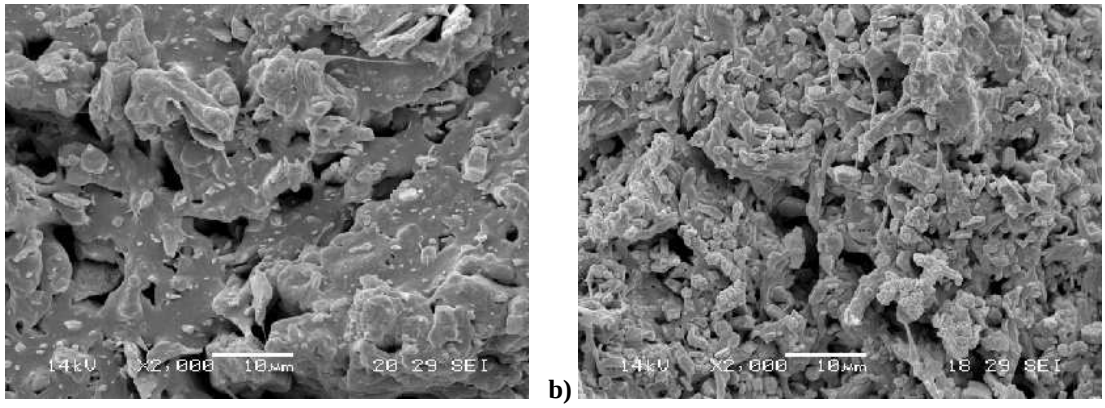

Figure 3.1.4.6: SEM micrographs of the fracture surface section of a) Hy_20 and b) H5_20 composites after tensile measurement.

H5_20 sample is characterized by evident proof of plastic deformation of the matrix: even if the filler content is high, the ligaments surrounding the filler particles are still deformable, creating a "fibril-like" structure which is strictly related to the high elongation limit data obtained. In this case more agglomerates of particles could be found than in Hy_20, as indicated by the theoretical approach on rheological properties (paragraph 3.1.2.1).

On the contrary, for Hy_20 fracture section, no significant plastic deformation can be observed due to the limited molecular chain mobility during tensile measurement. Analysing the micrograph relative to Hy_20 it is possible to highlight even that the polymer matrix looks like "cut" in many points of the fracture surface. This could lead to a second factor responsible for the lower elongation at break of Hy composite: Hy particles, with their long and irregular shape, could act as blades thereby helping the formation of crack points and their propagation.

However the elongation property of Hy composite could be improved by the use of filler surface treatment as reported for other fillers[91, 120-123]. Specifically in a previous work[94] it was found that the use of an organic treatment on a natural magnesium hydroxide

(produced by the same company with the same process, but characterized by lower average particle size than Hy) led to higher maximum elongation data of the EVA based composites than the incorporation of the virgin filler (respectively ≈ 120% and ≈ 60%). It was also confirmed that an increase in elongation at break for the coated-filler composite takes to a decrease of yield strength (from 16 to 10 MPa). It can be pointed out that a possible improvement of deformation property for Hy composite with an organic coating would damage its reinforcing performance.

3.1.5. Thermal degradation behaviour of highly filled EVA composites

The evaluation of the effects that the natural fillers Hy, Mf and SM on thermal degradation of poly(ethylene-co-vinyl acetate) have been performed by TGA-FTIR analysis. The measurements have been carried out from 50 to 1000°C at heating rate of 20°C/min in order to obtain good compromise between the TGA and FTIR analysis on evolved gases. In fact a slow heating rate is good from TGA point of view because it avoids overlapping of degradation steps when they happen at close temperatures, but according to Berbenni et al.[124], high heating rate is necessary to achieve the best quality of FTIR results.

3.1.5.1. TGA study of the natural fillers (Hy, Mf and SM) influence on EVA thermal degradation

It is widely reported that the thermal degradation of unfilled poly(ethylene-co-vinyl acetate) takes place in two steps, which change slightly with the vinyl acetate content. The first one occurs mainly between 315 and 415°C and it corresponds to the deacylation of the vinyl acetate groups in EVA. The second step is attributed to the degradation of the hydrocarbon chains and it occurs in the range of 415-530°C. In the case of EVA matrix with vinyl acetate content of 27.7 wt% the deacylation stage results in a weight loss of around 19%. All these information can be found in Figure 3.1.5.1.1, where TGA curve is reported together with those of Hy composites.

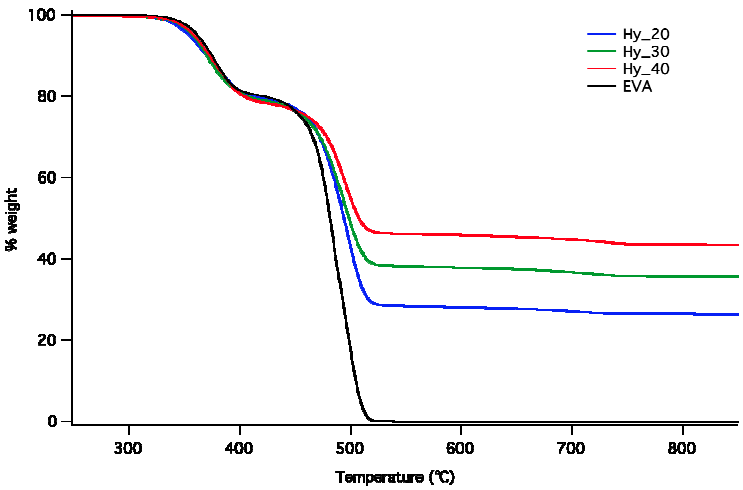

Figure 3.1.5.1.1: TGA curves of EVA and Hy composites at different filler content (N_2, 20°C/min).

By comparing the TGA curves, it is observed that the decomposition of the Hy filled composites seems to follow the same trend for the first step of degradation, while the composites are slightly more stable in the second step and the thermal stability increases with the filler content. Finally it is possible to see a third step of degradation, related to the decomposition of magnesium and calcium carbonate in the range of temperature 550-750°C.

The similarity between EVA and Hy composites curves during the first step of degradation is due to the dehydration of magnesium hydroxide, which is anticipated in the composite, as can be observed in the Figure 3.1.5.1.2 where the derivative TGA curve of Hy_40 is compared with those of EVA matrix and the filler Hy.

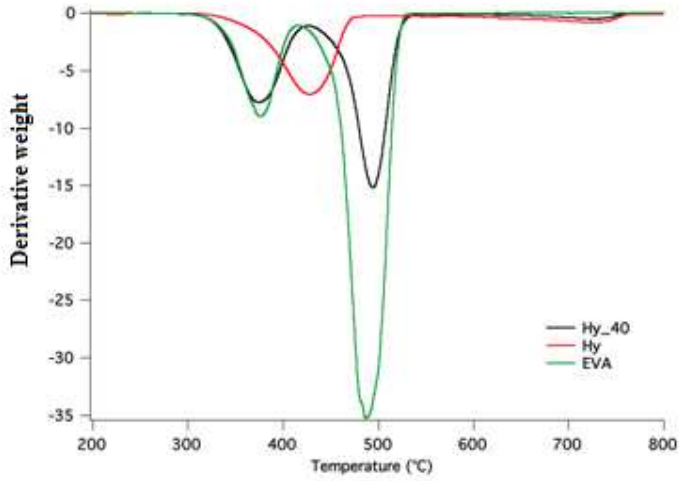

Figure 3.1.5.1.2: DTG curves of Hy_40 compare with EVA and Hy curves (N_2 ,20°C/min).

It has already reported that in EVA composites, filled with magnesium hydroxide, the loss of acetic acid from the polymer and water from hydroxide occur almost at the same temperature and this is one of the factors makes magnesium hydroxide an effective flame retardant additive for EVA compounds[5].

The experimental TGA curves of EVA, Mf_40 and SM_40 are reported in Figure 3.1.5.1.3, together with the calculated TGA curves in order to highlight the effects of magnesium and calcium carbonate in EVA during the degradation process.

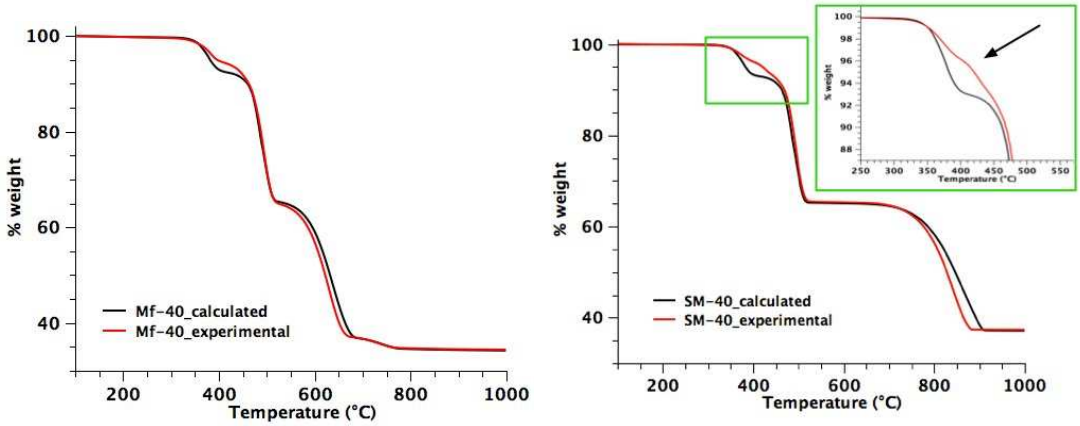

Figure 3.1.5.1.3: Comparison between experimental and calculated TGA curves of Mf_40 and SM_40 composites (N_2, 20°C/min).

This kind of approach takes in account a linear combination for predicting the thermal behaviour of the composites, assuming no interactions between the filler and the matrix: their theoretical TGA curves can be obtained by the sum of the component curves multiplied by their weight fraction[125]. The calculated curves are obtained following the mixture equation:

$$M_{theo}(T) = x_{filler} \cdot M_{filler}(T) + x_{polymer} M_{polymer}(T)$$

where M_{filler} and $M_{polymer}$ are the experimental TGA curves of the filler and the polymer matrix respectively, while x_{filler} and $x_{polymer}$ are the weight fractions. The differences between the calculated and the experimental curve point out the possible effects coming out by filler-polymer interaction. In Figure 3.1.5.1.3 it is possible to appreciate a shift towards higher temperature for the first degradative step for both Mf and SM composites. This could be in witness of the interaction between filler and polymer, corresponding to higher thermal stability of the composites compare to the theoretical curve. The result is in agreement with what reported by previous work on the use of filler in polyolefin compounds[126]. In this specific case of EVA matrix the enhanced stability characterized

mostly the step of acetic acid loss. In particular SM_40 experimental TGA curve shows the presence of a weak additional step during the loss of acetic acid, which is highlighted in the zoomed area.

In Figure 3.1.5.1.4, where the derivative curve of TGA of Mf_40 and SM_40 are reported in comparison with that of pristine EVA, sample Mf_40 shows the two steps corresponding to EVA degradation with maximum rate of weight loss ($T_{max\ rate}$) at 382° and 493°C and further two steps due to thermodegradation of magnesium carbonate and calcium carbonate impurities ($T_{max\ rate}$ of 629° and 735°C).

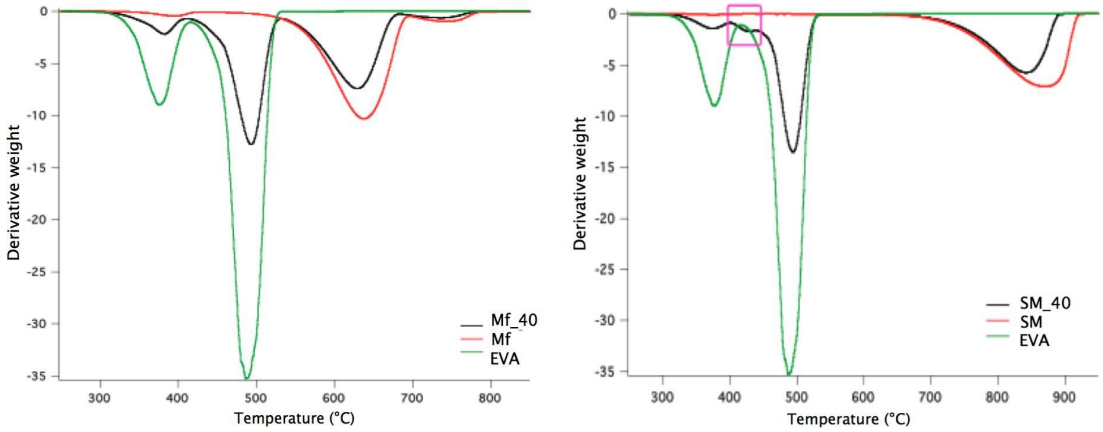

Figure 3.1.5.1.4: Derivative curves of TGA of EVA matrix, Mf_40 and SM_40 composites (N_2, 20°C/min).

Observing the DTG of SM_40 a shoulder with minimum at 429°C appears in addition to the expected peaks of EVA degradation (maximum rate at 373° and 494°C) and calcium carbonate degradation ($T_{max\ rate}$= 843°C). The presence of this additional peak on DTG curve could indicate a new degradation step in calcium carbonate composite, which happens between the loss of acetic acid and the pyrolysis of residual hydrocarbon chains.

3.1.5.2. FTIR study of the evolved gases during thermal degradation of natural carbonates SM and Mf filled EVA composites

The thermal degradation behaviour of the composite SM_40 has been more deeply analyzed in order to understand what happens during the further degradation step found in the TGA at 429°C and so deduce how the incorporation of natural calcium carbonate should influence the EVA degradation behaviour. For this kind of study, the combination of thermo-gravimetric analysis or laser Pyrolysis and Fourier transform infrared

spectroscopy (FTIR) can be employed[127]. These techniques are considered good for probing the chemical species in the gases evolved during thermal degradation[128, 129], giving information about the composition and the rate of emission of the species in the time of analysis. In particular, in addition to the FTIR spectra of the evolved gases, it is possible to evaluate the Gram-Schmidt curve (G-S), a reconstruction of the acquired interferograms based on vector analysis, which shows the trend of the total ejected gases detected by the spectrometer, and the three dimensional diagrams, which show the absorbance corresponding to the vibrational modes versus the wavenumber and versus the time. In this specific study the three-dimensional diagrams are reported as 2D-maps (absorbance is reported as colour intensity) because they give a more clear qualitative picture of the overall evolution of the FTIR spectra[130].

In Figure 3.1.5.2.1 the DTG curve and the corresponding Gram-Schmidt (G-S) infrared thermogram obtained for the SM_40 composite are reported.

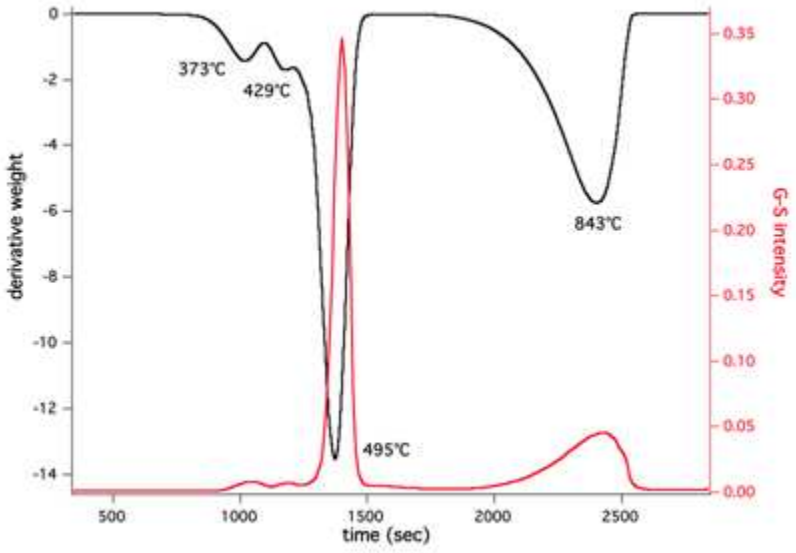

Figure 3.1.5.2.1: Derivative curve of TGA (black line) and Gram-Schmidt thermogram (red line) of SM_40 composite.

The G-S thermogram shows a trend versus time, which seems to correspond completely to the minimum peaks of the DTG curve. This result indicates that even by evaluation of the evolved gases, two peaks appear in the first part of G-S curve for composite degradation, corresponding to the DTG peaks at 373° and 429°C.

The 2D-maps of evolved gases for pristine EVA and SM_40 is shown in Figure 3.1.5.2.2.

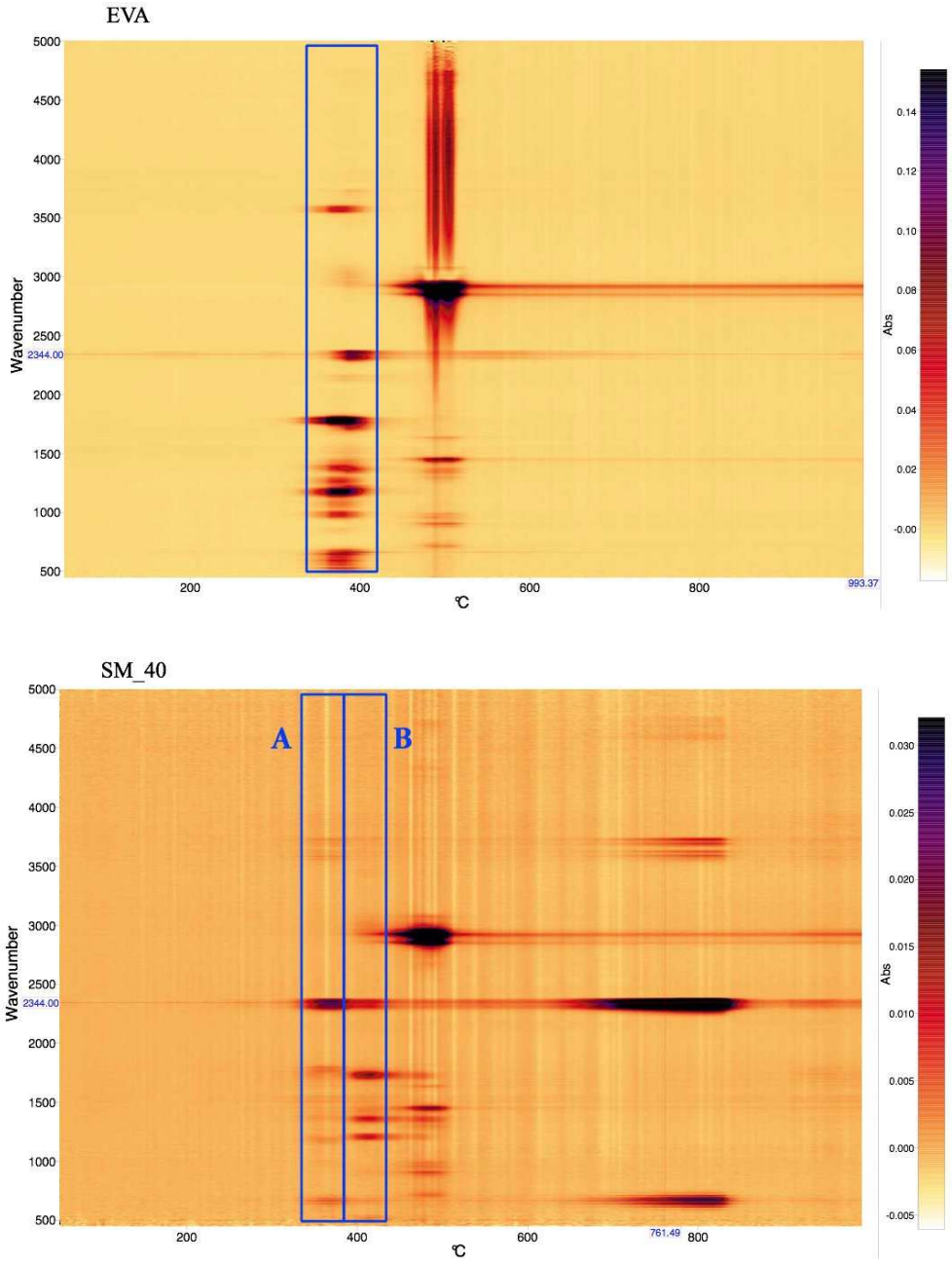

Figure 3.1.5.2.2: 2D-maps of FTIR spectra for the evolved gases of EVA matrix and SM_40 composite.

Comparing the 2D-maps related to EVA and SM_40 degradation, two events (A and B) can be clearly observed in the composite map in the range of 900-1300 seconds, together with the shift of some FTIR signals. The second step, corresponding to pyrolysis, is almost the same for both the samples, except for the higher absorbance of signals in EVA 2D-map. The FTIR shift of the signals should indicate the evolution of different species during the first (A) and the second (B) degradation steps of SM_40 composite.

In order to analyse better the evolved gases, the FTIR spectra obtained at the maxima of the Gram-Schmidt thermogram have been selected in the range of temperature between 300 and 450°C. In Figure 3.1.5.2.3 the spectra at 373°C and 429°C for SM_40 are compared with the spectrum at 376°C for EVA.

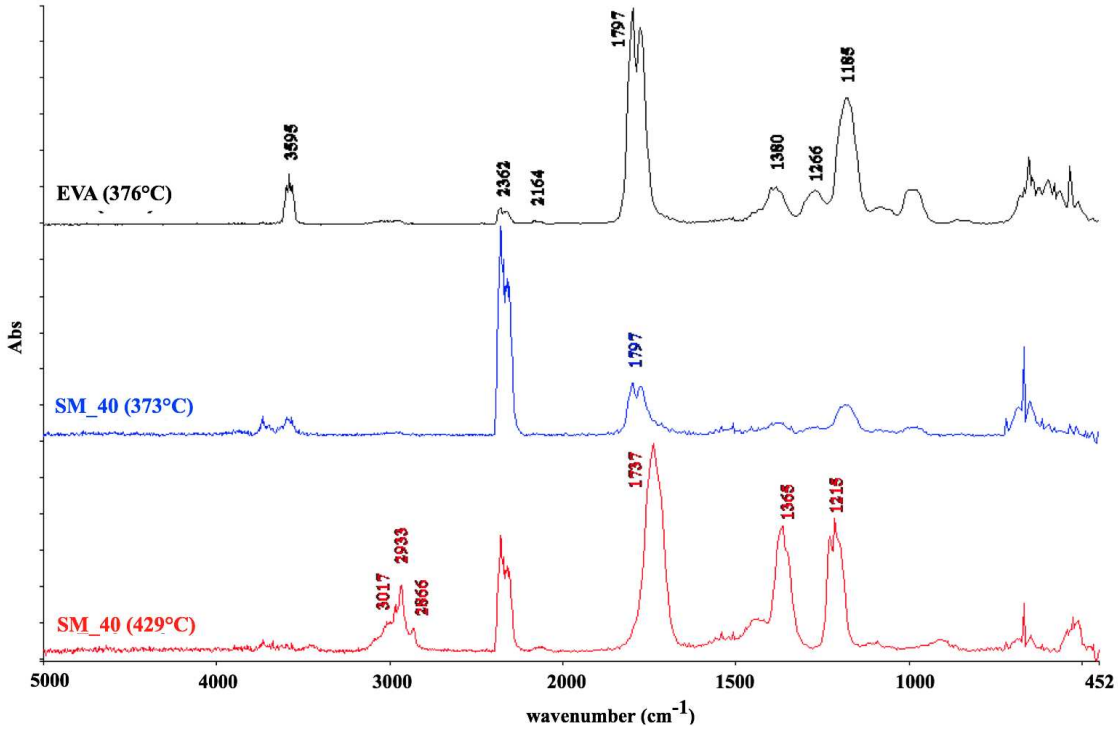

Figure 3.1.5.2.3: FTIR spectra of the gases obtained at the maxima of Gram-Schmidt profiles of EVA (at 376°C), and of SM_40 (at 373°C and 429°C).

The spectrum at 376°C for EVA matrix corresponds primarily to acetic acid, with the typical bands at 3595, 1797, 1380, 1266 and 1185 cm^{-1}. It is possible to see the presence of the signals at 2164 and 2362 cm^{-1} corresponding respectively to CO and CO_2 and the bands in the region 3000-2850 cm^{-1}, indicating the presence of small amount of CH_4. These species could indicate the secondary acetate pyrolysis, which has been already reported by thermal degradation study on EVA copolymer using heating rate higher than 10°C/min[130].

The SM_40 spectrum at 373°C is similar to that of EVA and this implies that the composition of the gaseous mixture for the first step of degradation of EVA and the composite is quite the same, in fact the typical signals of acetic acid are present. However some differences can still be envisaged: the presence of a small amount of water (band around 3700 cm^{-1}) and a huge amount of carbonic anhydride compare to

EVA. The latter result could indicate an enhancement of secondary acetate pyrolysis due to the less concentration in the evolved gases flux.

The spectrum obtained from G-S plot of SM_40 at 429°C, corresponding to the further step of degradation, shows still the presence of CO_2 and CO in small amounts and strong absorptions at 1737, 1365 and 1215 cm^{-1}. Table 3.1.5.2.1 shows the assignments of the main IR bands to vibrational modes of atomic groups found in the spectrum. On the whole, the assignments should indicate the typical vibrational modes of aliphatic ketone species, which should be the main compound in the evolved gaseous mixture.

Table. 3.1.5.2.1: Assignments of the IR bands to vibrational modes of atomic groups for the spectrum at 429°C.

Wavenumber (cm^{-1})	Vibrational mode
3017-2866	C-H stretching vibration
2359	CO_2
2150	CO
1737	C=O stretching (carbonyl)
1365	C-H bending
1215	C-C stretching

The presence of the signal at 1737 cm^{-1} (bands in the range 1740 - 1720 cm^{-1}) has been reported by previous studies on thermal degradation of pristine EVA as formation of some species with carbonyl groups different from acetic acid. Marcilla et al.[131] indicated the possibility of aliphatic aldehydes formation, but they could see the specific signals mostly when the degradation analyses were carried out in oxidative atmosphere. Sultan et al.[132] reported the presence of acetaldehyde, ketone groups and trace of lactones in the evolved gases coming from EVA degradation. In particular they justified the formation of acetaldehyde by introducing the concept of a competitive reaction for vinyl acetate decomposition, which could follow radical or molecular mechanism, taking to the formation of ketone groups on the main polymer chain instead of double bonds:

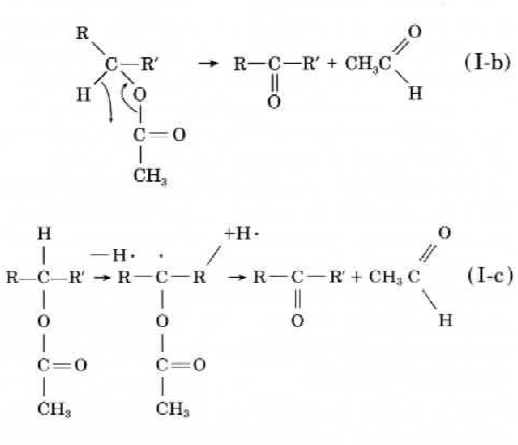

Figure 3.1.5.2.4: Schemes of reaction of acetaldehyde formation during thermal degradation of EVA taken from Sultan et al.[132] with the molecular (I-b) and radical mechanism (I-c).

In our thermal degradation study, the TGA-FTIR analysis carried out on EVA matrix doesn't show clearly the presence of carbonyl group in the evolved gaseous mixture and this could be due to an instrumental limit; furthermore none of the aldehyde bands (especially that at 2747 cm^{-1}) could be found both in the EVA and SM_40 spectra. These results point out that the formation of carbonyl functional group on the main chain of polymer could be possible and the reaction could be amplified by the presence of calcium carbonate, but there is no confirmation about this mechanism cause no trace of aldehydes could be detected.

The other possibility, which could explain the further degradation step beyond the loss of acetic acid in SM composite, takes into account that the spectrum obtained at 429°C for SM_40 could be that of a short aliphatic ketone like acetone. The spectrum of acetone (vapour phase) and the spectrum at 429°C for SM_40 are compared in Figure 3.1.5.2.5, where it is possible to appreciate the similarities of almost all the signals.

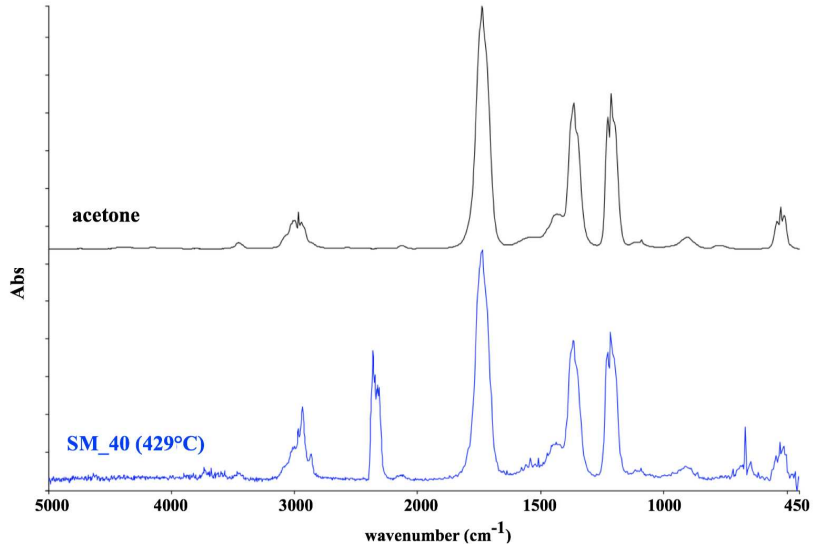

Figure 3.1.5.2.5: Comparison between FTIR spectrum of pure acetone (vapour phase) and the spectrum obtained at 429°C for SM_40 during thermal degradation.

There are many works on the thermal decomposition of different acetates or conversion of acetic acid forming acetone[133, 134]. It is known that acetone can be produced by acetate thermal decomposition[135] and the process was used for industrial production before the method of hydrolysis of cumene hydroperoxide has been introduced. In particular calcium acetate was widely used as raw material for acetone production, exploiting the reaction (temperatures around 400°C):

$$Ca(CH_3COO)_2 \rightarrow CH_3COCH_3 + CaCO_3$$

Many studies have been carried out also on the conversion of acetic acid into acetone in gas phase using different hydroxides, oxides and carbonates as catalyst. Depending on the used temperature together with the adsorptive and catalytic interactions of gas phase acetic acid with the solid surfaces, different degree of conversion could be obtained, following the reaction[136]:

$$2CH_3COOH_{(g)} \rightarrow CH_3COCH_{3\,(g)} + CO_{2\,(g)} + H_2O_{(g)}$$

In the decomposition process of the SM composite, the acetic acid released for decomposition of the vinyl acetate groups of EVA matrix, could interact with the calcium carbonate, such as a "solid surface" or probably it could form directly calcium acetate reacting with calcium carbonate. In both cases the conversion of acetic acid into acetone seems to be possible also in the EVA composite filled with calcium carbonate. In particular these mechanisms could be supported by the temperature value at which the ketone species are obtained by FTIR analysis: it corresponds to the temperature of acetic

acid conversion in the presence of the most of catalysts and to the decomposition of calcium acetate (Figure 3.1.5.2.6).

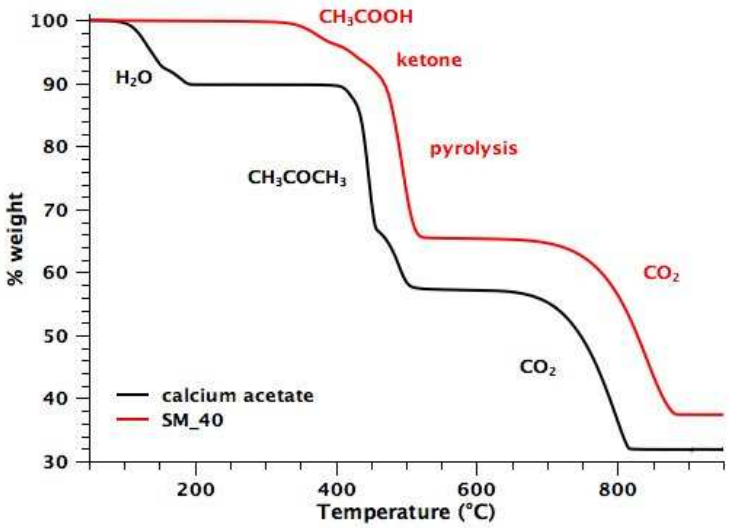

Figure 3.1.5.2.6: TGA curves of hydrate calcium acetate and SM_40 (N_2 ,20°C/min) with the main evolved species in the steps.

The FTIR analyses of the evolved gases have been carried out also on the sample Mf_40 in order to understand if magnesium carbonate could show a comparable effect to calcium carbonate on EVA degradation path. As reported previously, in the TGA curve of Mf composite no different step can be seen as in the case of SM_40 and the same trend is obtained for the G-S diagram, which does not show any further moment of gases emission (Figure 3.1.5.2.7).

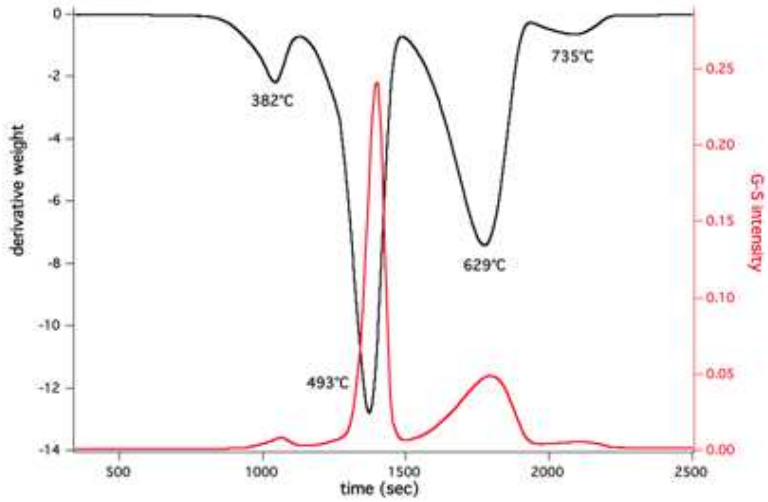

Figure 3.1.5.2.7: Derivative curve of TGA (black line) and Gram-Schmidt thermogram (red line) of Mf_40 composite.

Analysing in detail the FTIR spectra at three points of G-S plot for the first step of degradation reported in Figure 3.1.5.2.8, it can be observed that it shows some differences compare to that of pristine EVA and it changes with increasing temperature.

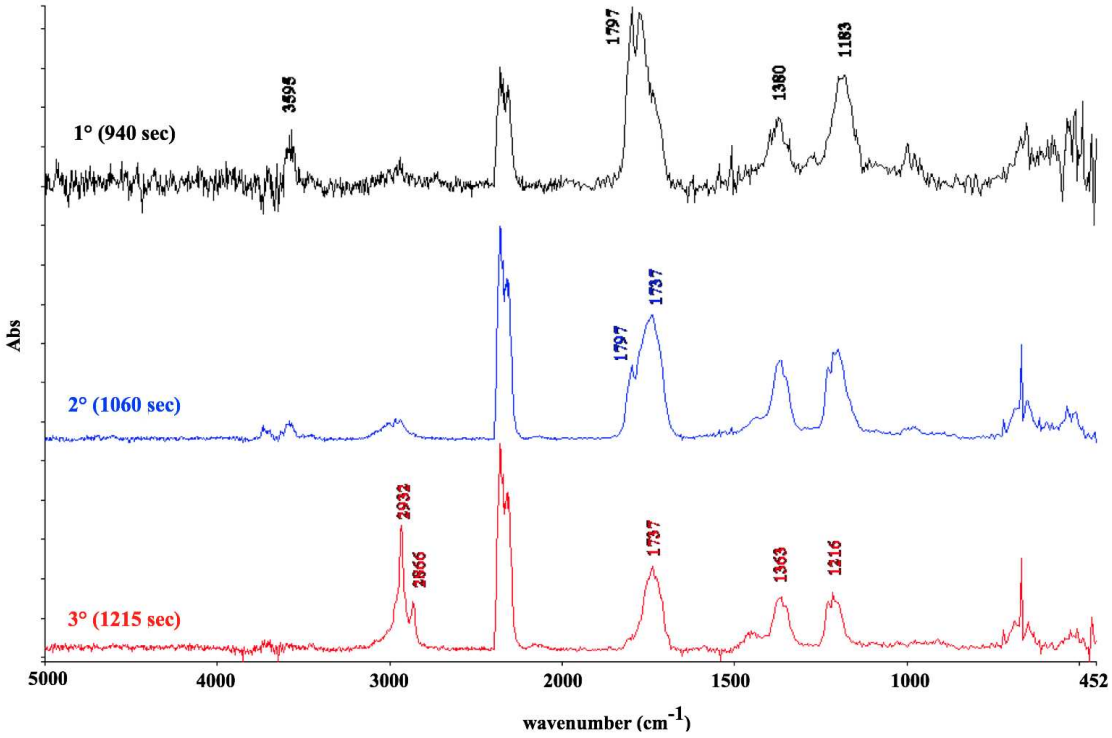

Figure 3.1.5.2.8: FTIR spectra obtained at different moments of the first degradation step for Mf_40.

The first spectrum related to the beginning of degradation indicates primarily the presence of CO_2 and acetic acid, even if the peak at 1797 cm^{-1} shows a shoulder at lower wavenumber, which is not evident in EVA spectrum (Figure 3.1.5.2.3). The second spectrum corresponds to the maximum of G-S plot and it shows a higher signal at 1737 than at 1797 cm^{-1}, together with the shift of the other main peaks (1367 and 1216 cm^{-1}): these changes indicate that the evolved gases mixture is not composed just by acetic acid, but also by species containing carbonyl group. The last spectrum taken at the end of the first degradation step is very similar to that obtained for SM_40 at 429°C (peaks at 2932, 1737, 1363 and 1216 cm^{-1}), confirming the emission of aliphatic ketones also in Mf composite. These results point out that both the calcium and magnesium carbonate show a similar effect on EVA first degradation step, with the formation and emission of ketone species, which can be detected by TGA-FTIR technique.

The main difference between the studied carbonates about the effect on EVA degradation behaviour is the temperature of formation and then of emission of the ketones. In Figure 3.1.5.2.9 the G-S plots with the absorbance intensity of IR bands related to acetic acid (1797 cm^{-1}) and ketone (1737 cm^{-1}) are reported for SM and Mf composites.

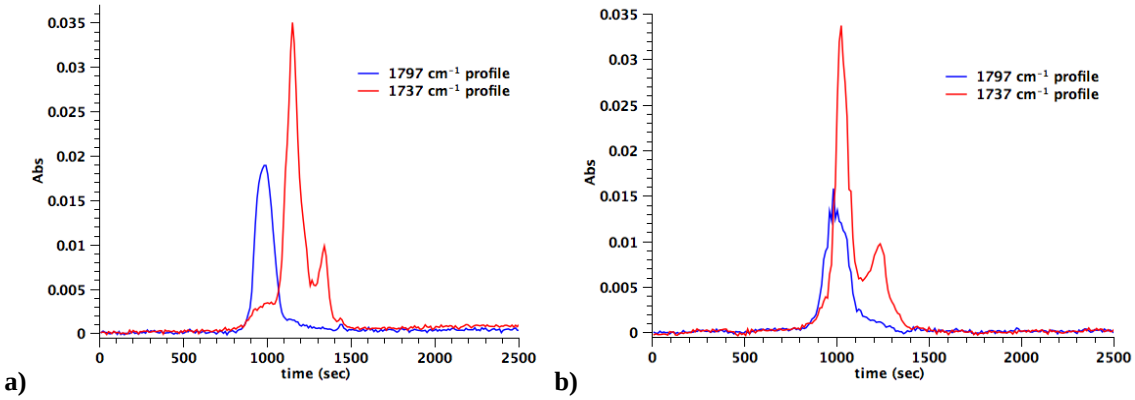

Figure 3.1.5.2.9: Gram-Schmidt profiles and absorbance intensity for acetic acid (1797 cm^{-1}) and ketone (1737 cm^{-1}) typical IR bands for (a) SM and (b) Mf composites.

As it can be observed in the Figure 3.1.5.2.9 the emission of ketone species for SM composite shows a strong delay compared to the emission of acetic acid confirming the two different moments of degradation. For Mf composite the emission of ketones is almost together that of the acetic acid, except for a little delay and presence of the second peak at higher temperature. This result should reinforce the hypothesis of acetic acid interaction with the filler and the probable acetate formation in situ during composite degradation. In fact acetic acid lost for vinyl acetate decomposition in Mf composite could be absorbed on magnesium carbonate and/or probably magnesium acetate could be formed. In this case the conversion to ketone carries out at lower temperature than that observed in the case of calcium carbonate (the decomposition temperature of magnesium acetate is around 330°C)[137], almost at the same temperature of acetic acid release.

All these results show that the introduction of both magnesium and calcium carbonate in EVA has a strong effect on the thermal degradation behaviour of the polymer, influencing the degradation path of the polymer during the first step, when vinyl acetate groups decompose and acetic acid is released. It is not possible to exclude that a similar effect happens also in the composites with Hy (and in general hydroxides), but the coexistence of dehydration reaction of the filler and acetic acid release of the polymer

makes impossible a clear analysis with this technique, cause the typical signals of water hide completely the other bands in the IR spectra.

3.2. Flame retardant properties of EVA composite filled with natural magnesium hydroxide (Hy) in combination with other flame retardant additives

It is possible to find a variety of papers in literature[138-140] on the use of different additives in combination with magnesium hydroxide in order to reduce the total filler content, improving rheological and mechanical properties, without damaging the flame retardant efficiency. Especially in case of natural magnesium hydroxide as flame retardant filler, the introduction of other additives is necessary for reducing filler amount and maintaining an acceptable flame retardant level. Despite the flame retardant efficiency of Hy is lower than H5, the natural brucite is a widely used (cheaper) alternative to synthetic MDH in halogen free flame retardant compounds for cable, roofing membranes, pipes and building panels.

Due to the huge variety of HFFR additives have been used in combination with magnesium hydroxide (paragraph 1.3.1 of Introduction) it has been decided to direct the research of the second part of this PhD thesis on methods for parameterization of burning behaviour, for screening among a series of FR additives in combination with Hy and then for rationalizing flame retardant mechanism of a specific selected combination. In literature, the most of the studies can be found on flame retardant additives for polymers, deal with the combination of two or three of them and usually the research methods follow "trial and error" approach. In this way the analysis of all the properties and influencing factors for a flame retardant system can be a complex and time-consuming process due to the large number of experiments required for obtaining information. However during the last decades, statistical approaches have been applied even to the analysis of flame retardant properties in order to provide efficient framework for systematically gaining information about the burn behaviour of polymer systems[141-144]. Concerning this research, statistical approach has been applied especially for the evaluation of a specific flame retardant system due to the necessity of finding fast, indicative and representative methods required by both the scientific and applicative research.

3.2.1. Flame retardant characterization of EVA composite with natural magnesium hydroxide (Hy)

The flame retardant efficiency of EVA based composites filled with the natural magnesium hydroxide Hy in comparison with the synthetic magnesium hydroxide H5 has been evaluated with Limiting Oxygen Index (LOI) and cone calorimeter test. The filler content of the composites is 60 wt% for both the hydroxides (this is a typical filler level used in EVA-based cable compounds) and the obtained results are reported in Table 3.2.1.1.

Table 3.2.1.1: Combustion parameters obtained from LOI and Cone Calorimeter.

Sample	LOI (%)	Cone calorimeter		
		TTI (s)	pkRHR (kJ/s*m^2)	pkRHR$_{time}$ (s)
EVA (pure)	20	35	465	160
Hy_60	36	76	172/155	124/555
H5_60	43	84	193	243

As expected, the limiting oxygen index values significantly increase with addition of the fillers in EVA, due to flame retardant effect of magnesium hydroxide, but also to the less amount of polymer present in the composites, which represents the combustible material. The sample containing Hy gave a lower LOI value than the H5 composite (36 against 43). Comparison of specimens behaviour points out that Hy composite has higher tendency to show the "afterglow" phenomenon, which slows down or avoids the complete extinguishing of the combustion even without the flame. The higher LOI value for H5 than Hy composite is reasonable taking into account a less percentage of hydroxide (around 90%wt, the effective endothermic flame retardant) in the natural brucite than into synthetic MDH (>99%wt pure); another influent aspect could be the irregular shape of Hy particles, which reduces the cohesion of filler particles in EVA matrix during combustion, with reduction of overall compound fire performances[145].

From the cone calorimeter experiments, comparative plots of rate of heat release versus time are shown in Figure 3.2.1.1, while data related to time to ignition (TTI), peak of rate of heat release (pkRHR) and time for the peak (pkRHR$_{time}$) are reported in Table 3.2.1.1.

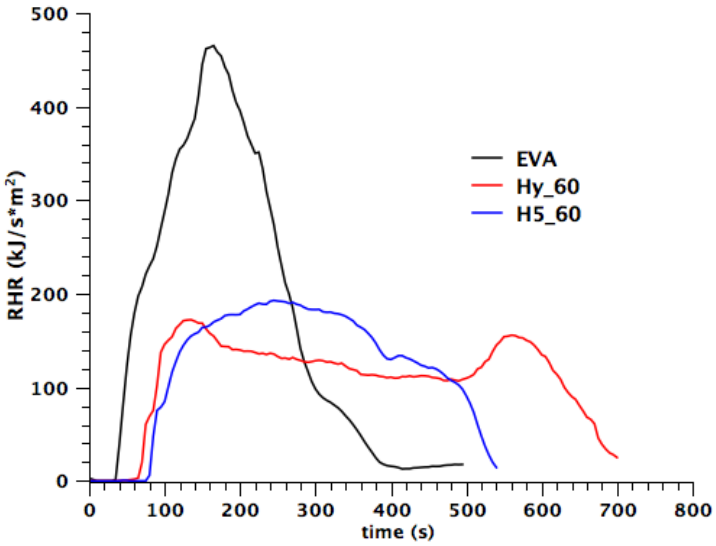

Figure 3.2.1.1: Comparison of Rate of Heat Release of EVA matrix and the composites Hy_60 and H5_60.

Both the composites show higher TTI and lower pkRHR than EVA and they are characterized by slight differences between them. From graph in Figure 3.2.1.1, the main differences between H5 and Hy compounds can be observed qualitatively in the shape of the RHR curve[70], which explains the presence of two peaks of RHR in the Hy_60 sample. H5 composite shows one maximum after more than 200 seconds, indicating a slow development of the combustion; Hy_60 shows the main maximum at the beginning of fire (around 50 seconds after the ignition), followed by a progressive decrease and then by a second peak between 500-600 seconds. This second peak corresponds to cracking of char formed during the first part of combustion and to the consequent re-increasing of fire intensity. These differences could be related to the formation of a different char structure during composite combustion with different physical stability[75].

a) 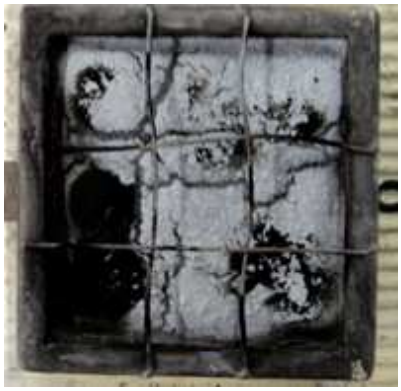 b) 

Figure 3.2.1.2: Photos of the residues after cone calorimeter test of the samples Hy_60 (a) and H5_60 (b).

As it is depicted in Figure 3.2.1.2 the residue of Hy composite is characterized by deep breaking lines, while the surface of H5_60 residue is clearly more compact and homogeneous. It could happen that in Hy_60 the char is formed during the first pkRHR, then it breaks in different points, giving the possibility for the polymer below to become available for pyrolysis. The pyrolysed material feeds the flame taking to an increase in rate of heat release, which is represented by the second peak. In H5_60 the char remains more stable and coherent during all combustion time, without so evident cracks on the surface. As reported for LOI analysis, the different morphology of the Hy and H5 particles can be a reason of the differences in the char structure: the regular shape of H5 particles produces a more uniform and homogeneous system, which promotes the formation of a char with "regular" and compact structure during combustion.

3.2.2. Screening study on flame retardant additives in combination with natural magnesium hydroxide and their performance

The screening analysis has been carried out on a variety of flame retardant additives combined in Hy composite in order to find a method for evaluating the performance of different formulations and the influence of the additives according to a new parameterization of burning behaviour. The chosen additives belong to different groups, each of which corresponds to a different flame retardant element (boron, phosphorous and nitrogen). In Table 3.2.2.1 the eight additives that have been selected for the study are listed.

Table 3.2.2.1: Additives chosen for flame retardancy screening study.

Boron-group additives	fixed wt%	Phosphorous-group additives	fixed wt%	Nitrogen-group Additives	fixed wt%
ZB Zinc borate	10	**Tpp** Triphenyl phosphite	2.5	**MC** Melamine cyanurate	5
CaB Calcium borate	10	**RP** Red phosphorus	2.5	**PPMt** PPM Triazine	5
BA Boric acid	5				
Tbb Tributyl borate	2.5				

Common characteristic of the additives is that they are all halogen free, and industrially used as ingredients to set up polyolefin compounds alternative to PVC based materials.

According to previous studies and applicative interest, some constraints have been established for tailoring formulations:

- fixed amount for each additive in the recipe (reported in Table 3.2.2.1);
- the formulations can be composed from 1 to 3 additives belonging to different classes;
- only one additive per class in each formulation;
- one additive of Boron group must be always present (ash cohesion desired)[76];
- Hy + additives = 60% by weight.

The base system used as substrate of this research is composed by EVA matrix, a fixed amount of compatibilizer, which corresponds to 4 wt% of maleic anhydride grafted poly(ethylene) (ULDPE-g-MAH), and 2.5 wt% of poly(dimethylsiloxane) (PDMS) as base additive (considered in the additives portion of formulations). This because the incorporation of compatibilizer and silicon is widespread in halogen free flame retardant compounds in order to guarantee mechanical, rheological and aesthetical properties[146]. This is generally true for highly filled composite production and it becomes a necessity in case of use of natural magnesium hydroxide Hy for the reasons analysed in a previous work[94] and in the first part of this research (chapter 3.1).

Evaluation of flame retardant efficiency

In industrial applications, vertical burning tests are widely used for flammability analysis as a screening, because they provide efficiency indication quite rapidly. This study is carried out in order to find a fast, but reliable and significant method for evaluation of the influence of flame retardant additives combination in compounds. Great importance is given to self-extinguish behaviour of the sample and to mechanical stability of the residue during combustion: in case of real fire conditions, dripping of flaming parts spread fire, by causing increase of victims.

For the screening purpose of this chapter the following vertical burning tests have been selected:

- Limiting Oxygen Index (LOI), with the application of the fire source from the top of the specimen; it can be still considered the most used FR test in the industrial

world as indicative for flammability of materials;

- DIN 4102 B2 vertical burning test, with the application of the fire source from the bottom of the specimen; the quite large size of the sample and the presence of the mask avoid specimen movement during combustion, taking to a clear identification of the material stability and burning tendency.

DIN 4102 B2 set up is useful for observing material burning characteristics. Some attempts on other flammability tests, such as UL-94, have been carried out, but final data were not as reliable as those of DIN 4102 B2 due to the large size of the specimen.
In particular for this study, specimens with thickness of about 1-1.2 mm have been used and specific stages during the test have been identified, which were related to the position of the flame during combustion. It has been possible to point out three main steps, which could be reported as parameters (time units) and they have been called *DIN-parameters* for easiness. The three *DIN-parameters* can be clearly identified during DIN 4102 B2 test, are:

1) **Time a (T_a)**: the flame top reaches the graduation line;
2) **Time b (T_b)**: the flame base reaches the graduation line;
3) **Time c (T_c)**: the flame base reaches the top of the specimen.

In Figure 3.2.2.1 a scheme of the *DIN-parameters* is reported.

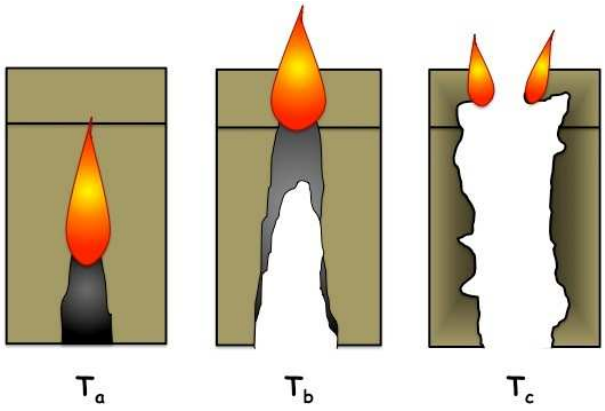

Figure 3.2.2.1: Schematization of the observable steps of combustion during vertical burning test DIN 4102 B2.

The analysis of the *DIN-parameters* leads to a classification of the studied materials in groups that are different for flammability behaviour depending on additives combination.

This classification is useful to rate the fire behaviour of compounds and to analyse the additives effects.

The proposed classification (*DIN-classification*) is relative to the observations of materials during vertical test DIN 4102 B2 and takes into account the flammability behaviour (self-extinguishing or not) and the material properties during combustion (dripping or stable residue). In particular three different behaviours have been distinguished during the test:

- fast and continuous fall of small fluid burning pieces, like drops (**Dripping**);
- slow fall of solid burning parts and/or extinguished pieces of sample (**Unstable residue**);
- burned part remains on the sample without falling pieces (**Stable residue**).

From these criterions three main classes come out (Figure 3.2.2.2), with some additional sub-classes introduced to describe specific burning features:

1. ***Class 1***: the combustion stops before T_a (very early), so the samples have no *DIN-parameter*. Some specimens are classified as ***Class 1a*** when they stop burning immediately after the flame is removed, while as ***Class 1b*** when they self extinguish after some time the flame is removed (in any case before T_a).
2. ***Class 2***: the combustion reaches T_a and stops before getting T_b (so in this case we have only T_a as *DIN-parameter*).
3. ***Class 3***: the combustion involves all the sample length, so T_a, T_b and T_c are recorded. Some specimens are classified as ***Class 3a*** when they show a residue, which remains stable for the most of combustion, and ***Class 3b*** when they show dripping or falling parts during all the burning test time.

A schematic description of the adopted *DIN-classification* is reported in the following Figure 3.2.2.2.

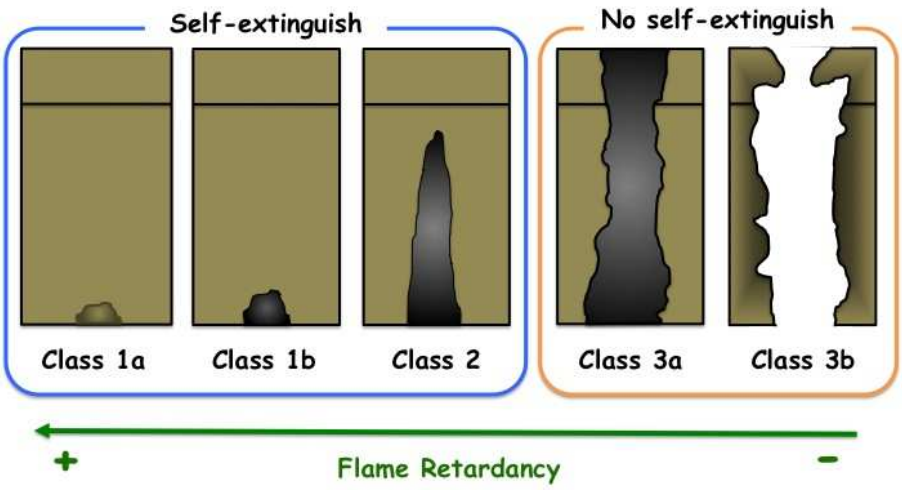

Figure 3.2.2.2: Classification of the analysed formulations depending on their behaviour during DIN 4102 B2 test.

Experimental results and evaluation of additive effects

In the Table 3.2.2.2, the formulations and the experimental results obtained from LOI and DIN 4102 B2 are reported, together with indications of material behaviour and the *DIN-class* belonging. The formulations are indicated by the sequences of additive abbreviation. The combinations of additives in the formulations have been randomly sampled, taking into account the chosen constraints; the formulations *base system* and *matrix+Hy*, respectively with and without PDMS, are included as references.

Table 3.2.2.2: Formulations and experimental results obtained from LOI and test following DIN 4102 B2.

Formulations	*LOI (%)*	*T a (s)*	*T b (s)*	*T c (s)*	*Dripping*	*Unstable residue*	*Stable residue*	*DIN-class*
matrix + Hy	32	128	205	245	No	Yes	No	3b
base system	36	113	-	-	No	No	Yes	2
ZB_Tpp_MC	29	61	132	172	Yes	No	No	3b
ZB_MC	34	128	-	-	No	No	Yes	2
CaB_Tpp_MC	33	41	116	130	Yes	No	No	3b
ZB_RP_MC	39	-	-	-	No	No	Yes	1b
CaB_Tpp	29	68	167	336	No	Yes	No	3a
CaB_MC	33	79	176	283	No	Yes	No	3a
BA_MC	38	61	-	-	No	Yes	No	2
Tbb_Tpp_MC	33	64	122	143	No	Yes	No	3b
Tbb_RP_MC	39	-	-	-	No	No	Yes	1a
Tbb_RP	42	-	-	-	No	No	Yes	1a
Tbb_MC	33	102	166	210	No	Yes	No	3b
ZB_Tpp	27	59	135	185	Yes	No	No	3b
ZB_RP	35	-	-	-	No	No	Yes	1b
CaB_PPMt	35	206	-	-	No	No	Yes	2
CaB_RP_PPMt	35	-	-	-	No	No	Yes	1b
CaB_RP	37	-	-	-	No	No	Yes	1b
BA_Tpp_PPMt	27	106	159	169	Yes	No	No	3b
BA_Tpp	29	66	118	127	Yes	No	No	3b
BA_PPMt	37	85	-	-	No	No	Yes	2

The reference samples are the base system (matrix + 57.5 wt% Hy + 2.5 wt% PDMS) and the composite without PDMS (matrix + 60 wt% Hy) in order to evaluate the flammability benefits that incorporation of PDMS can take, comparing the formulations properties. The base system is characterized by improved LOI value in respect to matrix+Hy (36 compare to 32), that could be related to industrially well-known effect of combination between silicon and maleic anhydride grafted PE into EVA+hydroxide compounds. The introduction of PDMS takes also to positive effect on *DIN-parameters*. The base system belongs to ***Class 2*** (it does not burn completely) with high stability of the residue, while the combustion of the sample matrix+Hy is complete (***Class 3b***), even if it proceeds slowly (quite high burning times).

About the other formulations it is possible to observed that almost all the various flammability performances, expressed by LOI, *DIN-parameters,* residue behaviour and thus *DIN-class* belonging are represented by the studied formulations. All the collected data have been evaluated by using multivariate linear regression analysis in order to find valid regression models for the parameters and then establish which additives of the

combinations determine significant variation of the analysed parameters. The goodness of the models is expressed by proportion of explained variance (determination coefficient R^2), which should be close to 1 in order to verify that it has been possible to model the system. The evaluation of the relative importance of the additives for the specific parameters has been possible by determination of the regression coefficients with Variable Importance in Projection (VIP), which provides also their signs ("+" or "–"), giving information about positive or negative effect of the component on the response (Appendix II).

The number of cases considered for each parameter, together with the proportion of explained variance obtained for their models and the most significant variables (higher VIP) with their signs are indicated in Table 3.2.2.3 for each response.

Table 3.2.2.3: Results from Multivariate Linear Regression algorithm analysis of the obtained responses.

Response variables	n° cases	Explained variance[1] (R^2)	main significant variables
LOI	21	0.787	RP (+), Tbb (+), Tpp (-)
T_a	15	0.736	PPMt (+), BA (-), MC (-), Tpp (-)
T_b	10	0.906	Hy (+), Tpp (-)
T_c	10	0.525	CaB (+), Tpp (-), BA (-)
Dripping	21	0.704	RP (-), Tpp (+)
Residue stability[2]	21	0.704	RP (+), Tpp (-)
DIN-class	21	0.955	RP (+), Tpp (-)

[1] explained variance is in calibration

[2] model takes into account the 3 responses together (Dripping, Unstable residue and Stable residue)

Almost all the analysed parameters show acceptable explained variance and in particular for T_b, *DIN-classification* and also LOI, R^2 values are quite high indicating the good "quality" of the models.

In Figure 3.2.2.3 the plots relative to LOI statistical results are reported.

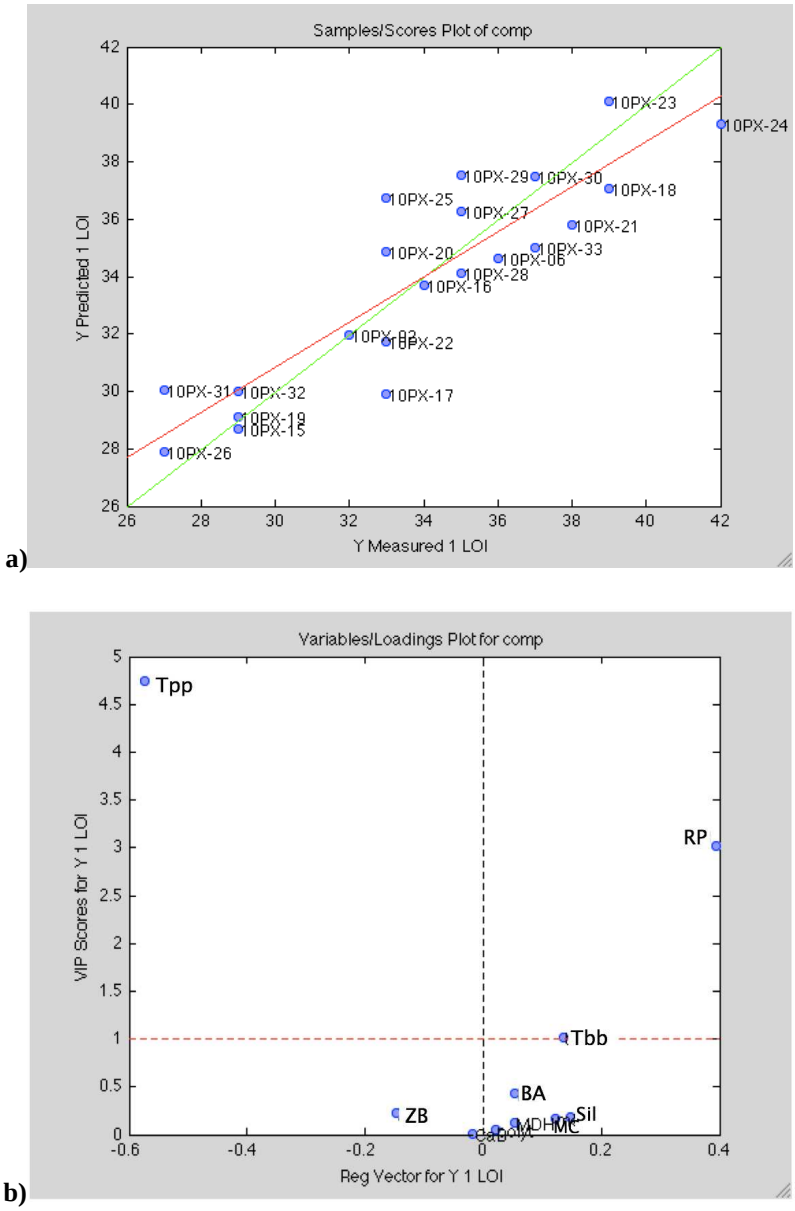

Figure 3.2.2.3: Experimental versus predicted values (a) and regression coefficient with VIP (b) for LOI results.

The plot of experimental versus predicted values in Figure 3.2.2.3 (a) is reported only for LOI data as example and it shows that the model satisfies quite well the assumptions of the analysis, confirming visually the R^2 datum of Table 3.2.2.3. The graph in Figure 3.2.2.3 (b) shows the regression coefficient with Variable Importance on the Projection (VIP): the components placed in the upper part of the graph (VIP > 1) are the relevant among the variables group; furthermore the components placed on the right part have positive influence (+) on the response, while those placed on the left have negative (-). About LOI results, the analysis of regression coefficients for the studied system points

out that they are deeply influenced by the presence of RP and Tpp in the recipes. In fact they are both placed in the upper part of the graph, but Tpp on the left and RP on the right side: this situation indicates the positive and negative considerable effect on LOI value of RP and Tpp respectively. Tbb seems also to impart some (positive) influence on LOI values, even if its importance is very lower compared to the Phosphorous group components. Among the less relevant additives (VIP < 1) it is interesting to point out also that just ZB shows negative effect on LOI (at this dosage ZB is a less effective flame retardant in comparison to magnesium hydroxide in EVA). This result can be considered in agreement with other works in literature[125].

In Table 3.2.2.3 it is possible to evaluate also the analysis of the *DIN-parameters* with the main relevant components (significant variables). The VIP regression analysis for T_a points out that, among the additives, Tpp shows the highest negative effect, while BA and MC have a small negative influence. All the other components have positive effect on T_a but only PPMt influences it considerably (VIP > 1). RP is not present because all the formulations containing RP in the studied system stop burning after removing the flame (***Class 1*****a** and ***Class 1b*** have not T_a).

Tpp, BA, MC and PPMt could have influence both on the flame size and on the burn rate of the compound. In fact it is important to consider that T_a is influenced by both the burn rate and by the height of the flame. For example, the same T_a result can be obtained for a compound, which burns slowly with long flame (left picture in Figure 3.2.2.4), and for another compound, which burns quickly with little flame (right picture in Figure 3.2.2.4). Both the cases are dangerous during a real fire, but they are related to different behaviours during combustion.

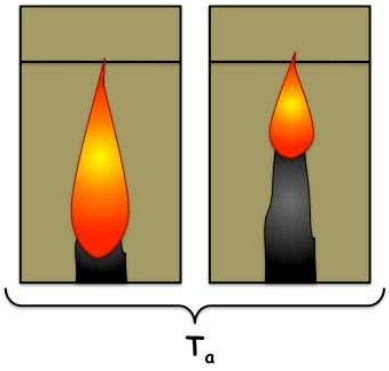

Figure 3.2.2.4: Different flame and burning behaviours of materials at the time T_a.

On the other hand T_b and T_c are connected only to the burning rate of the formulations: higher are their values, slower is the spread of fire. It has been noted by our analysis that for the formulations of ***Class 3***, higher times of combustion are generally related to higher stability of the residue. In particular very high T_c values characterize the ***Class 3a*** formulations (Table 3.2.2.2), which show a stable residue for most of the combustion process, loosing extinguished parts only when the flame is close to the top of the specimen.

About T_b, Tpp shows negative effect and the amount of Hy has considerable positive effect (Table 3.2.2.3), while the most effective components on T_c are CaB as positive influence and Tpp and BA as negative: in comparison with what is reported for T_a, the results should indicate that these additives have higher effect on the burn rate of material rather than on the flame size. Overall the presence of fillers (Hy and CaB) makes higher the burning times and it can influence positively the char stability of the formulations, which remains compact for most of the burning test time.

The regression coefficients with VIP of Dripping is shown in Figure 3.2.2.5.

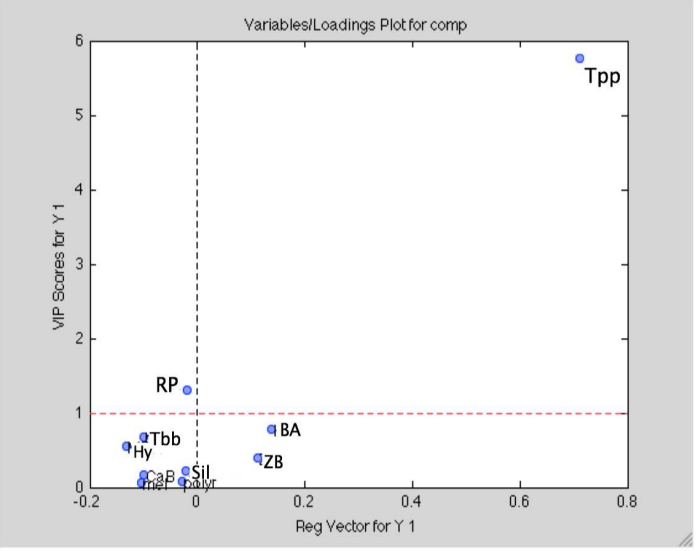

Figure 3.2.2.5: Regression coefficients with VIP for dripping behaviour during vertical burning test DIN 4102 B2.

In the graph Tpp and RP are the most discriminating additives also on Dripping (VIP>1). In fact Tpp promotes dripping effects and it contrasts with stable char formation, while RP avoids dripping and, for the burning formulations, it confers stability to the material.

The analysis on the identifiable class of the formulations has been done taking into account the main *DIN-classes*, corresponding to 1, 2 and 3 (without sub-classes) in order to give the most of importance to the self-extinguishing capacity of the samples. As it can be observed in Table 3.2.2.3, RP and Tpp are again the most considerable components, showing a VIP higher than 1. In particular all the formulations containing RP are labelled as ***Class 1*** (Table 3.2.2.2), so it can be considered the distinctive component of formulations of ***Class 1***, while Tpp the main component of ***Class 3*** formulations. No relevant difference could be evaluated among the other additives influence, confirming that in the studied system the chosen Phosphorous-group additives are the most influent on burning properties of this kind of compounds.

In order to support the validity of classification method based on *DIN-parameters* and observations, an attempt of correlation between the results obtained from LOI and DIN 4102 B2 tests has been done. In Figure 3.2.2.6 the formulations corresponding to the FR additives combinations and belonging to the different *DIN-classes* are reported versus their LOI results.

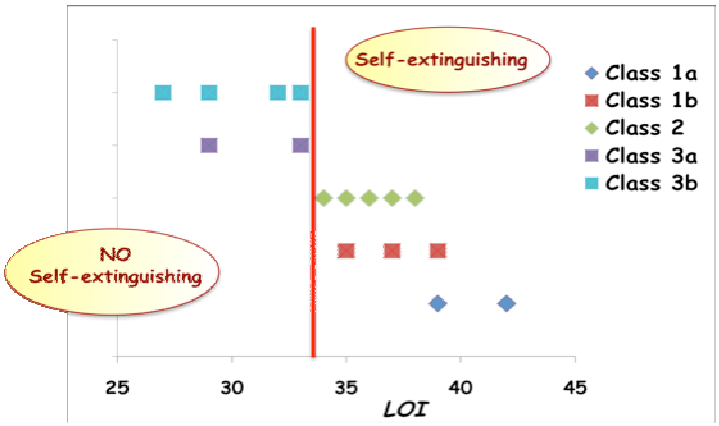

Figure 3.2.2.6: Correlation between *DIN-classification* and LOI values.

The results point out that the formulations with Self-extinguishing behaviour (***Class 1*** and ***Class 2***) have the highest LOI values, while ***Class 3*** formulations show lower LOI results (the red line should have only marker meaning). This is a quite unexpected result because usually correlation between LOI and vertical burning tests are difficult to appreciate[13]. The clear indication of the above data is that RP and Tpp are the most positive and negative relevant additives on both LOI and DIN 4102 B2 results.

All these results confirm that it is possible to perform a screening approach and the new parameterization method can be applied on the system studied in this thesis (chosen base formulation and flame retardant additives) in order to evaluate the performance of additives combinations in Hy composites and select them on the base of the desired material properties. The method points out useful indications about samples combustion behaviour and additives effect, such as their relative importance in the influence on a specific parameter. Beyond the high efficiency of red phosphorus against the negative effects of triphenyl phosphite, which tend to hide all the information on the other additives in the studied system, general good results are indicated for the use of calcium borate among the boron additives, especially concerning slower burn rate and stability of the residue. In particular the approach showed good capacity to evaluate and to classify the residue stability and self-extinguishing behaviour of different formulations. On the whole the method has pointed out promising results for application on further system of different matrix and /or flame retardant additives.

3.2.3. Study on a quaternary system based on natural magnesium hydroxide filled EVA composite

The additives, chosen for improving flame retardant properties of EVA composite decreasing magnesium hydroxide amount, are a poly(dimethylsiloxane) gum (PDMS) with silica as carrier and a natural mineral filler composed mostly by micronized calcium hydrate borate. These co-additives have been selected for their applicative interest: PDMS component is already used in similar compounds especially for improving rheological and mechanical properties. Calcium borate has been chosen because of the practical interest in using boron containing additive (alone or in combination with silicon additives) and for its natural origin; furthermore because it has shown interesting effect on residue stability and in reducing burn rate in the screening study (paragraph 3.2.1) and finally the existence of just a few literature works on its use makes interesting the study of its incorporation in highly Hy filled EVA compound for evaluating the possible application for cable and wire materials[76]. This study, based on natural magnesium hydroxide filled EVA composite, would like to open prospects of calcium borate use as flame retardant co-additive and to study its behaviour in such polyolefin systems.

The approach to this study has been carried out by using Design of Experiment (DoE), followed by analysis of the coefficients. The method allows the analysis of a wide variety of different parameters and the translation of them as responses into predictive mathematical models within the operating range of controllable variables[142]. The analysis of the coefficients in the models is of great practical importance to understand the effects of different additives and the possible interactions among them[144], in order to be able to forecast composite properties based on the acquired knowledge.

3.2.3.1. Experimental design approach: constraints, formulations and parameters

The chosen quaternary system is studied by Mixture Design[147-149] (specifically D-optimal mixture design), where the components are the natural magnesium hydroxide (Hy), the poly(dimethylsiloxane) based additive (Sil) and calcium borate (CaB); the matrix is mostly composed by EVA and it is also considered a variable. Matrix amount can change because it is established that the sum of the additives must be less than or equal to 60 wt% for evaluating the possible decrease of additives total content. A fixed amount of compatibilizer (ULDPE-g-MAH) has been introduced in the matrix composition, which is kept constant at 4 wt% in order to analyse a system as close as possible to the interesting industrial application, without introducing other variables. The components are expressed as the fraction of total amount of their experimental ranges and they sum up to one. Constraints on the component proportions are selected in order to focus the exploration of the entire simplex region of compositions only on the region of interest: concerning this study constraints have been selected in accordance with prior knowledge on industrially used FR compounds. Components and constraints of the quaternary system are listed in Table 3.2.3.1.1.

Table 3.2.3.1.1: Constraints for controllable input variables corresponding to the additives.

Variable	Lower limit (weight fraction)	Upper limit (weight fraction)
X_1 : Hy	0.3	0.6
X_2 : Sil	0	0.1
X_3 : CaB	0	0.2
X_4 : matrix	0.4	0.7

According to these assumptions, the statistical program has set up 18 run design, that are reported in the Table 3.2.3.1.2. Among the indicated 18 formulations, 15 are relative to different compositions and 3 repetitions (see formulations 3, 10 and 14, which are the repetitions of 2, 4 and 6 respectively) have been randomly selected.

Table 3.2.3.1.2: D-optimal mixture design formulations.

Component	Formulation n°								
	1	**2**	**3**	**4**	**5**	**6**	**7**	**8**	**9**
X_1 : Hy	0.300	0.300	0.300	0.600	0.300	0.300	0.450	0.493	0.500
X_2 : Sil	0	0	0	0	0.100	0.100	0	0.021	0.100
X_3 : Cab	0.100	0	0	0	0	0.200	0	0.043	0
X_4 : matrix	0.600	0.700	0.700	0.400	0.600	0.400	0.550	0.443	0.400
	10	**11**	**12**	**13**	**14**	**15**	**16**	**17**	**18**
X_1 : Hy	0.600	0.400	0.400	0.343	0.300	0.343	0.400	0.450	0.300
X_2 : Sil	0	0.100	0	0.046	0.100	0.071	0	0.050	0.050
X_3 : Cab	0	0	0.100	0.043	0.200	0.093	0.200	0.100	0.200
X_4 : matrix	0.400	0.500	0.500	0.568	0.400	0.493	0.400	0.400	0.450

The experimental responses selected as dependent variables are taken from different flame retardant tests, in order to have an overview of the different aspects of flame retardant behaviour for the samples and to discover potential correlations among parameters coming from different measurements. The chosen tests are:

- Limiting Oxygen Index (LOI);
- vertical burning tests UL94-V and DIN 4102 B2;
- Cone Calorimeter

Both the American UL94-V and German DIN 4102 B2 tests have been chosen as vertical burning tests for a comparison of the information they can point out. DIN 4102 B2 has been selected for the evaluation of the residue stability (Dripping, Unstable residue and Stable residue) and the burning time t_a (the top of the flame reaches the graduation line), while UL94-V for the measurement of average burning rate.

Concerning cone calorimeter it has been established to carry out the analysis and evaluation of most of the parameters provided by the used instrument, together with other calculated parameters. The collected data are the time to ignition (TTI), the peak of rate of heat release (pkRHR), the time at which there is the peak of rate of heat release ($pkRHR_{time}$) whose determination is reported in Figure 3.2.3.1.1 for some formulations.

The average rate of heat release in the first 180 seconds after ignition ($avRHR_{180}$) and the total heat release (THR) have been determined; the average effective heat of combustion (avEHC) the peak of smoke temperature (Tsmoke) and the time at which there is the peak of smoke temperature ($Tsmoke_{time}$) have been selected from their plots respectively. For avEHC it has been chosen approximately the average in the first 300 seconds as shown in Figure 3.2.3.1.1. The indices of flammability performance, such as the fire performance index (FPI=TTI/pkRHR) and the fire growth rate (FIGRA=pkRHR/$pkRHR_{time}$) are calculated by using experimental data.

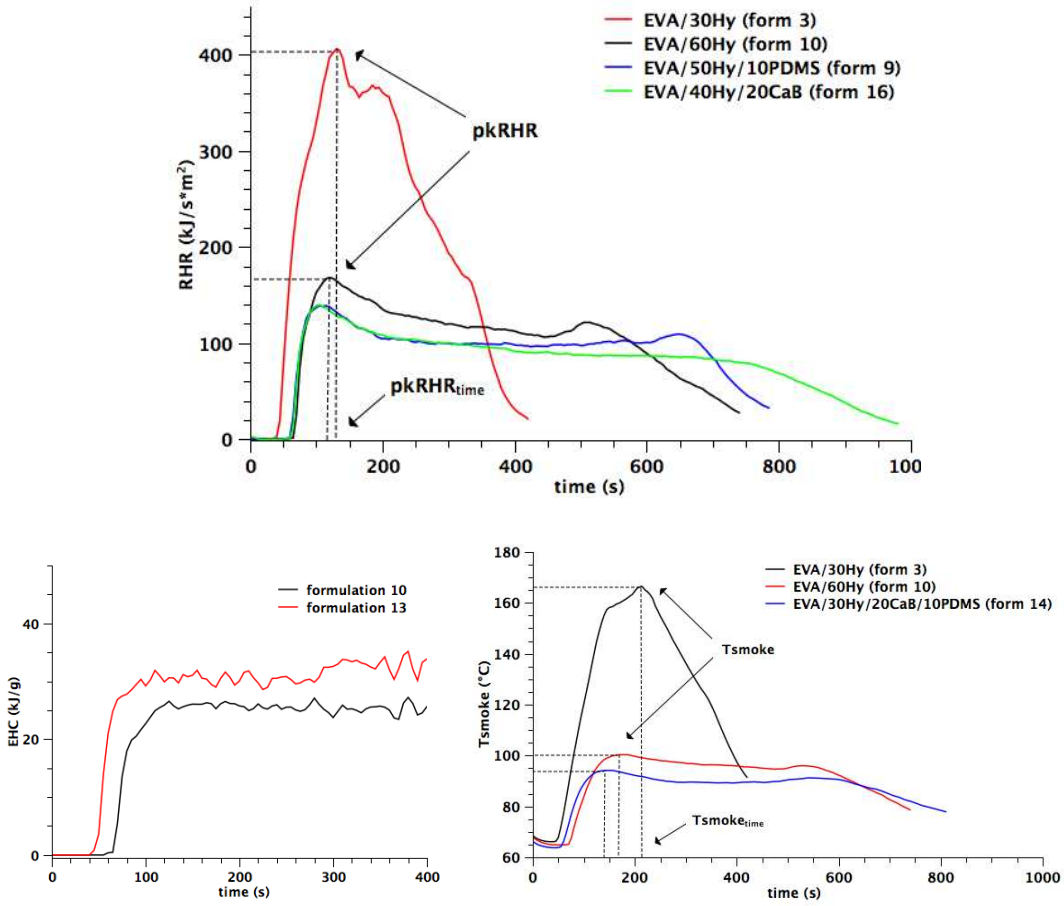

Figure 3.2.3.1.1: Indication of some of the cone calorimeter parameters chosen in the RHR, EHC and Tsmoke plots for the analysis of quaternary system (for some significant formulations as examples).

In Table 3.2.3.1.3 the analysed parameters for each kind of test are reported, with their optimization targets and their relative importance (weight factors) expressed by a scale of "+" symbols ranging from 1 to 3.

Table 3.2.3.1.3: Experimental parameters with their target of optimization and relative importance.

Flame retardancy test	Parameter	Importance	Target
LOI	% O_2	++	max
DIN 4102 B2	t_a (s)	++	max
	Dripping	+++	min (No)[1]
	Unstable residue	+++	min (No)[1]
	Stable residue	+++	max (Yes)[1]
UL94-V	burn rate (cm/min)	+	min
Cone Calorimeter	TTI (s)	+++	max
	pkRHR (kJ/s*m^2)	+++	min
	$pkRHR_{time}$ (s)	+	max
	avEHC (kJ/g)	+	min
	Tsmoke (°C)	+	min
	$Tsmoke_{time}$ (s)	+	max
	FPI (m^2*s/kW)	++	max
	FIGRA (kW/m^2*s)	++	min
	$avRHR_{180}$ (kJ/s*m^2)	++	min
	THR (MJ/m^2)	+	min

[1]These parameters indicate physically the presence or the absence of the specific property.

Experimental data collected from the flame retardant measurements carried out on the 18 formulations revealed by the program, are reported in Table 3.2.3.1.4 and Table 3.2.3.1.5.

Table 3.2.3.1.4: Flammability test results as responses of the mixture design formulations.

Response	Formulation n°								
	1	**2**	**3**	**4**	**5**	**6**	**7**	**8**	**9**
LOI (%)	24	20	20	31	31	35	24	30	40
t_a (s)	40	38	37	-	46	-	62	-	-
Dripping	Yes	Yes	Yes	No	Yes	No	Yes	No	No
Unstable residue	No	No	No	No	No	No	No	No	No
Stable residue	No	No	No	Yes	No	Yes	No	Yes	Yes
burn rate (cm/min)	6.10	6.41	6.41	0.32	7.07	3.49	6.20	3.26	2.88
	10	**11**	**12**	**13**	**14**	**15**	**16**	**17**	**18**
LOI (%)	30	34	25	29	35	31	27	36	30
t_a (s)	-	-	66	61	-	64	-	-	104
Dripping	No	No	No	No	No	No	No	No	No
Unstable residue	No	No	Yes	Yes	No	Yes	No	No	Yes
Stable residue	Yes	Yes	No	No	Yes	No	Yes	Yes	No
burn rate (cm/min)	0.31	4.24	5.07	6.41	3.79	5.36	0.52	3.36	4.60

Table 3.2.3.1.5: Cone calorimeter test results as responses of the mixture design formulations.

Response	Formulation n°								
	1	**2**	**3**	**4**	**5**	**6**	**7**	**8**	**9**
TTI (s)	54	48	50	82	50	64	66	64	68
pkRHR (kJ/s*m^2)	283	378	404	160	245	150	234	170	138
$pkRHR_{time}$ (s)	95	135	135	140	100	85	140	110	110
avEHC (kJ/g)	30	31	30	25	31	32	31	28	26
$avRHR_{180}$ (kJ/s*m^2)	260	340	321	146	237	114	211	139	114
THR (MJ/m^2)	84	89	89	69	82	70	81	75	71
Tsmoke (°C)	137	173	166	115	120	90	121	100	93
$Tsmoke_{time}$ (s)	210	210	215	190	220	150	230	165	155
FPI (m^2*s/kW)	0.19	0.13	0.12	0.51	0.20	0.43	0.28	0.38	0.49
FIGRA (kW/m^2*s)	2.98	2.80	2.99	1.14	2.45	1.76	1.67	1.55	1.25
	10	**11**	**12**	**13**	**14**	**15**	**16**	**17**	**18**
TTI (s)	76	56	64	56	58	65	72	67	59
pkRHR (kJ/s*m^2)	168	213	208	263	159	180	140	151	173
$pkRHR_{time}$ (s)	120	95	120	105	85	110	105	100	85
avEHC (kJ/g)	25	28	28	30	31	32	27	28	29
$avRHR_{180}$ (kJ/s*m^2)	139	169	176	226	125	139	114	116	133
THR (MJ/m^2)	73	80	80	82	72	85	77	75	73
Tsmoke (°C)	100	106	114	125	94	96	90	90	94
$Tsmoke_{time}$ (s)	180	145	220	220	145	250	175	165	140
FPI (m^2*s/kW)	0.45	0.26	0.31	0.21	0.36	0.36	0.51	0.44	0.34
FIGRA (kW/m^2*s)	1.40	2.24	1.73	2.50	1.87	1.64	1.33	1.51	2.04

Before studying the Mixture Design, an attempt of finding any correlation between the parameters has been done by means of Principal Component Analysis (PCA). Evaluation has been provided about LOI, cone calorimeter data and UL94 burn rate (using autoscaling as preprocessing). The PCA plot of the parameters is reported in Figure 3.2.3.1.2.

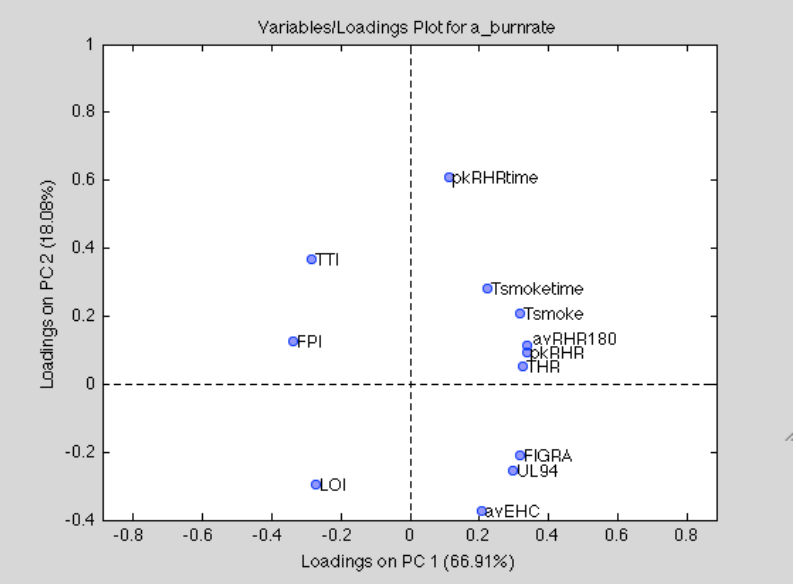

Figure 3.2.3.1.2: PCA plot of the parameters.

It should be noted that approximately most of the cone calorimeter parameters can be found in the same area of the graph, while UL94 and LOI lay in different regions indicating the absence of correlations among the FR parameters. This result points out that there are no strong correlations among the common flame retardant tests, indicating the completely different nature of them. This is in agreement with what has been widely reported on literature about the three flame retardant measurements: limiting oxygen index, vertical burning test UL94 and cone calorimeter are influenced by different material effects (dripping, flame spread, fire growth, etc) and they provide results that correspond to different flame retardant characteristics[13, 85, 150].

In the graph it is possible to spot only very weak correlations between LOI, TTI and FPI and between UL94 burn rate and FIGRA. The correlation between LOI and FPI (or TTI) is not easy to explain, even if both are in relation with the rate of decomposition to flammable small molecules and it is in agreement with recent results reported for other systems[151]. Furthermore the correlation between FIGRA and UL94 burn rate can be

related to the same nature of the parameters, which are both strongly linked to the capacity of the flame of spreading through the material.

Multivariate linear regression models have been developed for each response variable. Models have been studied by means of backward linear regression selecting and including in each model only statistical significant coefficients. First order terms are always present, while the upper order terms (interactions) depend on model efficiency and performance. Some response variables, such as FPI, dripping, unstable residue, stable residue and t_a have been transformed in different mathematical expressions because they were without normal distribution of residues with zero mean (necessary characteristics for elaborating a linear regression model). It could be possible that the optimization targets for these transformed variables change in respect to the mathematical expression. Models validation has been carried out by applying the leave one out cross-validation. Some further details and definitions about statistical method and parameters are reported in Appendix II. The numbers of terms (first order and interaction) for each parameter model are reported in Table 3.2.3.1.6, together with the model performance parameters (R^2, R^2-adjusted, R^2-prediction and Adequate Precision) in order to evaluate the goodness of the models in fitting the data and in prediction (Appendix II).

Table 3.2.3.1.6: Number of coefficients and performance parameters of the multivariate linear regression models.

Model	n° coeff	Performance parameter			
		R^2	R^2-adjusted	R^2-prediction	Adeq Precision
LOI	8	0.983	0.971	0.949	31.37
UL94-V	10	0.957	0.909	0.427	12.81
TTI	4	0.900	0.878	0.847	18.63
pkRHR	4	0.944	0.932	0.899	23.96
pkRHRtime	4	0.769	0.719	0.623	11.04
avECH	6	0.879	0.828	0.734	12.04
Tsmoke	7	0.972	0.957	0.922	25.17
Tsmoketime	4	0.668	0.592	0.439	8.86
ln(FPI)	4	0.963	0.955	0.939	30.00
FIGRA	12	0.989	0.968	0.831	19.95
avRHR	4	0.963	0.955	0.941	30.58
THR	4	0.837	0.802	0.744	13.35
$(t_a)^{-2.7}$	4	0.939	0.903	0.825	11.59
1.0/Sqrt(Dripping + 0.01)	4	0.701	0.637	-	-
1.0/(Unst res + 0.01)	11	0.923	0.812	-	-
Ln(Stab res + 0.01)	14	0.993	0.971	-	-

It is possible to observe that most of the obtained models are linear, showing 4 as number of coefficients: this result points out that for many of the flame retardant parameters considered, interactions have not significant effect.

Concerning the models performance, many dependent variables have shown very good models with R^2 and R^2-adjusted upper than 0.9 and Adequate Precision values more than 20 (its desired value is 4 or more)[152]. R^2-prediction values indicate also good capacity of the models to predict the experimental parameters even in points of the experimental range, where no test has been done. In particular for UL94 burn rate it is obtained good coherence of the model with the results rationalization (high R^2 and R^2-adjusted), but it is not so reliable in prediction (R^2-prediction < 0.5). Among the very "high-performance" models there are LOI, pkRHR, Tsmoke, FPI, FIGRA and avRHR. However almost all the obtained models could be considered acceptable. Only those related to the time parameters coming from cone calorimeter measurements ($pkRHR_{time}$ and $Tsmoke_{time}$) have shown lower quality and this result should indicate that the evaluation of their models coefficients is not so significant. Overall the general result on the performance analysis is really positive regard to the chosen system complexity and the high number of response variables.

3.2.3.2. Evaluation of components influence on flame retardant behaviour of the system

The analysis of the most interesting parameters has been carried out and the main results are reported: this is useful for evaluating the significant effects (main effects and possible interactions among the components) and their correlations with composite properties. Therefore it is of great importance to point out the phenomenological aspects indicated by the model coefficients for the different responses: the determination of these effects, which can support the model analysis, takes to the practical validation of the method.

In this kind of design, where the interested region is defined by upper and lower constraints, a simplification of the analysis would be reached by the introduction of pseudo-components. However model plots reported and prediction of the data are obtained by using actual components.

Evaluation of Limiting Oxygen Index parameter

The evaluation of LOI data takes to a mathematical model that shows some quadratic factors, as it can be observed for the trends of LOI model versus Sil additive fraction at different CaB amounts (fixing 40 wt% of matrix and 60 wt% of total additives amount), which are reported in Figure 3.2.3.2.1.

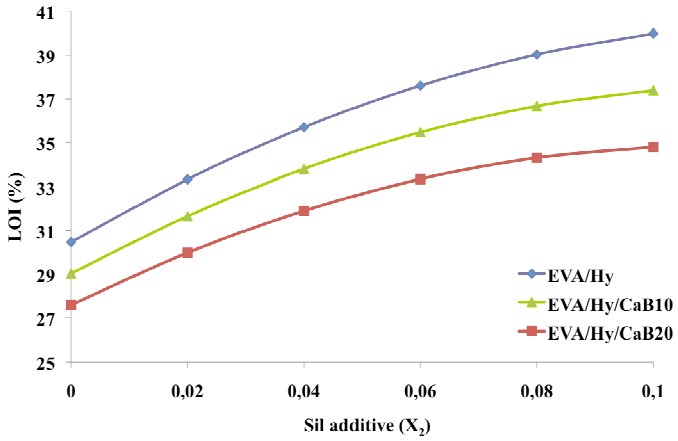

Figure 3.2.3.2.1: LOI model plots versus Sil additive weight fraction at different amounts of CaB additive (0, 10 and 20 wt%) fixing 40 wt% of matrix and 60 wt% of total additives amount.

The coefficients from the regression equation for LOI response are as follows:

terms	X_1	X_2	X_3	X_4	X_1X_2	X_1X_4	X_2X_3	X_2X_4
LOI coefficients	+30.5	+23.4	+26.2	+20.6	+53.5	-7.6	+43.1	+40.7

Among the linear coefficients related to the variables, Hy (X_1) shows the highest positive effect, but looking at the second order terms we can note just one negative coefficient relative to Hy-EVA matrix interaction (X_1X_4). Although it is very low as absolute value, it is indicative of the negative afterglow effect on LOI of composites with aluminium and magnesium hydroxide. Afterglow avoids the complete combustion extinguishing even if there is no flame on the sample, reducing LOI performance[67].

According to the graph in Figure 3.2.3.2.1 for formulations with 40 wt% of matrix, between the additives, Sil (X_2) is influent on limiting oxygen index increase, while CaB takes to the reduction of LOI. Despite the linear coefficients of the components are almost similar (respectively 23.4 and 26.2), X_2 appears in the second quadratic terms with all the other components and with "+" sign. The interaction coefficients of the regression equation for Sil additive can be ranked as follows:

$$X_1X_2 \text{ (Hy} \times \text{Sil)} > X_2X_3 \text{ (CaB} \times \text{Sil)} > X_2X_4 \text{ (matrix} \times \text{Sil)}$$

It may be deduced that PDMS shows a strong tendency of interacting with the other additives concerning LOI results, especially with magnesium hydroxide. For this reason increasing the Sil additive concentration in the compound LOI increases and it could be considered the most influent additive for this measurement.

Experimentally the influence of PDMS, indicating by the interaction coefficient of the model, can be observed during measurement and on LOI residues with a solid phase effect shown in Figure 3.2.3.2.2.

Figure 3.2.3.2.2: LOI residues of the sample (a) EVA/Hy and (b) EVA/Hy/10Sil.

It should be noted that in the EVA/Hy specimen (60 wt% of Hy) the edges are burnt because of the afterglow effect, while in the EVA/Hy/10Sil specimen (50 wt% of Hy and 10 wt% PDMS) the char is just on the top, without spreading down the edges. During combustion poly(dimethylsiloxane) degradation takes to lower molecular weight products, which are able to migrate on the sample surface: part of them is released as volatile products and part is blocked on the surface forming silica[122, 123, 153]. In the case of LOI measurement the sample shape and size (small surface available for combustion), together with the starting point for vertical combustion from the top of the specimen, make the structure formed in solid phase by silica with the presence of fillers (Hy and CaB) strong and coherent enough to stop both the flame and the afterglow. The effect can be observed during LOI test on a sample containing PDMS additive as a strong flame on the top of specimen, that does not spread along the edge because of a charred strip formation (see Figure 3.2.3.2.2), leading to self-extinguishing even at high oxygen percentage.

Evaluation of Cone Calorimeter parameters

Statistical analysis of cone calorimeter results points out that all the components have significant influence as main effect on most of the chosen parameters. In fact most of the cone calorimeter parameters are described by linear equations (4 coefficients as reported in Table 3.2.3.1.6), where no statistically significant interactions appear.

According to literature, time to ignition (TTI) and peak of rate of heat release (pkRHR) are the main parameters usually reported for evaluation of flame retardant properties concerning cone calorimeter measurements. In the PCA on the studied system it has been pointed out that these two parameters are not correlated, while approximately all the other parameters are in correlation with pkRHR. So it is possible to detect two main groups of cone calorimeter parameters, which correspond respectively to the ignition (including TTI) and the heat released during combustion, involving pkRHR and the correlated parameters (avRHR, THR,Tsmoke, etc).

In Figure 3.2.3.2.3 the plots of TTI versus Sil additive fraction for compositions with a fixed amount of matrix (0.4), at different CaB amounts are reported.

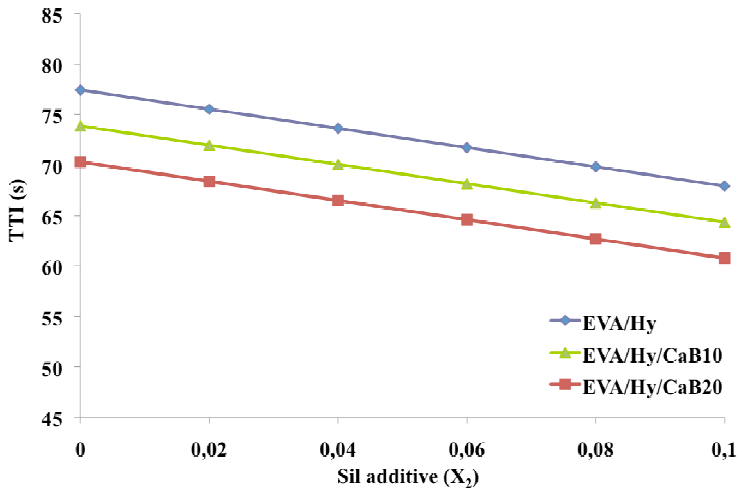

Figure 3.2.3.2.3: TTI model plots versus Sil additive weight fraction at different amounts of CaB additive (0, 10 and 20 wt%) fixing 40 wt% of matrix and 60 wt% of total additives amount.

The coefficients from the regression equation obtained for time to ignition are as follows:

terms	X_1	X_2	X_3	X_4
TTI coefficients	+77.5	+48.9	+66.8	+49.4

The highest factors, indicating positive effect, are those related to the fillers and especially magnesium hydroxide. The flame retardant action of magnesium hydroxide

can explain this high influence on the time necessary for ignition, due to the endothermic reaction of dehydration but mainly for the dilution of the pyrolysis gases with release of steam and char formation on the surface[96]. The effect could be supported by the presence of calcium borate as it should be indicated by the second linear coefficient value (66.8): calcium borate can contribute to time to ignition increase due to a combination of effects like thermal stability, gases dilution and char formation[76, 154]. The coefficients of EVA matrix and PDMS additive are lower and this is understandable because they are the polymeric components and during exposure at cone heater their thermal degradation process leads to evolution of pyrolysis gases.

Even the peak of rate of heat release mixture model is linear and the coefficients are reported below:

terms	X_1	X_2	X_3	X_4
pkRHR coefficients	+152.7	+99.9	+151.6	+364.6

The analysis of the coefficients points out that EVA matrix coefficient is the highest as it would be expected, because the polymer represents the combustible material in the system leading to the release of heat during combustion. Thus the general negative effect of polymer matrix on flame retardant properties of composite, about ignitability and combustion capacity, is underlined by both the models of TTI and pkRHR.

Almost the same trends can be found for the average rate of heat release during 3 minutes after ignition (avRHR) and the total heat release (THR). The mixture model coefficients for avRHR and THR are as follows:

terms	X_1	X_2	X_3	X_4
avRHR coefficients	+129.7	+75.4	+115.3	+319.8
THR coefficients	+72.7	+70.6	+74.4	+89.7

For all these models, among the flame retardant additives, Sil (X_2) shows the lowest coefficients, pointing out the weakest contribution of silicon additive in the heat release rate increase: both magnesium hydroxide and calcium borate show higher coefficient than Sil additive on heat release analysis.

The temperature of the smoke (Tsmoke) corresponds to the temperature of the flux of gases, which come out from the burning material (mostly air, steam water, smoke and

other gases depending on sample composition). It is strictly correlated to the heat released during cone calorimeter test as confirmed by PCA plot in Figure 3.2.3.1.2. In the case of Tsmoke the mixture model contains interaction terms and the coefficients are as follows:

terms	X_1	X_2	X_3	X_4	X_1X_2	X_1X_4	X_2X_4
Tsmoke coefficients	+106.9	+116.9	+77.5	+168.9	-75.9	-57.5	-136.7

Among the main components and interactions, CaB and Sil additives are indicated as the most effective on reducing Tsmoke. In Figure 3.2.3.2.4 the plots obtained by the model for Tsmoke at different percentage of the components are reported.

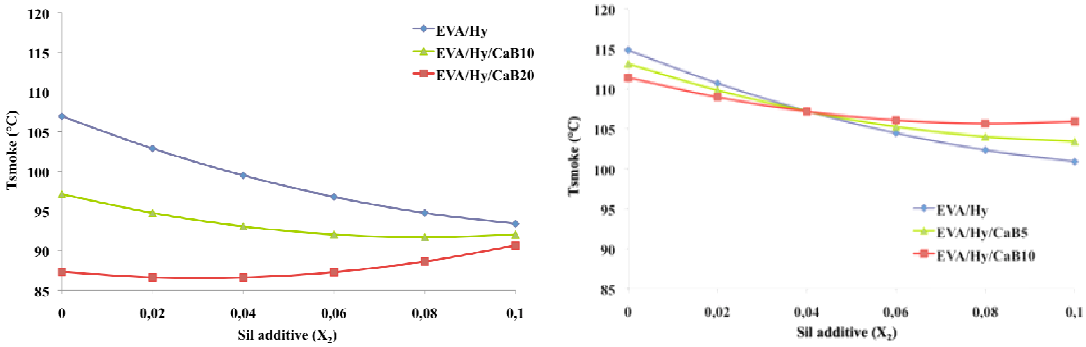

Figure 3.2.3.2.4: Tsmoke model plots versus Sil additive weight fraction at different amounts of CaB additive (0-10-20 wt%) and with EVA matrix fixed at 40 wt% (a) and at 50 wt% (b).

The plots of the model versus Sil additive weight fraction reported in Figure 3.2.3.2.4, indicate that CaB is more effective at lower EVA matrix amount (40 wt%), while Sil effect on Tsmoke is quite similar at different matrix percentage. The main evidence from the reported plots is that both Sil and CaB can influence more Tsmoke when they are not used as coadditives: if they are combined together in the composite with EVA matrix and Hy, their relative influence is strongly decreased. For example in Figure (a) the model indicates that it is possible to have a decrease of 20°C for Tsmoke by incorporation of 20 wt% of CaB (in place of Hy), while the decrease is just around 5°C when 10 wt% of Sil is incorporated. Taking into account this model indication, CaB and Sil additives can be considered like competitors in decreasing Tsmoke: they impart almost the same effect, but their effective coefficients in the model (main for CaB and interaction for Sil), should indicate different mechanisms, which should involve also Hy and matrix in case of Sil additive.

One of the main effects due to the use of flame retardant additives acting in solid phase and that can take to the reduction of rate of heat release (and also Tsmoke), is the formation of a protective barrier on the sample during combustion. Both Sil and CaB are effective as flame retardants in solid phase leading to the formation of different structures on surface sample as it is possible to see in Figure 3.2.3.2.5: CaB takes to the formation of a glassy, but porous surface on the residue (b), while the presence of Sil additive can be recognized by the presence of the brittle protective layer on the sample (a).

a)  b) 

Figure 3.2.3.2.5: Cone calorimeter residues of a) formulation 9 (with 10 wt% of Sil) and b) formulation 16 (with 20 wt% of CaB)

According to previous works, silicon compounds effect on flame retardant properties have been evaluated even in combination with MDH in EVA composites: it was found that the replacement of a magnesium hydroxide percentage with silicon rubber could improve cone calorimeter performance, especially in decreasing the rate of heat release[85, 155]. Fu et al.[83] reported that partial substitution of magnesium hydroxide with fumed silica in EVA takes to the drastic reduction of pkRHR and avRHR: in the presence of other flame retardants, like magnesium hydroxide, borates etc, silica can form a silicaceous layer that acts as heat and mass transfer barrier[156]. In the studied system Sil additive, that is a silicone deposited on silica as carrier, shows positive influence on rate of heat released, which generally decreases by increasing Sil amount, and it has negative influence on TTI, leading to earlier ignition.

In Figure 3.2.3.2.6 the TGA curves of the formulation containing 60 wt% of Hy (form 10), the formulation with substitution of 10 wt% of Hy with Sil (form 9) and the formulation with substitution of 20 wt% with CaB (form 16) are reported.

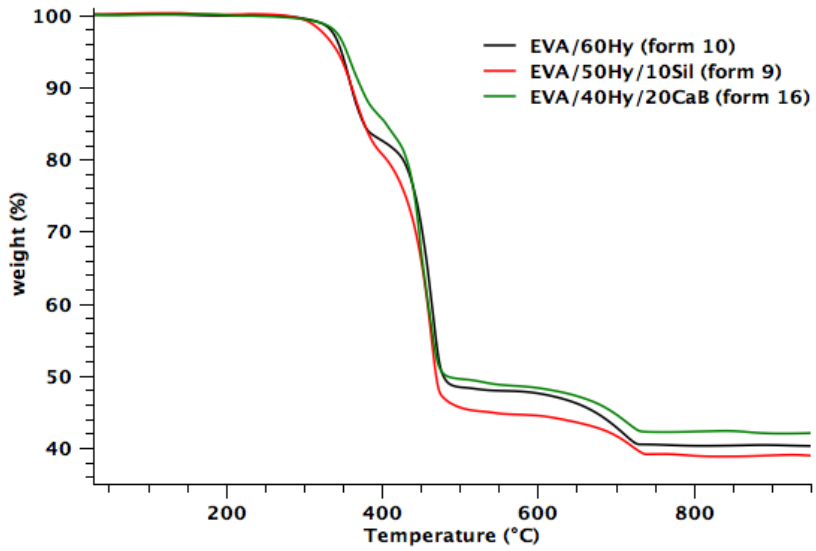

Figure 3.2.3.2.6: TGA curves of formulations 9, 10 and 16 in air flow (10°C/min).

Thermal degradation in air of formulation 9 starts at lower temperature than that of formulation 10 and 16, pointing out the lower thermal stability of compound with PDMS in comparison with the other formulations. The earlier degradation of formulation with PDMS can be related to the low coefficient in TTI model: the rapid pyrolysis forms gases and accelerates the ignition in cone calorimeter. On the contrary the positive influence of Sil additive on RHR reduction can be related to the solid phase effect coming from PDMS degradation. During combustion, Sil additive takes to the formation of the brittle and light protective barrier on the surface of the specimen (Figure 3.2.3.2.5). The main constituent of the surface layer should be silica, due to the silica contained by the additive and due to PDMS oxidative degradation products: it appears on the top of the structure, which is composed by the degradation products of filler. The presence of this silicaceous surface should decrease the burning tendency of the material, reducing the rate of heat release in the studied system more than magnesium hydroxide and calcium borate, as indicated by the model coefficients.

Most of the analysed cone calorimeter parameters are described by linear mixture models, with the exception of Tsmoke. Specifically the interactions indicated by Tsmoke model involve mostly Sil additive with matrix and Hy, but no interaction is indicated for CaB, pointing out that no particular synergistic and/or antagonistic effect can be found in the studied system and in the chosen range of composition. In literature the synergistic effects of borates as co-additives of aluminium and magnesium hydroxide in polyolefin

matrix have been widely reported even in combination with silicon containing compounds[79], but most of the researches are on zinc borates[77, 125, 139] and almost nothing on calcium borate. The main successful commercial application of calcium borate as flame retardant is for rubber modified roofing membrane production. In other markets, it is usually incorporated into ceramic glass frits[157], in epoxy compositions[158, 159] but not so much has been reported about its use in thermoplastic polymers in combination with hydroxides: this study would be a deeper research about the calcium borate additive flame retardant effects in thermoplastic EVA composite and in combination with PDMS as co-additive.

TTI, pkRHR, avRHR and Tsmoke results confirm that the calcium borate flame retardant effect is quite similar to that of magnesium hydroxide concerning the rate of heat release, while it is slightly lower for the ignition time. In particular the analysis of the coefficients indicates that CaB has more positive influence on rate of heat release that Hy, taking to a slighter reduction of the peak, more evident in the average RHR due to the coefficients difference (Figure 3.2.3.2.7).

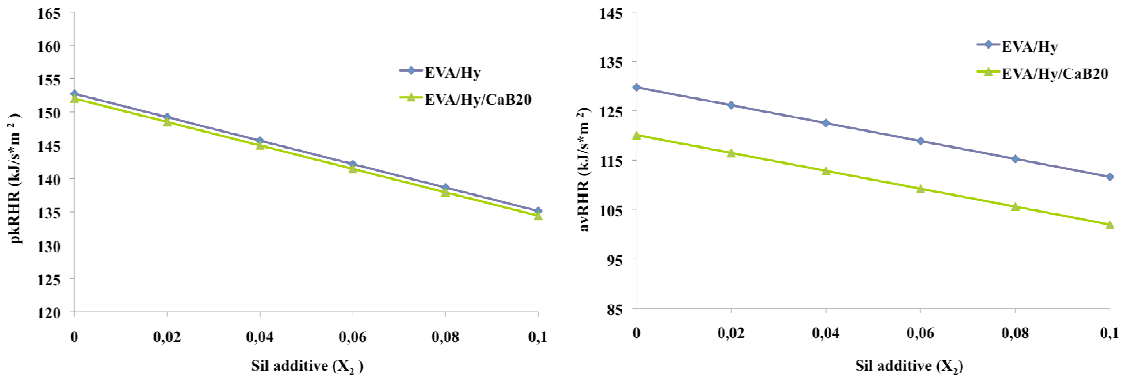

Figure 3.2.3.2.7: pkRHR and avRHR model plots versus Sil additive weight fraction at different amounts of CaB additive (0 and 20 wt%) fixing 40 wt% of matrix and 60 wt% of total additives amount.

.

In Figure 3.2.3.2.8 the rate of heat release curve of composite containing 60 wt% of CaB compare to that with 60 wt% of Hy are reported (obtained by mass calorimeter).

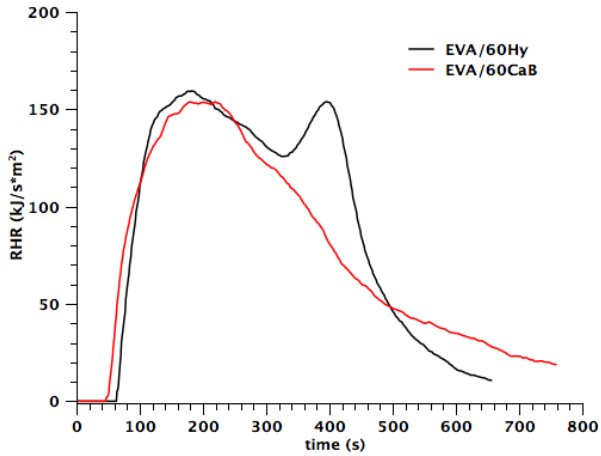

Figure 3.2.3.2.8: Mass calorimeter RHR results of composites (matrix EVA+ compatibilizer) with natural magnesium hydroxide and the used calcium borate additive (both 60 wt%).

The comparison between RHR curves indicates that the information obtained by statistical analysis of TTI and pkRHR models are in agreement with the reported fillers effects: the composites have similar combustion behaviour (almost the same pkRHR), even if Hy composite has higher ignition time and it shows a second peak due to the different residue stability of the samples. The absence of the second peak in CaB sample is an indication of calcium borate tendency to form a more cohesive and compact residue in EVA than the natural magnesium hydroxide.

Calcium borate can act as flame retardant mostly due to the dehydration reaction in the temperature range of 250-500°C and the formation of glassy matters, which can insulate oxygen, inflammable gas and heat transfer[158]. However the total flame retardant effect is lower than magnesium hydroxide also because of the lower amount of water released (Figure 3.2.3.2.9).

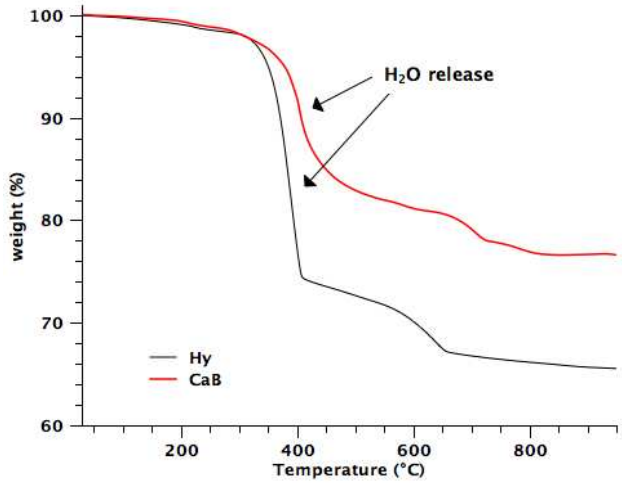

Figure 3.2.3.2.9: TGA curves of natural magnesium hydroxide and the calcium borate additive (nitrogen, 10°C/min).

So calcium borate can positively influence the time to ignition, because it increases thermal stability of compounds (Figure 3.2.3.2.6) and it improves the smoke temperature and the stability of residues. However its flame retardant effect depends by its own properties without any relevant interaction effect with the other components as indicated by statistical analysis on cone calorimeter responses.

Among the all cone calorimeter parameters considered in this study there are also some indices, often used especially from applicative point of view, because they could summarize the flammability performance. These indices are related to full-scale fire situation and they can give an indication of the time available for people to escape. FPI represents a kind of compromise between the main cone calorimeter parameters (TTI and pkRHR) while FIGRA could be related to the flame spreading rate at the beginning of the fire[160].

The coefficients from the regression equation of FPI (obtained by mathematical modification) have the following values:

terms	X_1	X_2	X_3	X_4
ln(FPI) coefficients	-0.69	-0.95	-0.82	-2.04

The analysis of the coefficients for this expression indicates that all the components have negative effect on FPI, but the EVA matrix shows the highest coefficient as absolute value. This is in agreement with what has been reported in the previous part of the statistical analysis for TTI and pkRHR. In fact polymer has double negative effect on

FPI: on time to ignition due to the thermal degradation and on the peak of rate of heat release because of its high burning disposition.

FIGRA is described by one of the most complex model of those obtained in this study. The coefficients of the regression equation are as follows:

terms	X_1	X_2	X_3	X_4	X_1X_2	X_1X_3
FIGRA coefficients	+1.27	-9.99	+2.40	+2.90	+16.77	-3.22
	X_1X_4	X_2X_3	X_2X_4	X_3X_4	$X_1X_2X_4$	$X_2X_3X_4$
	-1.70	+15.92	+17.35	+1.04	+16.02	-38.24

A so complicated regression equation points out that all the components affect the FIGRA parameter both the single and the interaction factors. In this case also cubic interactions appear among EVA matrix, Sil additive and the fillers separately. It is not easy to explain the coefficients of the FIGRA expression and it is not useful for a complete comprehension of the system, because they involve too many aspects of horizontal burning behaviour of the chosen system.

Vertical burning test evaluation

Two attempts of vertical burning tests have been carried out on the studied system: UL94 considers smaller samples, just hung at the top, while in DIN 4102 B2 samples are considerably larger and they are kept by a mask, avoiding specimen movement during flame application and burning process.

For DIN 4102 B2 the burning time t_a is the only numerical parameter could be analysed and it is obtained for the non self-extinguishing formulations: higher is t_a value (with the limit of self-extinguishing), slower is the burning rate and/or lower the height of flame.

The regression model for t_a is reported below:

terms	X_1	X_2	X_3	X_4
$(t_a)^{-2.7}$ coefficients	-2.97E-5	- 2.78E-5	+ 4.60E-6	+ 5.78E-5

EVA matrix coefficient (X_4) is the highest and it indicates a negative influence on t_a value. The matrix is the most burning component and it causes the decrease of time of combustion. Not all the formulations would have t_a as a result because they could stop burning before the top of the flame can reach the marker and this self-extinguishing behaviour represents even a better result than a high value of t_a. A more clear evaluation of the flame retardant effect for the additives could be extracted by the determination of

the maximum matrix percentage is required in order to have self-extinguishing behaviour. The t_a results, determined by the model for three composites with different compositions, are reported in Figure 3.2.3.2.10 as function of the matrix percentage. The chosen compositions are EVA with 60 wt% of Hy and the composites with replacement of 5 wt% of Hy with Sil and CaB additive.

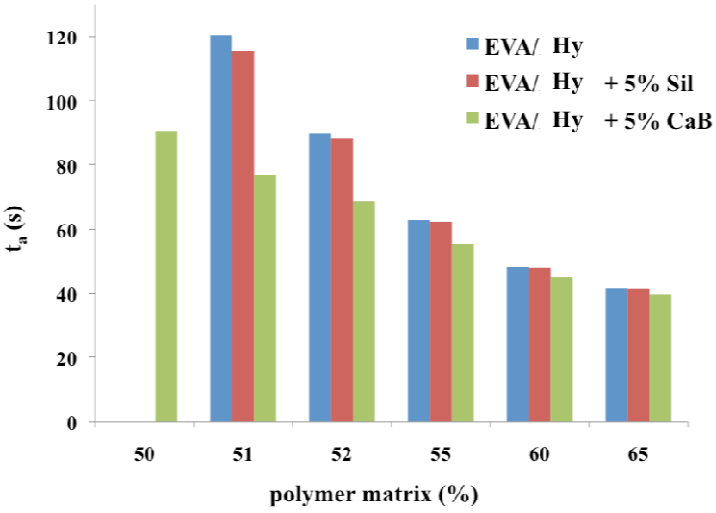

Figure 3.2.3.2.10: Predicted t_a values versus matrix amount for the composite containing only Hy and the composites with 5% of Sil additive and CaB in combination with Hy.

It is possible to note that the composites with Hy alone and in combination with Sil additive could take to self-extinguishing behaviour until 51% of matrix (that is the last value it is possible to calculate t_a), while the combination with CaB requires lower amount of matrix (< 50%) for obtaining the same result. Even if the difference is not so high, the result points out the higher burning tendency of the material with CaB than the other composites (as indicated by the coefficient) and underlines the lower flame retardant effect for vertical burning test compare to the other additives in the studied system.

The further information we obtained from the set up of DIN4102 B2 deals with the stability of the sample during combustion, because the method allows us to distinguish clearly if a formulation could have a stable residue, avoiding dripping and flammable parts loosing. Three possible choices have been detected (*Dripping*, *Unstable residue* and *Stable residue*), with the condition that one excludes the others. All the DIN-response variables have been mathematically transformed, considering the response Yes as the maximum value (1) and No as the minimum (0) as indicated in the Table 3.2.3.1.3: the

obtained models are almost good and quite complex (Table 3.2.3.1.6). A detailed evaluation of model coefficients has not been done, because it is not useful for a real comprehension of the system: their models have been developed in order to tailor the residue behaviour in such system.

In the application of vertical UL94 test, the chosen parameter is the calculated average burn rate that is based on the time necessary to the sample to burn completely. Among the studied formulations, **4**, **10** (that is a repetition) and **16** show self-extinguishing behaviour with burning time close to 10 seconds, thus they have been ranked by considering the burned length. The formulations contain 60 wt% of filler and an overall ranking of burn rate on the 18 formulations points out the general tendency of composites with higher filler content to show lower burn rates. This result highlights the strong effect of the fillers (mostly Hy) on flammability performance and burning material stability. The coefficients from regression model for UL94 burn rate are as follows:

terms	X_1	X_2	X_3	X_4	X_1X_2
UL94-burn rate coefficients	+0.5	-5.5	-0.6	+6.5	+17.6
	X_1X_3	X_1X_4	X_2X_3	X_2X_4	X_3X_4
	+4.9	+8.7	+26.5	+17.0	+8.9

The trends of UL94 burn rate model as a function of CaB weight fraction at different Sil content are reported in Figure 3.2.3.2.11 (fixing 40 wt% of matrix and 60 wt% of total additives amount).

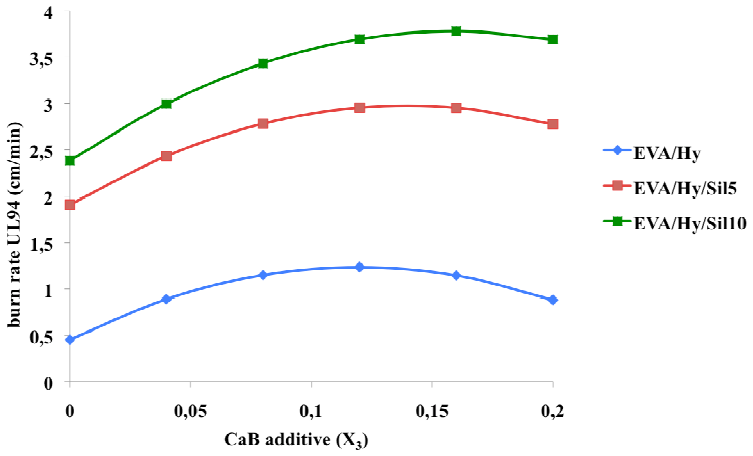

Figure 3.2.3.2.11: UL94 burn rate model plots versus CaB additive weight fraction at different amounts of Sil additive (0, 5 and 10 wt%) fixing 40 wt% of matrix and 60 wt% of total additives amount.

Many interaction coefficients appear in the model and all of them indicate the effect of increasing burning rate. Sil additive shows negative influence on burn rate as single component, but it is involved in the interaction terms with the highest values of the coefficients and, observing the plots in Figure 3.2.3.2.11, totally its effect in the reported formulations is the increase of burn rate in UL94-V test. From the graph, also CaB takes to the increase of burn rate, but it is much lower than Sil. Furthermore the use of Sil and CaB as co-additives takes to higher increase of burn rate, rather than the case they are not used together.

Comparing Sil effect indicated by UL94 burn rate model with that one of LOI, it is possible to point out an opposite flame retardant effect. Sil shows positive interaction coefficients with all the other components in both the models: they lead to a general positive contribution in increasing LOI parameter, while they lead to the increase of burn rate in the case of UL94 (with no self-extinguish behaviour), which is a FR negative contribution. This result can be related to the differences between the tests: in LOI test the combustion moves from the top to the bottom, while in UL94 the combustion proceeds in the opposite direction and moreover the flame involves the upper part of the specimen. Sil additive displays effective action in LOI, but it falls in a strict test such as vertical UL94, where the formation of silicaceous barrier, which would be very important to interfere with combustion, is not enough. Furthermore in the studied system it has been possible to appreciate experimentally that a slower combustion rate characterizes samples with higher char forming capacity and residue stability. This correlation between burn rate and residue stability can be observed in the graph reported in Figure 3.2.3.2.12.

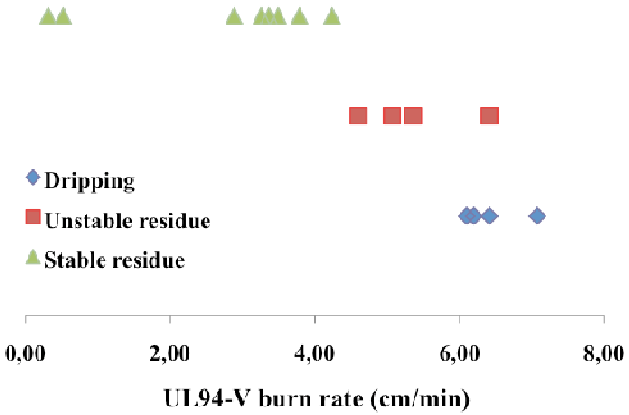

Figure 3.2.3.2.12: Correlation between the formulations residue behaviour during DIN 4102 test and the burn rate in UL94 vertical test.

The formulations with a stable residue during vertical burning test (DIN 4102 B2) are characterized by a slower burn rate, while higher burn rates correspond to the samples showing dripping or flammable parts falling. Even if it is only a qualitative indication, it confirms that the formation of a strong and stable residue is related to the lower burning tendency of the studied formulations.

Overall, the results of the analysis of the coefficients allow the determination of the specific additive effects (as single component or interaction) and of the responses, which are more influenced by them. Unsurprisingly the matrix influences negatively all the responses (decreasing LOI and TTI, increasing RHR, etc), suggesting that in the composite the polymer must be the lowest possible concentration in order to have good flame retardant properties. Another important point is that it is not possible to strongly decrease natural magnesium hydroxide amount to achieve good flame retardancy: among the components Hy is positively effective especially on LOI, TTI, t_a and UL94 burn rate.
Sil additive influence is mostly related to its degradation effect and formation of a silica barrier on the sample: the first is recognized in the negative effect on TTI, while the latter mostly in its influence in decreasing RHR. The action of Sil can be enhanced by the presence of other components, especially Hy, which can cooperate in the stable barrier formation: it is indicated by the presence of interaction terms in the models, such as the positive effect on LOI, Tsmoke and the negative effect on UL94 burn rate due to the typology of test.
CaB does not show any particular cooperative effect with the other components and it shows similar beneficial influence of Hy even if it is almost lower, except for RHR and Tsmoke, where its influence on thermal stability and residue stability becomes important.

3.2.3.3. Search for *optimal* compositions

Based on the analysis of the models used for describing the parameters, some optimal compositions of EVA based quaternary system have been planned. The *optimization method* has been used in order to evaluate the possibility of tailoring materials with the desired properties, depending on their application. As it is possible to image there are several paths of optimization: in fact it is possible to optimize more than one parameter at the same time, or even all together. Therefore the crucial step is the ranking of the flame

retardant properties, because the path of optimization needs to find compromise among different variables in order to reach higher values in others.

The optimization is solved by a backward process from selected response variables, whose importance (*weight factors*) and targets are indicated in Table 3.2.3.1.3. The process takes to a list of formulations as possible solutions, ordered taking into account the desirability of their responses. The desirability parameter is used to determine how close the solution result is to the desired one and its maximum value is "1" for the best solutions (Appendix II). In this study on EVA system, different paths of optimization are studied, focusing on different parameters. The stability of the residue is the basing characteristic for the chosen optimization attempts, expressed by the stable residue classification. Thus the common response for the attempts of optimization is that they must have “Yes” as outcome of stable residue parameter (following the relative models of Table 3.2.3.1.6).

Two optimization paths have been planned:

- LOI-optimal formulation (A): the aim is the highest LOI value.
- CCT-optimal formulation (B): the aim is the highest Time to Ignition (TTI) simultaneously with the lowest peak of Rate of Heat Release (pkRHR).

Three of the most desirable formulations given by the program for the optimization paths are listed in Table 3.2.3.3.1 and Table 3.2.3.3.2 together with their predicted optimal results and desirability.

Table 3.2.3.3.1: Composition of the LOI-optimal formulations and their desirability.

n°	Hy (X_1)	Sil (X_2)	CaB (X_3)	matrix (X_4)	LOI	Stable residue	*desirability*
1	0.500	0.100	0	0.400	40.0	Yes	1
2	0.508	0.092	0	0.400	39.7	Yes	0.992
3	0.525	0.075	0	0.400	38.8	Yes	0.968

Table 3.2.3.3.2: Compositions of the CCT-optimal formulations and their desirability.

n°	Hy (X_1)	Sil (X_2)	CaB (X_3)	matrix (X_4)	TTI	pKRHR	Stable residue	*desirability*
1	0.560	0.000	0.040	0.400	76.0	152.6	Yes	0.920
2	0.560	0.013	0.027	0.400	75.2	150.2	Yes	0.914
3	0.539	0.000	0.061	0.400	75.3	152.5	Yes	0.912

Among the formulations given by the program, two have been chosen as LOI_{opt} (A) and CCT_{opt} (B) are reported in Table 3.2.3.3.3.

Table 3.2.3.3.3: Compositions of the "optimal" formulations and their desirability.

Component		Formulation	
	Unit	A (LOI_{opt})	B (CCT_{opt})
Hy	%	50.0	56.0
Sil	%	10.0	1.3
CaB	%	0	2.7
Matrix	%	40.0	40.0
Desirability		1.000	0.914

It can be observed that the formulation B is not the first reported in Table 3.2.3.3.2 , but it has been chosen the second formulation in terms of desirability. Both for LOI_{opt} and CCT_{opt} lists of formulations the predicted optimal results are very close each other, indicating that it is possible to select one of the given formulations expecting good results anyway. Formulation B contains both CaB and Sil additives, even if as small amount, and this composition with similar properties of the others has been selected as the most interesting from an applicative point of view.

Some of the experimental results for the optimal formulations A and B are reported in Table 3.2.3.3.4 together with the results range obtained in the 18-run system investigation (min-max range).

Table 3.2.3.3.4: Experimentally measured test results for optimal formulations in comparison with the experimental range obtained for the 18-run system.

Component		Formulation		
	Unit	A (LOI_{opt})	B (CCT_{opt})	min-max range
LOI	%	40	32	20-40
Stable residue		Yes	Yes	No-Yes
TTI	s	64	74	48-82
pkRHR	$kJ/s*m^2$	145	160	138-404
$pkRHR_{time}$	s	110	115	85-140
$avRHR_{180}$	$kJ/s*m^2$	118	145	114-340
Tsmoke	°C	97	96	90-173

It should be noted that the achieved results are all inside the experimentally obtained range and for each parameter they are almost in agreement with the specific target (Table 3.2.3.1.3). The analysis points out the compromise characteristic of the formulations,

especially for B, where a higher pkRHR value than A formulation is measured in order to achieve higher time to ignition.

It is possible to deduce some considerations about the given optimized compositions: first of all a common result for the paths of optimization is that the amount of polymeric matrix must be the lowest established; in fact its weight fraction is always equal or very close to 0.4 that is our system lowest limit for it.

Furthermore in the optimization paths Hy weight fraction is almost close to 0.5, underlining that high amount of magnesium hydroxide are required for optimal performance in the chosen range.

For LOI path of optimization the highest desirability is reached without CaB and with the highest amount of Sil additive, in the range imposed by our constraints. Combination of Sil and Hy additive improves LOI values of our formulations according to the interaction coefficients of the model.

On the other hand it is possible to note the presence of CaB as common additive of all the listed formulations for CCT optimization (Table 3.2.3.3.2). This result points out that the studied system considers effective a small amount of calcium borate in combination with Hy, when compromise between the main cone calorimeter parameters (TTI and pkRHR) is required, especially for its reported influence on pkRHR (CaB coefficient). For B formulation, where both CaB and PDMS are in combination with Hy, slightly lower value of pkRHR than the other formulations is predicted due to the reported CaB and Sil coefficients and this combination does not reduce TTI considerably.

A comparison between the predicted and the experimental data for the optimal formulations has been evaluated. The experimental results compare with the predicted are reported in Table 3.2.3.3.5 and Table 3.2.3.3.6.

Table 3.2.3.3.5: Comparison between the experimental and the predicted results for A(LOIopt).

Response	Predicted results		Experimental results
	Mean	A 95% confidence interval	Value
LOI	40	38-42	40
Stable residue	Yes	-	Yes
TTI	68	64-72	64
pkRHR	135	111-160	145
$pkRHR_{time}$	106	94-117	110
$avRHR_{180}$	112	94-130	118
Tsmoke	93	83-103	97

Table 3.2.3.3.6: Comparison between the experimental and the predicted results for B(CCTopt).

Response	Predicted results		Experimental results
	Mean	A 95% confidence interval	Value
LOI	32	31-33	32
Stable residue	Yes	-	Yes
TTI	75	72-78	74
pkRHR	150	130-170	160
$pkRHR_{time}$	123	113-132	115
$avRHR_{180}$	126	111-141	145
Tsmoke	101	96-108	96

Many experimental results are in agreement with the predicted values and however most of them are included in the 95% confidence intervals. The confidence limits for the reported parameters should be considered acceptable because for most of them they are less than 20%.

Another interesting attempt of optimization has been performed including the parameters coming from vertical burning test DIN 4102 B2: even in this case the stability of the residue has been maximized together with the maximization of the burning time t_a. The analysed formulation with the highest desirability, called C, is composed by 42 wt% of Hy, 6.4 wt% of Sil, 11.5 wt% of CaB and 40 wt% of matrix. The predicted and experimental results are reported in Table 3.2.3.3.7.

Table 3.2.3.3.7: Comparison between the experimental and the predicted results for the formulation C composed by 42 wt% of Hy, 6.4 wt% of Sil, 11.5 wt% of CaB and 40 wt% of matrix.

Response	Predicted results		Experimental results	
	Mean	A 95% confidence interval	Value	min-max range (18 formulations)
LOI	35	34-37	36	20-40
Stable residue	Yes	-	Yes	No-Yes
TTI	67	65-70	69	48-82
pkRHR	141	127-156	136	138-404
$pkRHR_{time}$	99	92-106	90	85-140
$avRHR_{180}$	113	102-123	111	114-340
Tsmoke	91	86-96	95	90-173

It is possible to observe from the composition that even in this case the amount of matrix is the lowest as established by the system, but it is interesting that the percentage of Hy is lower than 50 wt% with the introduction of 11.5 wt% of calcium borate, taking to the total content of filler less than 55 wt%. The most interesting characteristic of formulation C (especially for an applicative point of view) is that the obtained results represent really

a good compromise among the series of parameters of LOI, cone calorimeter and vertical burning test, by using a lower amount of filler than 60 wt% and not using too high amount of PDMS additive, which could have a negative influence on rheological and mechanical composites properties (and also on the cost of material).

Even in this case the evaluation of the predicted and experimental results points out that most of them are in agreement, confirming the good prediction performance of the models. However, taking into account all the analysed optimal formulations, the most dependable parameters in prediction are verified as LOI value, TTI, Tsmoke and the stability of the residue. Considering pkRHR and avRHR, they show good models quality (Table 3.2.3.1.6), but the confidence intervals relative to their predicted results are quite wide in comparison with the rate of heat release variations of the analysed formulations. In Figure 3.2.3.3.1, representative RHR curves obtained for the optimal formulations in comparison with that of formulation **10** are shown.

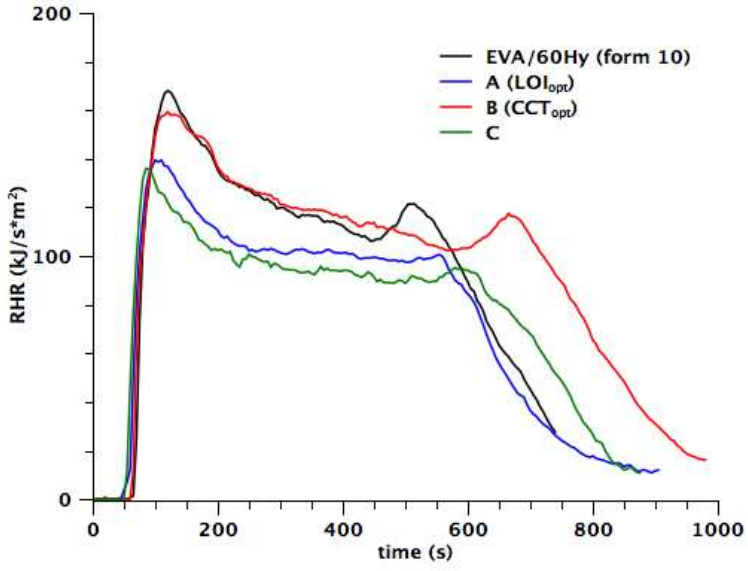

Figure 3.2.3.3.1: Cone calorimeter results of optimal formulations A and B and C in comparison with formulation 10 (EVA/60Hy).

It can be observed that for the reported formulations, all with the lowest content of matrix (40 wt%), the RHR curves are quite similar and the obtained data are close each other. This could be related also to what has been reported by statistical analysis of RHR, where the absence of interaction factors and the closer coefficient values for Hy, Sil and CaB in comparison with that of the matrix, confirm the slight variation of responses by changing additives proportions with fixed amount of EVA matrix.

However the study on the chosen optimal formulations has pointed out that it can be possible to forecast compounds by using in prediction some of the models obtained for the analysed parameters in order to get materials with specific flame retardant performance.

4. Conclusions

The physicochemical analysis of the natural fillers, magnesium hydroxide (**Hy**) and the natural carbonates (**Mf**) and (**SM**), in comparison with the synthetic aluminium and magnesium hydroxides, pointed out different aspects, which were proved as crucial factors for highly filled EVA composite properties. Hy and Mf were characterized by irregular shape, wider particle size distribution and the presence of impurities. Specifically Hy showed the most irregular particle shape, even if needle-like shape could be ascribed to most of the particles, and the lowest tap density, indicating lower aggregation tendency than the other fillers. Among natural fillers, calcium carbonate SM showed properties more similar to those of the synthetic fillers (regular shape, narrow particle size distribution, low amount of impurities).

The rheological properties of EVA highly filled composites, studied by using a capillary rheometer, showed that all the composites were characterized by pseudoplastic behaviour, that shear viscosity increased with incorporation of filler and that it became higher with increasing filler loading as expected. Furthermore the introduction of any type of the chosen fillers did not modify the influence of temperature on EVA viscosity and therefore no additional effect of this parameter must be considered in setting the process condition for composites. The rheological study was a successful method for evaluating filler influence on the processing behaviour of the highly filled composites. In fact among the analysed EVA composites, those containing Hy showed the lowest increase of shear viscosity due to the particle morphology and their rheological behaviour was less influenced by filler concentration: these aspects indicate that the process conditions for composites with the natural hydroxide are less expensive respect to those with the synthetic hydroxyde, even at the high filler loading required. The theoretical approach carried out on the composites with hydroxides allowed the rationalization of their rheological behaviour and of the most influent properties. In particular the study showed that the "favorable" rheological behaviour of Hy composites could be referred to the higher maximum loading tendency, to the better dispersion capacity and to the lower tendency of clustering than the synthetic hydroxide composites. Among the filler properties the particle size distribution and the average particle shape of Hy were indicated as the most influent on the filler dispersion and rheology of the composite.

About the melt elasticity properties of the materials, EVA composite filled with Hy showed better swelling behaviour than composites filled with synthetic aluminium hydroxide, while Hy composites showed the worst extrudate aesthetic quality among the studied composites. In particular both Hy and ATH took to a reduction of swelling behaviour of extrudates respect to the pristine EVA and the reduction increases with increasing filler loading. However the effect is more evident in Hy composites, due to the combination of particle shape, size distribution and specific surface, which took to the less elastic recovery of the material. On the other hand the introduction in EVA of Hy and, with different aspects, of Mf took to extrudates with very rough surface at the most of experimental conditions. The negative influence of these fillers on extrudate morphology was attributed to the lack of adhesion between filler and polymer in the case of Mf and for Hy to particle morphology. However the research pointed out also that it was possible to control extrudate aesthetic quality of Hy composite decreasing surface roughness by increasing temperature, by decreasing filler loading and by mixing Hy with another filler, which took to good extrudate morphology by itself, such as the used synthetic aluminium hydroxide.

The introduction of Hy took to better reinforcing effect than the other selected fillers in EVA composites. In fact the natural magnesium hydroxide showed the highest increase of yield strength and modulus with increasing filler loading and the main reason was found in the stronger filler- matrix interaction due to the higher interfacial adhesion of Hy. However the irregular shape of Hy particles and the stronger filler-matrix interaction took to limited deformability of composites and so to the lowest elongation at break.

While natural magnesium hydroxide incorporation did not show any particular effect on thermal degradation behaviour of EVA, it was found that the analysed natural carbonates, SM and Mf, influenced degradation of the polymer on the step corresponding to the release of acetic acid. In particular the presence of a subsequent degradative step for SM composite was determined and FTIR analysis of the evolved gases during degradation indicated the emission of aliphatic ketone species with a spectrum very similar to that of acetone. In the case of Mf composite the emission of acetic acid and ketone compound was detected almost together. The observed formation of ketone species allowed to advance a main hypothesis, supported by the ranges of degradation temperature and

related to the interaction between the fillers and acetic acid formed in-situ by degradation of vinyl acetate groups.

The evaluation of flame retardant properties of Hy composites, carried out during the second part of this PhD study, confirmed that Hy is a valid and cheaper alternative to the synthetic hydroxide despite its less efficiency due to the presence of impurities and the irregular shape of particles. The screening approach and the new parameterization method proposed for analysing a variety of flame retardant additives in combination with Hy in EVA, showed successful evaluation and classification especially of the residue stability and self-extinguishing behaviour of the analysed formulations. Moreover the approach allowed us to obtain useful indications about the chosen additives, such as their relative importance in the influence on a specific flame retardant parameter. All the results for the selected system pointed out that the method could be of high applicative interest and they are promising for the use with different matrices and/or flame retardant additives in order to obtain a stronger validation.

The flame retardant study of a quaternary system composed by the natural magnesium hydroxide and EVA as matrix, together with calcium borate and a poly(dimethylsiloxane) gum as additives, by application of Mixture Design, allowed us to understand the behaviour of the complex system by the analysis of a variety of parameters (coming from the main flame retardant tests). Only a few interactions among the components have been pointed out by the analysis of the mathematical models obtained for describing the parameters, because most of them showed only the main terms. Furthermore the models allowed the prediction of formulations with desired properties; predicted data were verified by experimental results and in most of the cases the good prediction performance of the models was confirmed.

The analysis of the coefficients obtained for the models can be considered a good method for determining the specific additives flame retardant effect, both in the case of single component and interactions. In particular, from the analysis of some models of the flame retardant parameters studied on this specific system and the evaluation of some phenomenological results (residue stability, thermal degradation behaviour, etc), it could be possible to point out useful indications about the chosen components:

1) matrix had to be always the lowest concentration was possible in order to achieve good flame retardant properties;

2) it was not possible to decrease strongly the natural magnesium hydroxide concentration to maintain a good flame retardant level of composite for most of the analysed parameters;

3) PDMS gum (called Sil additive) had good effect on Limiting Oxygen Index and heat release and this was mainly due to its capacity of forming a protective layer on the sample, enhanced by the presence of the other components, especially natural magnesium hydroxide;

4) calcium borate showed positive influence on thermal and residue stability of composites, even if it did not show any particular cooperative effect with other components.

Despite the study on the analysed quaternary system (EVA/Hy/Sil/CaB) has shown partial improvements respect to the reference composite (EVA+ magnesium hydroxide), it can be concluded that the applied method for evaluating flame retardant properties of additives combination results suitable both for scientific and industrial field. For this reason the used chemometrich approach could be useful for the analysis of different systems (different matrix, filler, additives, etc) in order to describe the burning behaviour of the formulations and the flame retardant effects of the components with a limited number of experiments.

Bibliography

1. Rothon, R. N., *Particulate-Filled Polymer Composites*. Longman: Harlow, 1995.
2. Rothon, R. N. *Adv. Polym. Sci.* **1999,** 139, (Mineral Fillers in Thermoplastics I), 67-107.
3. Miller, F., *Introduction to Plastics and Composites Mechanical Properties and Engineering Applications*. Marcel Dekker Inc.: New York, 1996.
4. Rothon, R. N. *Macromol. Symp.* **1996,** 108, (Eurofillers 95), 221-229.
5. Hornsby, P. R. *Int. Mater. Rev.* **2001,** 46, (4), 199-210.
6. Donnet, J.-B. *Carbon* **1994,** 32, (7), 1305-1310.
7. Leblanc, J. L. *Prog. Polym. Sci.* **2002,** 27, (4), 627-687.
8. Hind, A. R.; Bhargava, S. K.; Grocott, S. C. *Colloid. Surface. A* **1999,** 146, (1-3), 359-374.
9. Atay, H. Y.; Celik, E. *Polym. Compos.* **2010,** 31, (10), 1692-1700.
10. Tjong, S. C. *Mat. Sci. Eng. R* **2006,** R53, (3-4), 73-197.
11. Galletti, F.; Perego, G.; Ferrari, A. M.; Holden, G. Low-smoke self-extinguishing cable and flame-retardant composition comprising natural magnesium hydroxide. 2005-IB3208 2007049090, 20051027., 2007.
12. Lipatov, Y. S., *Polymer Reinforment*. ChemTec Publishing: Toronto, 1995.
13. Hull, R.; Witkowski, A.; Hollingbery, L. *Polym. Degrad. Stab.* **2011,** 96, (8), 1462-1469.
14. Leong, Y. W.; Abu Bakar, M. B.; Mohd. Ishak, Z. A.; Ariffin, A.; Pukanszky, B. *J. Appl. Polym. Sci.* **2004,** 91, (5), 3315-3326.
15. Lawandy, S. N.; Halim, S. F.; Darwish, N. A. *eXPRESS Polym. Lett.* **2009,** 3, (3), 152-158.
16. Chen, X.; Yu, J.; Guo, S.; Luo, Z.; He, M. *Polym. Compos.* **2009,** 30, (7), 941-947.
17. Rothon, R. N.; Liauw, C. M.; Lees, G. C.; Schofield, W. C. E. *J. Adhes.* **2002,** 78, (7), 603-628.
18. Hutley, T. J.; Darlington, M. W. *Polym. Commun.***1985,** 26, (9), 264-267.
19. Liauw, C. M.; Lees, G. C.; Hurst, S. J.; Rothon, R. N.; Dobson, D. C. *Angew. Makromol. Chem.* **1996,** 235, 193-203.
20. Hutley, T. J.; Darlington, M. W. *Polym. Commun.* **1984,** 25, (8), 226-228.
21. da Silva, A. L. N.; Rocha, M. C. G.; Moraes, M. A. R.; Valente, C. A. R.; Coutinho, F. M. B. *Polym. Test.* **2001,** 21, (1), 57-60.
22. Ahmed, S.; Jones, F. R. *J. Mater. Sci.* **1990,** 25, (12), 4933-4942.
23. Fu, Q.; Wang, G. *J. Appl. Polym. Sci.* **1993,** 49, (11), 1985-1988.
24. Fu, Q.; Wang, G.; Shen, J. *J. Appl. Polym. Sci.* **1993,** 49, (4), 673-677.
25. Demjen, Z.; Pukanszky, B.; Nagy, J. *Compos. Part A-Appl. S.* **1998,** 29A, (3), 323-329.
26. Pukanszky, B.; Fekete, E. *Adv. Polym. Sci.* **1999,** 139, (Mineral Fillers in Thermoplastics I), 109-153.
27. Liauw, C. M.; Lees, G. C.; Hurst, S. J.; Rothon, R. N.; Ali, S. *Compos. Part A-Appl. S.* **1998,** 29A, (9-10), 1313-1318.
28. Zuiderduin, W. C. J.; Westzaan, C.; Huetink, J.; Gaymans, R. J. *Polymer* **2002,** 44, (1), 261-275.
29. Azizi, H.; Faghihi, J. *Polym. Compos.* **2009,** 30, (12), 1743-1748.
30. Yang, W.; Liu, Z.-Y.; Shan, G.-F.; Li, Z.-M.; Xie, B.-H.; Yang, M.-B. *Polym. Test.* **2005,** 24, (4), 490-497.
31. Coussot, P.; Ancey, C. *Phys. Rev. E* **1999,** 59, (4), 4445-4457.
32. Malkin, A. Y. *Adv. Polym. Sci.* **1990,** 96, (Filled Polym. 1), 69-97.
33. Song, H. J.; White, J. L.; Min, K.; Nakajima, N.; Weissert, F. C. *Adv. Polym. Technol.* **1988,** 8, (4), 431-449.
34. Kaully, T.; Siegmann, A.; Shacham, D. *Polym. Compos.* **2007,** 28, (4), 512-523.
35. Kaully, T.; Siegmann, A.; Shacham, D. *Polym. Compos.* **2007,** 28, (4), 524-533.
36. Yang, J.; Liang, J. Z.; Tang, C. Y. *Polym. Test.* **2009,** 28, (8), 907-911.

37. Osman, M. A.; Atallah, A. *Polymer* **2005,** 46, (22), 9476-9488.
38. Wang, Y.; Wang, J.-J. *Polym. Eng. Sci.* **1999,** 39, (1), 190-198.
39. Osanaiye, G. J.; Leonov, A. I.; White, J. L. *J. Non-Newtonian Fluid Mech.* **1993,** 49, (1), 87-101.
40. Bomal, Y.; Godard, P. *Polym. Eng. Sci.* **1996,** 36, (2), 237-243.
41. Medalia, A. I. *J.Colloid Interf. Sci.***1970,** 32, (1), 115-131.
42. Kovalchuk, N. M.; Kuchin, I.; Starov, V.; Uriev, N. *Colloid J+* **2010,** 72, (3), 379-388.
43. Nielsen, L. E., *Mechanical Properties of Polymers and Composites*. Marcel Dekker: New York, 1974; Vol. 2.
44. Kaully, T.; Siegmann, A.; Shacham, D. *Polym. Adv. Technol.* **2007,** 18, (9), 696-704.
45. Focke, W. W.; Molefe, D.; Labuschagne, F. J. W.; Ramjee, S. *J. Mater. Sci.* **2009,** 44, (22), 6100-6109.
46. Hornsby, P. R.; Mthupha, A. *J. Mater. Sci.* **1994,** 29, (20), 5293-5301.
47. Liu, X.; Li, H. *Polym. Eng. Sci.* **2005,** 45, (7), 898-903.
48. Liang, J.-Z. *Polym. Test.* **2004,** 23, (4), 441-446.
49. Lapasin, R., Reologia dei polimeri fusi. In *Seminario di reologia*, Università di Padova, 2008.
50. Muksing, N.; Nithitanakul, M.; Grady, B. P.; Magaraphan, R. *Polym. Test.* **2008,** 27, (4), 470-479.
51. Dangtungee, R.; Supaphol, P. *Polym. Test.* **2008,** 27, (8), 951-956.
52. Chen, D.; Zhang, W.; He, P. *Polym. Polym. Compos.* **2005,** 13, (3), 271-280.
53. Bhagawan, S. S.; Tripathy, D. K.; De, S. K.; Sharma, S. K.; Ramamurthy, K. *Polym. Eng. Sci.* **1988,** 28, (10), 648-654.
54. Liang, J.-Z. *J. Appl. Polym. Sci.* **2007,** 104, (1), 70-74.
55. Petraru, F.; Popa, M.; Tudose, R. *Polym.-Plast. Technol. Eng.* **2003,** 42, (4), 555-568.
56. Liang, J.-Z.; Yang, J.; Tang, C.-Y. *Polym. Test.* **2010,** 29, (5), 624-628.
57. Samsudin, M. S. F.; Mohd. Ishak, Z. A.; Jikan, S. S.; Ariff, Z. M.; Ariffin, A. *J. Appl. Polym. Sci.* **2006,** 102, (6), 5421-5426.
58. Tordella, J. P. *Rheol. Acta* **1958,** 1, 216-221.
59. Han, C. D.; Lamonte, R. R. *Polym. Eng. Sci.* **1971,** 11, (5), 385-394.
60. Inn, Y. W.; Fischer, R. J.; Shaw, M. T. *Rheol. Acta* **1998,** 37, (6), 573-582.
61. Abdul Rahim, N. A.; Ariff, Z. M.; Ariffin, A.; Jikan, S. S. *J. Appl. Polym. Sci.* **2011,** 119, (1), 73-83.
62. Hornsby, P. R. *Macromol. Symp.* **1996,** 108, (Eurofillers 95), 203-219.
63. Hornsby, P. R.; Wang, J.; Cosstick, K.; Rothon, R.; Jackson, G.; Wilkinson, G. *Prog. Rubber Plast. Technol.* **1994,** 10, (3), 204-220.
64. Yeh, J. T.; Yang, H. M.; Huang, S. S. *Polym. Degrad. Stab.* **1995,** 50, (2), 229-234.
65. Rothon, R. N.; Hornsby, P. R. *Polym. Degrad. Stab.* **1996,** 54, (2-3), 383-385.
66. Rychly, J.; Vesely, K.; Gal, E.; Kummer, M.; Jancar, J.; Rychla, L. *Polym. Degrad. Stab.* **1990,** 30, (1), 57-72.
67. Delfosse, L.; Baillet, C.; Brault, A.; Brault, D. *Polym. Degrad. Stab.* **1989,** 23, (4), 337-347.
68. Hughes, P.; Jackson, G. V.; Rothon, R. N. *Makromol. Chem., Macromol. Symp.* **1993,** 74, (4th Meeting on Fire Retardant Polymers, 1992), 179-183.
69. Huang, H.; Tian, M.; Liu, L.; Liang, W.; Zhang, L. *J. Appl. Polym. Sci.* **2006,** 100, (6), 4461-4469.
70. Haurie, L.; Fernandez, A. I.; Velasco, J. I.; Chimenos, J. M.; Lopez Cuesta, J.-M.; Espiell, F. *Polym. Degrad. Stab.* **2006,** 91, (5), 989-994.
71. Hollingbery, L. A.; Hull, T. R. *Polym. Degrad. Stab.* **2010,** 95, (12), 2213-2225.
72. Laoutid, F.; Bonnaud, L.; Alexandre, M.; Lopez-Cuesta, J. M.; Dubois, P. *Mat. Sci. Eng. R* **2009,** R63, (3), 100-125.
73. Bourbigot, S.; Duquesne, S. *J. Mater. Chem.* **2007,** 17, (22), 2283-2300.

74. Haurie, L.; Fernandez, A. I.; Velasco, J. I.; Chimenos, J. M.; Lopez Cuesta, J.-M.; Espiell, F. *Polym. Degrad. Stab.* **2007,** 92, (6), 1082-1087.
75. Marosfoi, B. B.; Garas, S.; Bodzay, B.; Zubonyai, F.; Marosi, G. *Polym. Advan. Technol.* **2008,** 19, (6), 693-700.
76. Shen, K. K.; Kochesfahani, S. H.; Jouffret, F. *Fire Retardancy of Polymeric Materials (2nd Edition)* **2009**, 207-237.
77. Bourbigot, S.; Le Bras, M.; Leeuwendal, R.; Shen, K. K.; Schubert, D. *Polym. Degrad. Stab.* **1999,** 64, (3), 419-425.
78. Carpentier, F.; Bourbigot, S.; Le Bras, M.; Delobel, R. *Polym. Int.* **2000,** 49, (10), 1216-1221.
79. Shen, K. K.; Kochesfahani, S.; Jouffret, F. *Polym. Advan. Technol.* **2008,** 19, (6), 469-474.
80. Chen, X.; Yu, J.; He, M.; Guo, S.; Luo, Z.; Lu, S. *J. Polym. Res.* **2009,** 16, (4), 357-362.
81. Durin-France, A.; Ferry, L.; Cuesta, J. M. L.; Crespy, A. *Polym. Int.* **2000,** 49, (10), 1101-1105.
82. Marosi, G.; Marton, A.; Anna, P.; Bertalan, G.; Marosfoi, B.; Szep, A. *Polym. Degrad. Stab.* **2002,** 77, (2), 259-265.
83. Fu, M.; Qu, B. *Polym. Degrad. Stab.* **2004,** 85, (1), 633-639.
84. Marosi, G.; Csontos, I.; Ravadits, I.; Anna, P.; Bertalan, G.; Toth, A. *Recent Advances in Flame Retardancy of Polymeric Materials* **1999,** 10, 88-99.
85. Huang, H.; Tian, M.; Liu, L.; He, Z.; Chen, Z.; Zhang, L. *J. Appl. Polym. Sci.* **2006,** 99, (6), 3203-3209.
86. Zilberman, J.; Hull, T. R.; Price, D.; Milnes, G. J.; Keen, F. *Fire Mater.* **2000,** 24, (3), 159-164.
87. Wang, Z.; Qu, B.; Fan, W.; Huang, P. *J. Appl. Polym. Sci.* **2001,** 81, (1), 206-214.
88. Burns, M.; Wagenknecht, U.; Kretzschmar, B.; Focke, W. W. *J. Vinyl Addit. Techn.* **2008,** 14, (3), 113-119.
89. Wang, G.; Jiang, P.; Zhu, Z.; Yin, J. *J. Appl. Polym. Sci.* **2002,** 85, (12), 2485-2490.
90. Pukanszky, B.; Voros, G. *Compos. Interface.* **1993,** 1, (5), 411-427.
91. Zhu, S.; Zhang, Y.; Zhang, Y. *J. Appl. Polym. Sci.* **2002,** 83, (1), 121-128.
92. Hornsby, P. R.; Cusack, P. A.; Cross, M.; Toth, A.; Zelei, B.; Marosi, G. *J. Mater. Sci.* **2003,** 38, (13), 2893-2899.
93. Keszei, S.; Anna, P.; Marosi, G.; Marton, A.; Bertalan, G.; Vallo, F. *Macromol. Symp.* **2003,** 202, (Reactive Modification and Stability of Multicomponent Polymeric Systems), 235-243.
94. Cardelli, A. Effetto del trattamento superficiale su cariche inorganiche utilizzate come ritardanti di fiamma in materiali polimerici termoplastici. Università di Pisa, Pisa, 2005.
95. Hamdani, S.; Longuet, C.; Lopez-Cuesta, J.-M.; Ganachaud, F. *Polym. Degrad. Stab.* **2010,** 95, (9), 1911-1919.
96. Camino, G.; Maffezzoli, A.; Braglia, M.; De Lazzaro, M.; Zammarano, M. *Polym. Degrad. Stab.* **2001,** 74, (3), 457-464.
97. Kaully, T.; Siegmann, A.; Shacham, D. *Polym. Compos.* **2008,** 29, (4), 396-408.
98. Mohanty, S.; Verma, S. K.; Nayak, S. K. *J. Appl. Polym. Sci.* **2006,** 99, (4), 1476-1484.
99. Kim, K.-J.; White, J. L.; Shim, S. E.; Choe, S. *J. Appl. Polym. Sci.* **2004,** 93, (5), 2105-2113.
100. Hwang, W. R.; Hulsen, M. A. *Korea-Aust. Rheol. J.* **2006,** 18, (4), 171-181.
101. Poslinski, A. J.; Ryan, M. E.; Gupta, R. K.; Seshadri, S. G.; Frechette, F. J. *J. Rheol. (N. Y., NY, U. S.)* **1988,** 32, (7), 703-735.
102. Basu, D.; Banerjee, A. N.; Misra, A. *J. Appl. Polym. Sci.* **1992,** 46, (11), 1999-2009.
103. Servais, C.; Jones, R.; Roberts, I. *J. Food Eng.* **2002,** 51, (3), 201-208.
104. Shenoy, A. v., *Rheology of Filled Polymer Systems*. Springer - Verlag: 1999.
105. Rong, S. D.; Chaffey, C. E. *Rheol. Acta* **1988,** 27, (2), 186-96.

106. Santamaria-Holek, I.; Mendoza, C. I. *J. Colloid Interf. Sci.* 346, (1), 118-126.
107. Honek, T.; Hausnerova, B.; Saha, P. *Polym. Compos.* **2005,** 26, (1), 29-36.
108. Osman, M. A.; Atallah, A.; Schweizer, T.; Ottinger, H. C. *J. Rheol. (N. Y., NY, U. S.)* **2004,** 48, (5), 1167-1184.
109. Hristov, V.; Vlachopoulos, J. *Polym. Compos.* **2008,** 29, (8), 831-839.
110. Ariffin, A.; Jikan, S. S.; Samsudin, M. S. F.; Ariff, Z. M.; Ishak, Z. A. M. *J. Reinf. Plast. Compos.* **2006,** 25, (9), 913-923.
111. Guriya, K. C.; Bhattachariya, A. K.; Tripathy, D. K. *Polymer* **1997,** 39, (1), 109-115.
112. Migler, K. B.; Son, Y.; Qiao, F.; Flynn, K. *J. Rheol. (N. Y., NY, U. S.)* **2002,** 46, (2), 383-400.
113. Gahleitner, M. *Prog. Polym. Sci.* **2001,** 26, (6), 895-944.
114. Park, D. H.; Ahn, M. J.; Kim, S. C.; Lee, G. J. *Proceedings of International Wire and Cable Symposium* **2001,** 50th, 409-414.
115. Liang, J.; Zhang, Y. *Polym. Int.* **2010,** 59, (4), 539-542.
116. Nielsen, L. E. *J. Compos. Mater.* **1967,** 1, (1), 100-119.
117. Yin, J.; Zhang, Y.; Zhang, Y. *J. Appl. Polym. Sci.* **2005,** 97, (5), 1922-1930.
118. Fernandez, A. I.; Haurie, L.; Formosa, J.; Chimenos, J. M.; Antunes, M.; Velasco, J. I. *Polym. Degrad. Stab.* **2009,** 94, (1), 57-60.
119. Yin, J.; Zhang, Y.; Zhang, Y. *J. Appl. Polym. Sci.* **2005,** 98, (3), 957-967.
120. Pukanszky, B. *Eur. Polym. J.* **2005,** 41, (4), 645-662.
121. Kiss, A.; Fekete, E.; Pukanszky, B. *Compos. Sci. Technol.* **2007,** 67, (7-8), 1574-1583.
122. Marosi, G.; Anna, P.; Bertalan, G.; Szabo, S.; Ravadits, I.; Papp, J. *ACS Symposium Series* **2001,** 797, (Fire and Polymers), 161-171.
123. Marosi, G.; Keszei, S.; Matko, S.; Bertalan, G. *ACS Symposium Series* **2006,** 922, (Fire and Polymers IV), 117-130.
124. Berbenni, V.; Marini, A.; Bruni, G.; Zerlia, T. *Thermochim. Acta* **1995,** 258, 125-133.
125. Carpentier, F.; Bourbigot, S.; Le Bras, M.; Delobel, R.; Foulon, M. *Polym. Degrad. Stab.* **2000,** 69, (1), 83-92.
126. Karlsson, L.; Lundgren, A.; Jungqvist, J.; Hjertberg, T. *Polym. Degrad. Stab.* **2009,** 94, (4), 527-532.
127. Bodzay, B.; Marosfoi, B. B.; Igricz, T.; Bocz, K.; Marosi, G. *J. Anal. Appl. Pyrol.* **2009,** 85, (1+2), 313-320.
128. Huang, N.; Wang, J. *J. Anal. Appl. Pyrol.* **2009,** 84, (2), 124-130.
129. McGrattan, B. J. *ACS Symposium Series* **1994,** 581, (Hyphenated Techniques in Polymer Characterization), 103-115.
130. Marcilla, A.; Gomez, A.; Menargues, S. *J. Anal. Appl. Pyrol.* **2005,** 74, (1-2), 224-230.
131. Marcilla, A.; Gomez-Siurana, A.; Menargues, S. *Thermochim. Acta* **2005,** 438, (1-2), 155-163.
132. Sultan, B. A.; Soervik, E. *J. Appl. Polym. Sci.* **1991,** 43, (9), 1737-1745.
133. Nakamura, R.; Niiyama, H.; Suzuki, K. Manufacture of ketones from aliphatic carboxylic acids or esters. 88-71206 01242546, 19880324., 1989.
134. Sultanov, A. S.; Babakhodzhaeva, S. A. *Doklady Akademii Nauk UzSSR* **1967,** 24, (3), 28-30.
135. Mora, F. M. Acetone from calcium acetate liquor. 2794838, 1957.
136. Hasan, M. A.; Zaki, M. I.; Pasupulety, L. *Appl. Catal. A-Gen.* **2003,** 243, (1), 81-92.
137. Niu, S.; Han, K.; Lu, C.; Sun, R. *Applied Energy* 87, (7), 2237-2242.
138. Bourbigot, S.; Duquesne, S.; Sebih, Z.; Segura, S. *PMSE Preprints* **2004,** 91, 154-155.
139. Genovese, A.; Shanks, R. A. *Polym. Degrad. Stab.* **2007,** 92, (1), 2-13.
140. Gui, H.; Zhang, X.; Dong, W.; Wang, Q.; Gao, J.; Song, Z.; Lai, J.; Liu, Y.; Huang, F.; Qiao, J. *Polymer* **2007,** 48, (9), 2537-2541.
141. Babcock, L. M.; Altekar, M. *Chemometr. Intell. Lab.* **1995,** 29, (1), 141-146.

142. Atikler, U.; Demir, H.; Tokatli, F.; Tihminlioglu, F.; Balkoese, D.; Uelkue, S. *Polym. Degrad. Stab.* **2006,** 91, (7), 1563-1570.
143. Wu, W.; Yang, C. Q. *Polym. Degrad. Stab.* **2004,** 85, (1), 623-632.
144. Dvir, H.; Gottlieb, M.; Daren, S.; Tartakovsky, E. *Compos. Sci. Technol.* **2003,** 63, (13), 1865-1875.
145. Hornsby, P. R. *Int. Mater. Rev.* **2001,** 46, (4), 199-210.
146. Hristov, V.; Vlachopoulos, J. *Adv. Polym. Technol.* **2007,** 26, (2), 100-108.
147. Cornell, J., *Experiments with Mixtures: Designs, Models and the Analysis of Mixture Data*. 2nd ed. ed.; John Wiley & Sons: New York, 1990.
148. Scheffé, H. *J. Roy. Stat. Soc. B* **1958,** 20, 344-366.
149. Scheffé, H. *J. Roy. Stat. Soc. B* **1965,** 25, 235-263.
150. Morgan, A. B.; Bundy, M. *Fire Mater.* **2007,** 31, (4), 257-283.
151. Gallo, E.; Braun, U.; Schartel, B.; Russo, P.; Acierno, D. *Polym. Degrad. Stab.* **2009,** 94, (8), 1245-1253.
152. Smith, W. F., *Experimental Design for Formulation*. ASA-SIAM Series on Statistics and Applied Probability, SIAM: Philadelphia, ASA, Alexandria, VA, 2005.
153. Camino, G.; Lomakin, S. M.; Lageard, M. *Polymer* **2002,** 43, (7), 2011-2015.
154. Toure, B.; Lopez Cuesta, J. M.; Longerey, M.; Crespy, A. *Polym. Degrad. Stab.***1996,** 54, (2-3), 345-352.
155. Hamdani, S.; Longuet, C.; Perrin, D.; Lopez-Cuesta, J.-M.; Ganachaud, F. *Polym. Degrad. Stab.* **2009,** 94, (4), 465-495.
156. Shen, K. K.; Kochesfahani, S.; Jouffret, F. In *Review of recent advances on the use of silicon-based flame retardants - Silicon/Boron synergy*, BCC FR Conference, 2011; 2011.
157. Crompton, G. Compositions for and manufacture of fire- and heat-resistant components. 1988-311509 322135, 19881205., 1989.
158. Ishii, T.; Kokaku, H.; Nagai, A.; Nishita, T.; Kakimoto, M. *Polym. Eng. Sci.* **2006,** 46, (6), 799-806.
159. Kodolov, V. I.; Shuklin, S. G.; Kuznetsov, A. P.; Makarova, L. G.; Bystrov, S. G.; Demicheva, O. V.; Rudakova, T. A. *J. Appl. Polym. Sci.* **2002,** 85, (7), 1477-1483.
160. Morgan, A. B.; Cogen, J. M.; Opperman, R. S.; Harris, J. D. *Fire Mater.* **2007,** 31, (6), 387-410.

APPENDIX I

Time-temperature superposition principle (TTS) [1,2]

The time-temperature principle superposition states that the viscoelastic behaviour (expressed for instance as storage or loss modulus vs. angular frequency) of a linear polymer, evaluated at a certain temperature and frequency, is the same as that obtained at a higher temperature and a higher frequency. This shift of the modulus curve is described by means of a shift factor for the frequencies as a function of the temperature (Figure AI.1). The concept of equivalent states underlying time-temperature superposition can be expressed in terms of an equation relating the property measured at a temperature T_1 to that at the reference temperature (T_2) using the shift factor a(T):

$$G(T_1,\omega)=G(T_2, a(T_2)\cdot\omega)$$

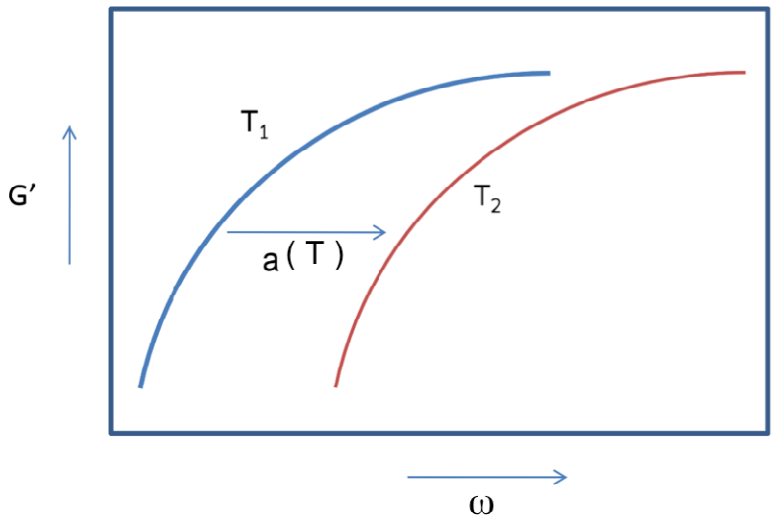

Figure AI.1: Schematic representation of the shift of the modulus curve on the anguar frequency axis.

If time-temperature superposition holds, the use of a shift factor allows to consctruct a master curve showing the viscoelastic behaviour at a reference temperature over a much larger range of frequencies than those experimentally accessible. An example of a master curve obtained for the storage modulus of a commercial polystyrene is reported in Figure AI.2.

[1] Ferry J. D., "*Viscoelastic Properties of Polymers*", 3rd edition, Wiley, New York (1980).
[2] Dealy, J.; Plazek, D. *Rheol. Bull.*, **2009**,78, (2), 16-31.

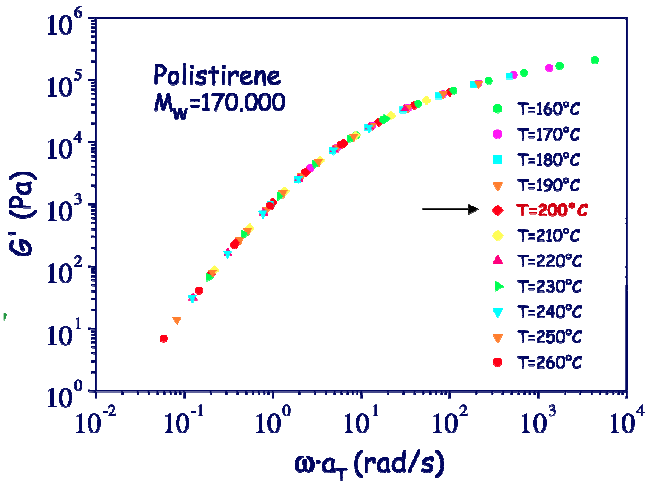

Figure AI.2: Master curve obtained by shifting modulus curves at different temperatures.

When viscosity is considered, the application of an additional vertical shift factor is necessary. The horizontal one accounts for the already mentioned time scale change with temperature, whereas the vertical one, whose value must be the same as the horizontal one, comes from the definition of complex viscosity (which is the complex modulus divided by the angular frequency).

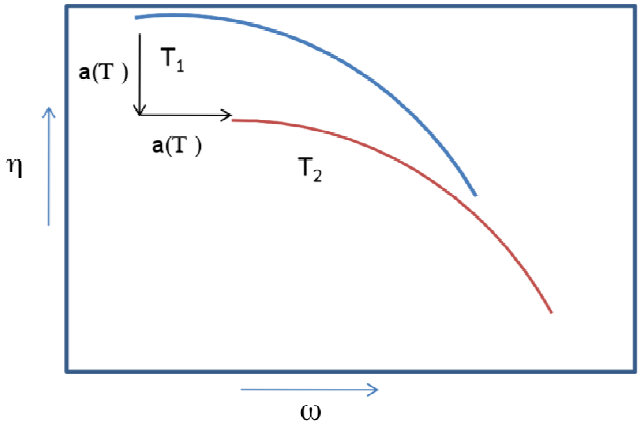

Figure AI.3: Schematic representation of the shift of the viscosity curve on the angular frequency axis.

The time-temperature superposition principle can generally be applied in the case of the terminal relaxation of linear homopolymers, which are consequently said to be "thermorheologically simple" materials. Branched polymers are another matter, as they are generally "thermorheologically complex" even materials in the terminal relaxation region. In this latter case TTS cannot be applied due to the simultaneous presence of

different mechanisms of relaxation (reputation and arm retraction). If the Cox-Merz rule is taken into account the same shifting procedure to build master curves can be applied to steady regime data, where the stress must be identified with the complex modulus and the shear rate must be identified with the angular frequency.

In this case the shift of shear stress as a function of shear rate can be expressed as follows:

$$\tau(T_1, \dot{\gamma}) = \tau(T_2, a(T_2) \cdot \dot{\gamma})$$

and considering the viscosity, both the horizontal and vertical shift have to be applied, leading to the following equation:

$$\eta(T_2, \dot{\gamma}_2) = \frac{\tau(T_2, \dot{\gamma}_2)}{\dot{\gamma}_2} = \frac{\tau(T_2, a(T_2) \cdot \dot{\gamma}_1)}{a(T_2) \cdot \dot{\gamma}_1} = \frac{\eta(T_1, \dot{\gamma}_1)}{a(T_2)}$$

APPENDIX II

Definitions about statistical methods used for flame retardant studies[3,4,5,6]*:*

In **mixture design**, the factors are proportions of different components or ingredients of a mixture. The factors are expressed as the fraction of total amount of their experimental ranges and they must sum up to 1. Generally in mixture experiments, the measured response is assumed to depend only on the relative proportions of the ingredients or components in the mixture and not on the amount of the mixture. Planning a mixture experiment typically involves the following steps[7]:

1. Define the objectives of the experiment.
2. Select the mixture components and any other factors to be studied. Other factors may include process variables or the total amount of the mixture.
3. Identify any constraints on the mixture components or other factors in order to specify the experimental region.
4. Identify the response variable(s) to be measured.
5. Propose an appropriate model for modelling the response data as functions of the mixture components and other factors selected for the experiment.
6. Select an experimental design that can fit the proposed model.

In many mixture designs, there are restrictions on the component proportions (x_i) that prevent from exploring the entire simplex region and thus focus the exploration only on the region of interest. These **constraints** are expressed as lower and upper boundaries of the component quantity and the resulting experimental domain is an irregular polytope. The general form to express **components** ($\boldsymbol{x_i}$) in a mixture design is:

$$\sum x_i = 1 \quad \text{and} \quad L_i \leq x_i \leq U_i$$

where L_i and U_i are the lower and the upper limit respectively.

[3] Smith, W.F., *Experimental design for formulation*. SIAM: Philadelphia, 2005
[4] http://itl.nist.gov/div898/handbook/pri/section5/pri5.htm
[5] Atikler, U.; Demir, H.; Tokatli, F.; Tihminlioglu, F.; Balkoese, D.; Uelkue, S. *Polym. Degrad. Stab.* **2006,** 91, (7), 1563-1570
[6] Dvir, H.; Gottlieb, M.; Daren, S.; Tartakovsky, E. *Compos. Sci. Technol.* **2003,** 63, (13), 1865-1875.
[7] Piepel, G.F.; Cornell, J.A. *J. Qual. Technol.*, **1994**, 26, (3), 177-196.

In these types of design it is considered convenient to simplify the analysis of the system by introducing **pseudo-components**, which allow the use of simplex type designs when lower bounds are employed in the experimental design. They are defined as:

$$x'_i = \frac{x_i - L_i}{(1 - \sum_{j=1}^{p} L_j)}$$

where *L* represents the lower bounds employed in the experimental design.

D-optimal design procedure can be useful for the types of design, where the experimental region is not a standard shape and classical designs cannot be applied. D-optimal criterion selects design points from a list of candidates so the variances of the model regression coefficients are minimized. It is a computer generated design, which maximizes the determinant of the X'X matrix, where X is the extended design matrix. Its application corresponds to laying out mixture experiments so that as large an experimental region as possible is well mapped.

The purpose of performing mixture experiments is to model the behaviour of the mixture in terms of a mathematical equation so that prediction of the response can be made empirically. In the study of the quaternary system reported in this PhD thesis the mathematical expression (*response surface*) assumed to be appropriate for the analysed responses can be represented by the following general regression formula:

$$E(y) = \sum_{i=1}^{p} \beta_i x_i + \sum \sum_{i<j}^{p} \beta_{ij} x_i x_j + \sum \sum \sum_{i<j<k} \beta_{ijk} x_i x_j x_k$$

where β values correspond to the coefficients of the component (β_i for first order, β_{ij} for second, etc), which are chosen by the program to achieve the best fitting of the model to the experimental data. The first order term represents the direct influence of the *i*-th ingredient on a certain response *E(y)* (*main effect*). The upper order terms express the interactions between the combined factors, which reflect the non-additivity in the influence of the factors on the response.

The coefficients of the models have been selected using a **stepwise backward selection procedure**. The process starts with fitting a model with all the variables of interest (following the initial screen); then the least significant variable is dropped, so long as it is not significant at the chosen critical level. Successively re-fitting reduces models and the same rule is applied until all remaining variables are statistically significant. First order

terms are always present, while the upper order terms depend on model efficiency and performance.

The **coefficient of determination** (***R²***) and the **adjusted coefficient of determination** (***R²adjusted***) have traditionally been used to measure goodness of fit of an estimated linear regression model.

The coefficient of determination R^2 measures the proportion of total variability explained by the model. It is generally defined as:

$$R^2 = \frac{SSR}{SST} = 1 - \frac{SSE}{SST}$$

where SSR stands for regression or model sum of squares, SST stands for total sum of squares and SSE for error or residual sum of squares.

The R^2-*adjusted* reflects the impact of increasing and decreasing the number of model terms. It is similar to R^2, but it is *adjusted* for the number of explanatory terms in a model and it is defined by the following general equation:

$$R^2_{adjusted} = 1 - \frac{n-1}{n-p}(1-R^2)$$

where n is the number of observation and p of the regressors in the model.

Values of R^2 and R^2-*adjusted* close to 1 and closer each other are desirable.

The **predictive capacity** of the regression model can be indicated by ***R²prediction*** which is calculated according to the following equation:

$$R^2_{prediction} = 1 - \frac{PRESS}{SST}$$

where *PRESS* stands for the prediction error sum of squares, which is a measure of how well the model will predict new data. Generally low value of PRESS and $R^2_{prediction}$ value closer to 1, indicates that the model is likely to be a good predictor.

Adequate Precision (*Adeq. Precision*) compares the range of the predicted values at the design points to the average predictor error and so it is related to the signal to noise ratio. A value of Adequate Precision greater than 4 is desirable, because it indicates adequate model discrimination.

The **leave-one-out Cross-Validation**[8], that has been used for validation of the models in the reported studies, is a statistical method of evaluating and comparing algorithms by dividing data into two segments: one used to train the model and the other used to validate the model. Specifically using the *leave-one-out* form, in each iteration nearly all the data, except for a single observation, are used for training and the model is tested on that single observation.

In order to achieve **numerical optimization** backward process has been used, where first the dependent variables (Y) are defined and then the independent variables (X), that can lead to the desired result, are found. It is necessary to choose the desired goal for each factor and response (maximize, minimize, etc), to provide a minimum and maximum level for each parameter and to assign a weight (importance) to each goal. The importance factor for each goal is indicated by a plus sequence (for example +++ is importance 3, ++ is importance 2, etc): more plus signs determine higher importance. The approach is to combine the goals of the factors and responses into an overall **desirability function**, with translation to a common scale ([0, 1]). The function shape is adjusted by the importance of the goals and the statistical program tries to maximize desirability in order to find the optimum. This corresponds to a specific composition of the mixture (best solution), which has 1 as desirability parameter if it satisfy completely the desired goals or lower desirability value if the goals are not perfectly reached. Usually the optimization process takes to a list of formulations as possible solutions, ordered taking into account the desirability of their responses.

Variable Importance in Projection (**VIP**) coefficients reflect the relative importance of the individual variables and specifically the influence on the Y-responses of every predictor X in the model. VIP coefficients allow to classify the X variables according to their explanatory power of Y. VIP values above 1 have significant influence on the model and are more relevant for explaining the variation of Y[9].

[8] Refaeilzadeh, P.; Tang, L.; Liu, H., *Cross Validation*. In Encyclopedia of Database Systems, Editors: M. Tamer Özsu and Ling Liu. Springer, 2009.
[9] Amaral, A.L.; Ferreira, E.C., *Anal. Chim. Acta*, **2005**, 544, 246–253.

Acknowledgments

I would like to extend my thanks to many people for their help during the entire period of my PhD thesis work.

First of all I would like to express my gratitude to professor Giacomo Ruggeri for allowing me to carry out this research in his laboratory and for all his support and encouragement throughout the course of this PhD thesis work.

I am grateful to professor Gyorgy Marosi from the Budapest University of Technology and Economics (Hungary) for his helpfulness during my research work in his laboratory and for following me during the thesis writing. I would also like to thank all the people of his research group at the Department of Organic Chemistry and Technology laboratory because of their technical support, and their friendship.

I especially thank Camillo Cardelli, Oleg Lednev and Elpidio Tombari of CNR. IPCF, UOS Pisa, for their scientific and practical support during these three years of experimental work: they have always been available with extremely valuable corrections and suggestions about my research work.

I am thankful to Marco Calderisi for his precious support on statistics, for all the analyses he has carried out on my results and for all the answers and explanations he has provided.

Thanks to Dino Ferri, Francesco Scavello and Paolo Lomellini of Polimeri Europa S.p.A, for their teachings and support with some measurements and for their explanations on the theoretical elaboration of the rheological results.

Naturally I would like to thanks Mixer S.p.A, Nuova Sima S.r.l. and Silma S.r.l. as they have provided most of the materials and allowed me to use many of the instruments of their internal laboratories during the three years of PhD work.
I would like to thank the technicians and researchers working there and in particular Paolo Lippera for the fillers analyses, Diego Tirelli, Andrea Galanti and Stefano Dossi, who explained perfectly how to proceed with rheological and thermal analyses and for always being available for scientific discussion.

I would like to thank professor Fernando Galembeck, Chemical Institute of University of Campinas, Brazil, for his useful suggestions and for providing some of the SEM analyses for filler dispersion studies in the composites.

I am really thankful to all the people, who have worked (or are still working) in the polymer laboratory especially Lucia Ricci, Andrea Pucci, Sabrina Bianchi and Antonella Manariti for their suggestions, for their friendship and obviously for being so patient with me!

It is a great pleasure to thank my entire family and all my friends, who have supported me throughout this time (especially my friends in Fabriano, who have been an incredible help during my stay there!).
Thanks especially to my parents for their ever present moral support!
Finally I am extremely grateful to Marco, who has become my husband during the last year, because he has trusted me and for his loving support.